SALTWATER INTRUSION MODELING IN JAGATSINGHPUR COASTAL AQUIFER SYSTEM, ODISHA

Ph.D THESIS

by

AJIT KUMAR BEHERA

DEPARTMENT OF EARTH SCIENCES
INDIAN INSTITUTE OF TECHNOLOGY ROORKEE
ROORKEE – 247 667 (INDIA)
DECEMBER, 2018

SALTWATER INTRUSION MODELING IN JAGATSINGHPUR COASTAL AQUIFER SYSTEM, ODISHA

A THESIS

Submitted in partial fulfilment of the requirements for the award of the degree

of

DOCTOR OF PHILOSOPHY

in

EARTH SCIENCES

by

AJIT KUMAR BEHERA

DEPARTMENT OF EARTH SCIENCES
INDIAN INSTITUTE OF TECHNOLOGY ROORKEE
ROORKEE – 247 667 (INDIA)
DECEMBER, 2018

©INDIAN INSTITUTE OF TECHNOLOGY ROORKEE, ROORKEE-2018
ALL RIGHTS RESERVED

INDIAN INSTITUTE OF TECHNOLOGY ROORKEE
ROORKEE

CANDIDATE'S DECLARATION

I hereby certify that the work which is being presented in the thesis entitled **"SALTWATER INTRUSION MODELING IN JAGATSINGHPUR COASTAL AQUIFER SYSTEM, ODISHA"** in partial fulfilment of the requirements for the award of the Degree of Doctor of Philosophy and submitted in the Department of Earth Sciences of the Indian Institute of Technology Roorkee, Roorkee is an authentic record of my own work carried out during a period from July, 2013 to December, 2018 under the supervisions of Dr. G.J. Chakrapani, Professor, Department of Earth Sciences, Indian Institute of Technology Roorkee, Roorkee and Dr. Sudhir Kumar, Scientist G, Hydrological Investigations Division, National Institute of Hydrology, Roorkee.

The matter presented in the thesis has not been submitted by me for the award of any other degree of this or any other Institution.

(AJIT KUMAR BEHERA)

This is to certify that the above statement made by the candidate is correct to the best of our knowledge.

(Sudhir Kumar)
Supervisor

(G.J. Chakrapani)
Supervisor

The Ph.D. Viva-Voce Examination of **Mr. Ajit Kumar Behera**, Research Scholar, has been held on 3rd July 2019.

Chairman, SRC **Signature of External Examiner**

This is to certify that the student has made all the corrections in the thesis

Signature of Supervisor (s) **Head of the Department**
Date: 03-07-2019

ABSTRACT

The present study dealt with saltwater intrusion modeling in a coastal aquifer system in the Mahanadi river delta region near the coast of Bay of Bengal. The aquifers of Mahanadi delta are characterized as shallow aquifers (< 50 m) and deeper aquifers (> 50 m). Electrical conductivity (EC) of groundwater varied from fresh of 146 µS/cm (NW of the Mahanadi delta) to a saline of 33900 µS/cm (close to sea coast) with cation dominance in the order $Na^+ > Ca^{2+} > Mg^{2+} > K^+$ and anion dominance of $Cl^- > HCO^-_3 > SO_4^{2-}$. The hydro chemical facies changed from Ca-Mg-Na-HCO_3 type to Na-Cl type along the groundwater flow direction due to ion exchange processes. A strong positive correlation ($r > 0.9$) between Cl^- with EC, Na^+, Mg^{2+}, Ca^{2+}, SO_4^{2-} and K^+ was observed, indicating the influence of seawater on coastal aquifer. The ionic ratios (Na^+/Cl^-, HCO^-_3/Cl^-, Mg^{2+}/Ca^{2+}, SO_4^{2-}/Cl^-, $Ca^{2+}/(HCO^-_3/SO_4^{2-})$) also suggested that the groundwater is affected by seawater intrusion. Stable isotope compositions ($\delta^{18}O$ and δ^2H) varied from -1.86 $^0/_{00}$ to -6.87 $^0/_{00}$ for $\delta^{18}O$ and from -10.79 $^0/_{00}$ to -45.42 $^0/_{00}$ for δ^2H, implying the mixing of saline water and fresh groundwater in the coastal region of the Mahanadi delta.

PHREEQC code was used to measure the saturation index of carbonate end minerals such as calcite and dolomite. The saturation index of calcite and dolomite minerals with < 1 is an indication of presence of fresh groundwater in Upper deltaic formation. This was supported by Ca-rich water with Mg^{2+}/Ca^{2+} ratio < 1. The proportion of seawater in groundwater was estimated to vary from 0% in the Upper delta formation to 72% in the Lower delta formation of the Mahanadi delta (close to sea coast), which is due to inland intrusion of seawater. A conceptual diagram was prepared to visualize the chemical variation in this coastal aquifer system. Shallow well close to Bay of Bengal showed less concentration of Na^+ and Cl^- content with low EC. The deep well close to the sea coast, showed high ionic concentration of Na^+ and Cl^- with an indication of seawater intrusion.

An appropriate groundwater flow model was developed to estimate seawater intrusion and understand the factors of groundwater dynamics in the Jagatsinghpur coastal district. The hydraulic head varied from 0.7 m to 15 m above mean sea level (MSL) with an average head of 6 m in the low-lying coastal region, where the groundwater is mainly abstracted (overdraft) for agricultural activities. Aquifer parameters were estimated using Parameter Estimation

Technique (PEST) module in Visual MODFLOW. The horizontal hydraulic conductivity and the specific yield values in the area were observed to vary from 40 m/day to 45 m/day and 0.05 to 0.07 respectively. The model has been calibrated for two years (2004 and 2005) by using these parameters, followed by validation of four years (2006 to 2009). The calibrated numerical model was used to calculate net recharge and groundwater balance and to infer interaction between river and coastal unconfined aquifer system and responses during different seasons.

The net groundwater recharge to coastal aquifer thus estimated, showed variations from 247.89 to 262.63 million cubic meter (MCM) for year 2006 and 2007. Similarly, the inflow from river boundary was calculated as 34 MCM during pre- and post monsoon period. In monsoon time, the costal aquifer discharged around 23 to 27 MCM of water to river system. Water level contour of this coastal aquifer was also studied, which showed high and low hydraulic gradient in the upper and lower part of the deltaic region respectively. The low hydraulic gradient and slugish movment of groundwater in the lower part of the study area was due to influence of seawater. Because of low net recharge, seawater ingress has been inferred. Other human factors such as, growing urbanization and industrialization also led to decline in the hydraulic head. Hence, appropriate recharge methods need to be adopted to reduce the seawater intrusion in the affected areas.

ACKNOWLEDGEMENTS

This thesis is the success of my endeavors that could have not been possible without the blessings of "**GOD**". His divine grace gave me strength, hope and determination to carry out this research and submit my Ph.D Thesis.

First and foremost, I would like to thank my Supervisor Prof. G.J.Chakrapani, Department of Earth Sciences, IIT Roorke, who believed in me and I am indebted for his valuable advice, support and criticism throughout my thesis work. I thank him for being a caring supervisor, who brings out the best in his students while giving them enough space to explore their own scientific potential. I sincerely appreciate his efforts for editing my thesis writing, and his immense support and critical reviews of my observations. I would like to thank Prof. Chakrapani for offering me the opportunity to work with him in his research group and an excellent lab setup.

I am highly delighted to express my gratitude to my supervisor Dr. Sudhir Kumar, Scientist G and Head, Hydrological Investigations Division, National Institute of Hydrology, Roorkee for his immaculate supervision, guidance, support and constant motivation throughout my research work. I deeply appreciate Dr. Kumar for his friendly behavior, which allowed me to express my ideas, thoughts to him. I would like thank Dr. Sudhir Kumar for being a caring mentor, who is always there to support me in any situation and also allowing me to work in Nuclear Hydrology Laboratory.

I would like to thank Dr. D.D. Pati, Director, Central Ground Water Board (CGWB), Bhubaneswar, for allowing me to discuss with his team for necessary data. I am very much thankful to Mr. Durjyoti Mandal (Scientist C), Mr. Prahallad Das (Scientist C) and Smt. Sanghamitra Mahapatra (Scientist C), CGWB, Bhubaneswar for providing me essential and necessary data for research work.

I am very much thankful to Dr. Sarada Prasad Pradhan, Assistant Professor, Department of Earth Sciences, IIT Roorkee, for motivating and supporting me during the end stage of my research work.

I would also like to thank Dr. Nachiketa Rai, Assistant Professor, Department of Earth sciences, IIT Roorkee, for his immense motivation and fruitful discussion during my Ph.D. work.

I am highly grateful to Dr. Pitambar Pati (Internal Expert, SRC) for supporting me throughout my research journey. I am very much thankful for suggesting critical reviews during this progress of work. He was always there, whenever needed.

I acknowledge my gratitude to Prof. R. Krishnamurthi (Chirman, SRC and DRC), Department of Earth Sciences, IIT Roorkee for his suggestions and encouragement throughout my research work. I am also thankful to Prof. Krishnamurthi for his immense support whenever approached.

I would like to thank Prof. A.K. Sen, for his support and encouragement throughout my research journey.

I would like to thank Dr. R.K. Peddinti (External Expert, SRC), Department of Chemistry, IIT Roorkee for giving valuable time and suggestions.

I express my gratitude to Dr. Suni Bajpai, Professor and Head, Department of Earth Sciences, IIT Roorkee for extending all necessary infrastructural facilities and cooperation.

I am highly indebted to the Foreign and Indian examiners of my thesis for their detailed review and comments, which improved the thesis presentation immensely.

My heartfelt thanks to Dr. Kiran Jyoti Mishra (Kiran Bhai), Geologist, Geological Survey of India (GSI), for his immense help, guidance and inspiration. I learnt many things from him.

I am very much thankful to Swopnasarika Swain (Sarika), Geologist, GSI for supporting me throughout my research work. I am also thankful to Muna for helping me in field work. I express my thanks to Charu Ji for her support and necessary help for research work.

I also express my thanks to Giris and Bubun, who helped me in fieldwork. Their help was great for me.

I am also thankful to Mr. Dinesh Rai and Mr. Jameer for helping me in laboratory, NIH, Roorkee.

Now the time for my friends in IIT Roorkee, who were there always to support and help me. To Chinmay (Universal Chinu Bhai), his funny behavior was always entertaining. I am thankful to him for his unconditional help. I am thankful to Arun (Structural Geologist) for his immense help and technical discussion during my research work. Thanks to Dr. Ajit Sahoo (Serious man) for his kind help.

I would like to thank Pipasa, Debasmita and Sujit for extending their helping hands for lab work. I also express my affection to my juniors, Amulya, Pipasa, Debasmita, Arun, Rudra and Rajesh being a part of my research Journey.

I also express my sincere thanks to Dr. Suman Bhai, Dr. Pursu Bhai, Dr. Tiku Bhai, Dr. Abhijeet Bhai, Dr. Sunil (Bada Bhai), Dr. Aditya, Chinu Bhai, Asit, Santanu and Jagannath for necessary help.

I would like to thank my senior lab mates Dr. Yawar, Dr. Sugandha and Dr. Anjali for helping me during initial phase of my research work.

Last but not the least, my deepest thanks to my parents, my elder brother (Pradeep) and sister-in-law (Priyadarshini) who blessed me and supported me for the successful completion of this research work. I express my affection to my younger sister (Kaltu), who always encouraged me throughout my journey of research. My parents, who always supported and stood by me throughout my research work. I will always remain grateful to my parents. My nephew (dugu) who also cooperated me during this work through his sweet wordings over phone.

TABLE OF CONTENTS

LIST OF FIGURES

LIST OF TABLES

CHAPTER 1 INTRODUCTION

1.1 INTRODUCTION

Over two billion people globally suffer from water scarcity caused by increased demands of water by a rapidly growing population and land use changes (Alcamo et al., 2000; Wada et al., 2010; Gleeson et al., 2016). Coastal aquifers are one of the most important water sources for people living along coastal regions (Ferguson and Gleeson, 2012). Due to over-exploitation of groundwater along the coasts to fulfil the ever growing demands for various water uses, and global warming related sea level rise phenomenon, seawater intrusion into coastal aquifers and associated contamination has been a major cause of concern in recent times (Wada et al., 2010).

Saltwater intrusion is the landward movement of seawater into the coastal aquifer system induced by groundwater development at sea coast. The depletion of groundwater level and contaminated productive wells with less than 1% of seawater are the primary effects of seawater intrusion (Werner et al., 2013). Several factors such as sea level changes, tidal fluctuations, long-term climate impacts, seasonal variations in recharge rates and evaporation, and impact of geological structures on aquifers are responsible for saltwater intrusion into the coastal aquifer system (Barlow, 2013). However, groundwater in coastal regions are often saline due to various other factors, such as past marine transgression (Post and Kooi, 2003; Delsman, 2015), percolation of saline surface water into the aquifer system (Smith and Turner, 2001), infiltration of sea salt driven by cyclonic storms etc. In addition, other processes and factors which are associated with seawater intrusion are dispersive mixing, paleo-hydrogeological conditions, density difference, anthropogenic influences and aquifer hydraulics and transportation characteristics (Custodio, 1987). It has become a great challenge for researchers to identify the primary source of seawater intrusion and evaluate management strategies for sustainable development of groundwater.

.

1.2 SALTWATER INTRUSION

Saltwater intrusion is a widespread environmental problem in most of the coastal regions of the world. Approximately two thirds of the world's population live within 400 km of the ocean shoreline, whereas over a half live within 200 km, which constitute only 10% of the earth's surface (Hinrichsen, 2007). According to Van Weert et al. (2009), globally the ground water basins of West and Central Asia are the largest areas with high groundwater salinity, and contribute 14% of the total groundwater salinity in comparison to the low lands of South America, Europe and eastern Australia, which constitute 6-7% of groundwater salinity (Fig. 1.1).

Saltwater intrusion are reported from different coastal parts of United States for a long time, which was first detected in coastal aquifers of North America as early as 1854 on Long Island, New York (Barlow and Reichard, 2010). The impact of saltwater intrusion on coastal regions of United States, Mexico and Canada was studied by Barlow and Reichard (2010). They interpreted that hydrogeological and geological setting controlled the extent and mode of occurrence of saltwater intrusion. Further, confining conditions and sluggish movement of groundwater caused the presence of saltwater which entered the aquifers of southern Florida during Pleistocene time (Sprinkle, 1989). Anthropogenic stress was also responsible for movement of saltwater into the coastal aquifers. Extraction of groundwater and construction of a dam in the Valley of Hermosillo on the Sonora River in 1940s caused drying up of a river, which reduced recharge to the aquifer system (Steinich et al., 1998), and resulted in saltwater intrusion into the alluvial aquifers (Flores-Márquez et al., 1998; Steinich et al., 1998). Groundwater pumping and land drainage were two major factors for saltwater intrusion in to the coastal regions of North America. In Cape May County, New Jersey, saltwater intrusion was first identified in 1980, where groundwater level went down below the sea level due to over pumping (Lacombe and Carleton, 2002) and led to lateral invasion of saltwater into the confined aquifer of Cape May County affecting more than 100 domestic wells (Barlow, 2013). Vertical migration of saltwater through geological structures such as fractures, joints, folds and faults, contaminated the aquifer systems of Florida, Georgia, Brunswick and Jacksonville (Spechler, 2001). In southeastern Florida, Biscayne an important unconfined aquifer supplied about 35.5 m^3/s water for agricultural activity in different places like Broward, Miami-

Dade, and Palm Beach Counties (Maupin and Barber, 2005). As a result, over drainage of aquifer system induced encroachment of seawater periodically into the groundwater system. Similarly, seawater intrusion in coastal regions of California resulted due to heavy withdrawal of groundwater, in addition to other factors such as, the complex structures, depositional basin, and presence of faults and folds.

Coastal aquifers make up a vital groundwater resources in Australia. An increasing population density and low recharge rate induced seawater intrusion in coastal fringe of Australia (Werner, 2010). Over exploitation of Australian coastal aquifers to meet the water demands for urban, industrial, and agricultural activities (Jacobson and Lau, 1994), led to depletion of groundwater storage and, hence resulted in seawater intrusion. In the lower Burdekin aquifers of Queensland, geological structures and heterogeneous nature of sediments affected the aquifer system and allowed seawater migration (Fass et al., 2007; Werner, 2010).

Different coastal parts in Africa are affected severely by seawater intrusion. The Nile delta of Northern Africa suffers from 60 km inland seawater intrusion due to excessive pumping (Sherif, 1999). Similarly, the aquifers in Cap-Bon and Libya have been facing seawater intrusion since the 1960s. Over pumping of groundwater and severe shortage of water are the main reasons for saltwater intrusion in these coastal regions. However, the higher rate of groundwater extraction compared to groundwater recharge (> 400%) in these regions exacerbate the seawater intrusion (Steyl and Dennis, 2010). Moreover, high rates of urbanization and agricultural activities caused seawater migration into the Libya and Algerian coastal aquifers (Sadeg and Karahanoðlu, 2001; Steyl and Dennis, 2010). In Morocco, saltwater intrusion is observed in fresh aquifer system due to presence of marine deposits, whereas, saltwater has been reported in eastern Africa as a result of over abstraction (95% groundwater is used for domestic and agricultural activities) and tidal effect (Steyl and Dennis, 2010). In drier countries such as, Ethiopia, Eritrea and Somali, seawater intrusion resulted due to over dependence on groundwater for domestic and agriculture purposes (Steyl and Dennis, 2010). In case of Niger delta aquifer system of western Africa, saltwater intrusion has been caused due to lack inland water resources and occurrence of marine sediments (Oteri, 1988; Adepelumi et al., 2009).

The coastal areas of Europe surrounded by the North Sea, the Atlantic Ocean, the Mediterranean Sea and the Baltic Sea, also show effects of groundwater salinity due to seawater intrusion (Custodio, 2010). In fact, Ghyben–Herzberg principle was developed based on the seawater intrusion problem in the northern Germany Baltic shore and the Dutch North Sea coast respectively (Todd, 1959). Multiple eustatic change during Quaternary period is the primary reason of seawater intrusion into the coastal aquifer. In Belgium and northern France, the shallow coastal aquifer consisting of Cenozoic sediments, contain partly fresh water and unflushed saline water driven by seawater transgression events (Custodio, 2010). Along the coastal line of the North Sea and the Baltic Sea, huge amounts of connate saline water trapped in the geological formation are suspected for groundwater salinity (IGRAC, 2009).

Several countries in Asia are affected by seawater intrusion along the coastal tracts. Japan, Taiwan, and Philippines receive severe cyclonic storms and typhoons. These events cause seawater intrusion as the low lying and flat coastal areas are affected by occurrence of floods. Moreover, a large portion of population living in coastal regions depend on groundwater for various purposes, which give rise to seawater intrusion because of over exploitation of groundwater (IGRAC, 2009). In the Western and Southern coasts of China and North and South Korea, intensive extraction of groundwater from shallow aquifers for irrigation purposes led to lateral migration of seawater into the coastal aquifer system. In South Asia, which is considered to be most densely populated area in the world, accounts 24% of world’s population (Mukherjee, 2018) excessive seawater intrusion result due to intensive exploitation of groundwater.

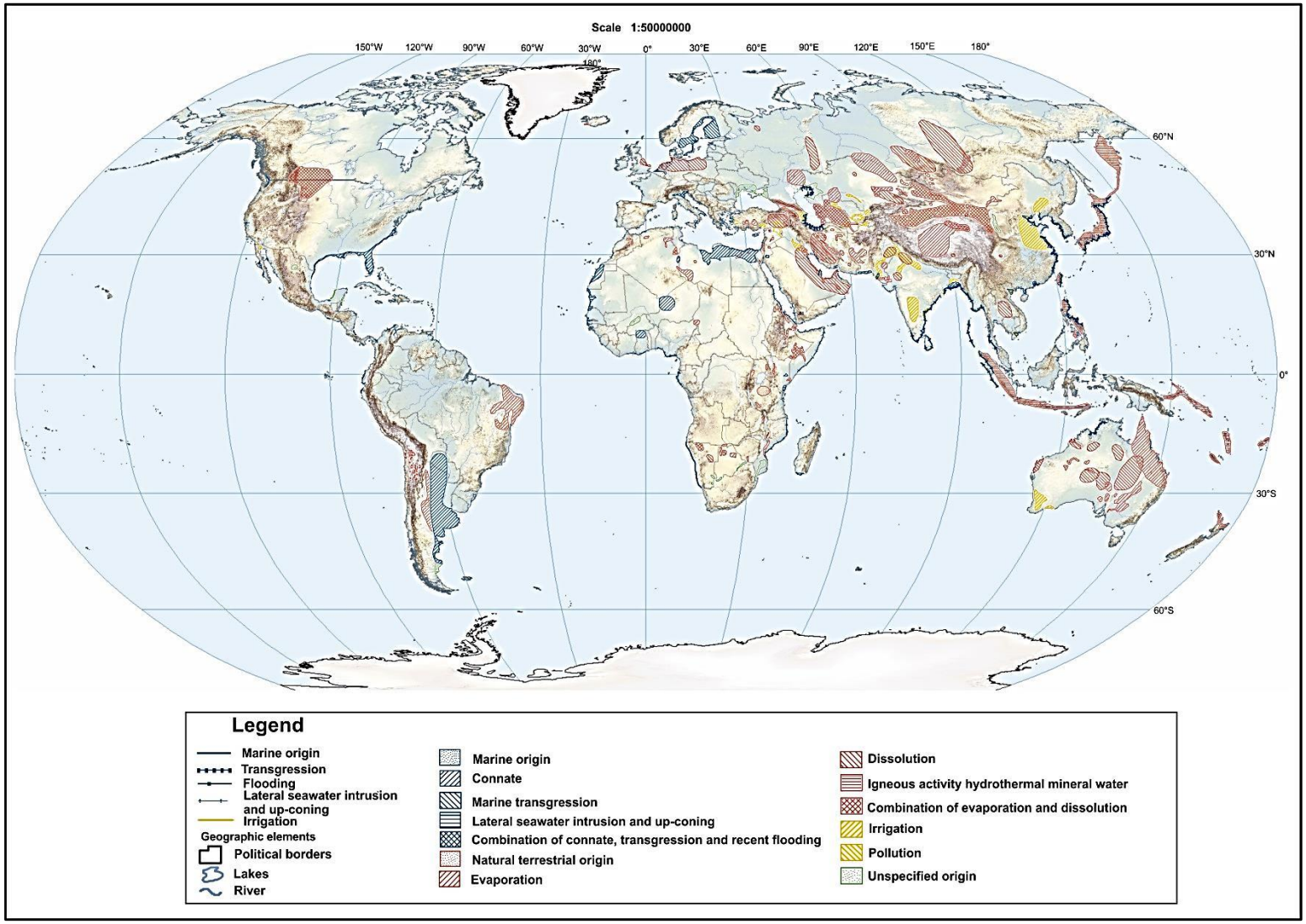

Figure 1.1 *Occurrence and genesis of saline groundwater (modified after, IGRAC Report 2009)*

1.3 SALTWATER INTRUSION IN INDIA

India has a large coast line along the Bay of Bengal and Arabian Sea and along several islands, with approximately 250 million people inhibiting within 50 km coast line (Sudha Rani et al., 2015). In recent years, greater abstraction of groundwater for irrigation and other domestic uses led to seawater intrusion in different regions along the coastal tracts of India. Other factors such as cyclonic storms, tidal effects and sea level rise also induce groundwater salinity in coastal regions.

1.3.1 Eastern Coast

The length of the east coast of India is around 3000 km, stretching from Sunderban in West Bengal to Kanayakumari, Tamil Nadu (CGWB, 2014). The eastern coast comprises four states of Tamil Nadu, Andhra Pradesh, Odisha, and West Bengal, adjoining the Bay of Bengal (Fig. 1.2). Most of the coastal aquifer systems near the Bay of Bengal are affected by seawater intrusion.

The groundwater salinity in coastal regions of Tamil Nadu, a densely populated area, is due to seawater intrusion. One of the saline water bearing aquifer systems of this state is Tiruvadanai aquifer, which is composed of Holocene to recent alluvium sediments (Saravana Kumar et al., 2009). Over a period of two decades, groundwater extraction led to decline of groundwater level and resulted in seawater intrusion into the aquifer system. The aquifer system in Kalpakkam receives seawater from the Edaiyur back-waters during high tide and causes groundwater contamination (Kanagaraj et al., 2018).

The Godavari delta in Andhra Pradesh is affected by saltwater intrusion due to increasing sea level and the growing demand of fresh water for agricultural, industrial, and domestic purposes (Bobba, 2002). Presence of faults and fracture also attribute to seawater intrusion along the coast of Vishakhapatnam (Subba Rao et al., 2005)

The costal tracts of Odisha cover approximately 8575 km^2 in Balasore, Bhadrak, Jajpur, Kendrapara, Jagatsinghpur, and Puri districts (CGWB, 2014). The coastal aquifer systems are composed of alluvial sediments, which also serve as potential aquifers. Due to over exploitation of groundwater for agricultural and

domestic purposes, groundwater level goes down below sea level and results in landward migration of seawater. However, the presence of pockets of saline groundwater derived by historical marine transgression and regression events, natural storms, and sea level changes escalates the groundwater salinity problems in coastal aquifers of Odisha (CGWB, 2014).

Along the coastal region of West Bengal, the growing demand of fresh water due to rapid growth population and urbanization led to seawater intrusion. The groundwater level dropped abruptly and reached to 3-7 meter below normal groundwater level (mbgl) during the last three decades, thus causing ingress of saltwater (CGWB, 2014). Over extraction of groundwater coupled with reduction of groundwater recharge is attributed as the main reason for saltwater intrusion into the coastal aquifer (Biswal et al., 2018).

1.3.2 Western Coast

The west coast of India encompasses four states named as Kerala, Karnataka, Maharashtra, and Gujarat (Fig. 1.2). The length of the Western coastal tract is about 1600 km, which extends from Tapti valley, north of Mumbai, to the southern tip of Kanyakumari (CGWB, 2014). The coastal aquifer system of the west coast faces salinity problem as it submerges within the Arabian Sea.

The Periyar river basin consists of shallow aquifer system of alluvial deposits, which also act as the source of freshwater (CGWB, 2014). The increasing demand of fresh groundwater led to seawater intrusion in shallow coastal aquifers. However, the occurrence of paleo- delta and paleo- beach deposits resulted in groundwater salinity (Kumar et al., 2015).

In the coastal tract of Karnataka, the encroachment of saltwater derived by high tides, cause salinity problems in coastal aquifers. Heavy pumping of groundwater near coast breaks the natural equilibrium condition of fresh - saline water interface and leads to seawater intrusion (Lathashri and Mahesha, 2015).

Along the Konkan coast of Maharashtra, the groundwater in coastal aquifer system is brackish to saline in nature. The tidal backwaters along the rivers recharge the groundwater system and contaminate the groundwater with salinity problem (CGWB, 2014). Along the Gujarat coast, groundwater occurs in the semi

consolidated to unconsolidated sediments of alluvial formation. The coastal aquifers suffer from groundwater salinity problem due to seawater ingress, as a result of intensive groundwater extraction (CGWB, 2014).

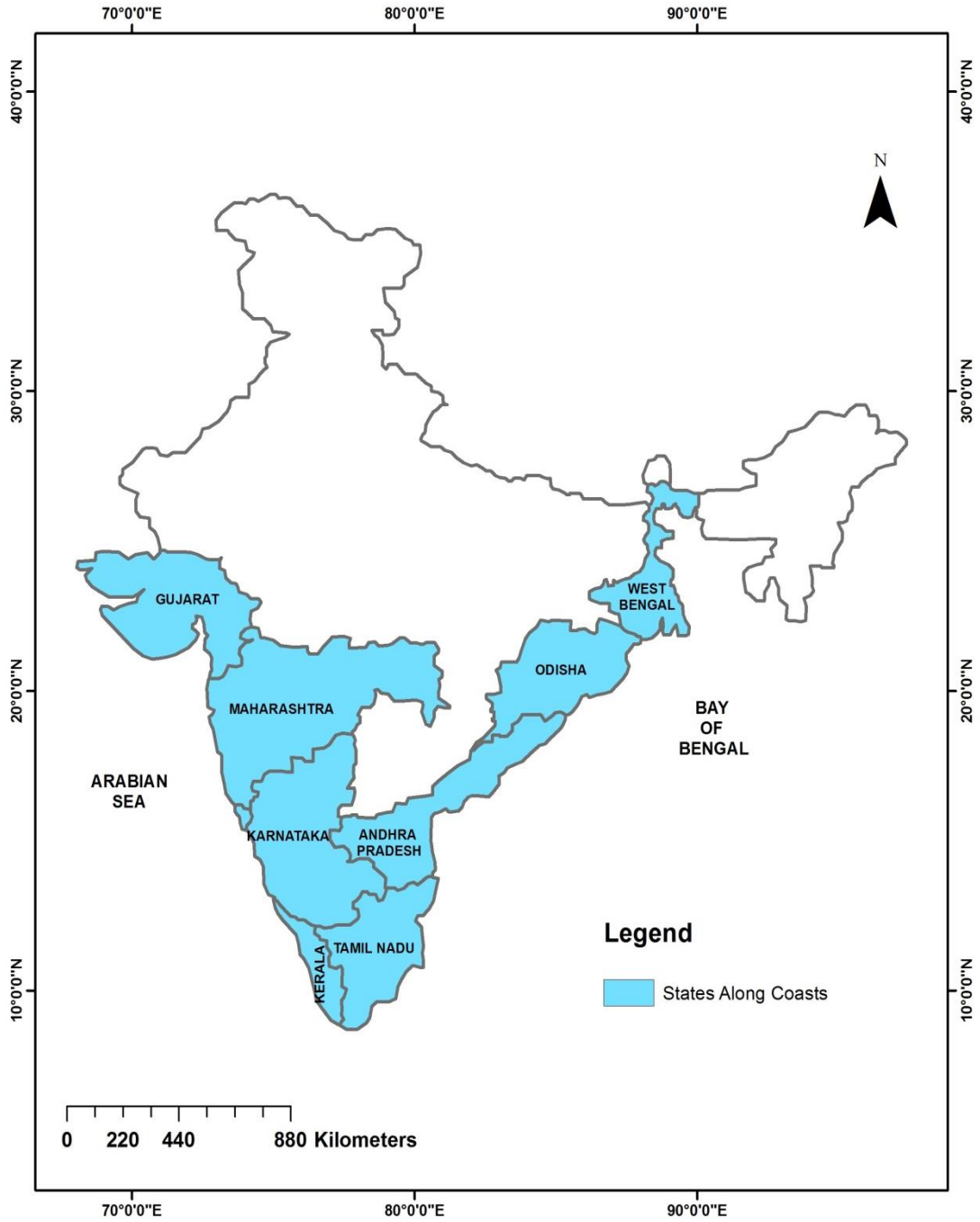

Figure 1.2 *Map of India with different states along the coasts (Modified after, Sudha Rani et al., 2015)*

1.4 WHY PRESENT STUDY?

Agriculture is the main water intensive activity in Jagatsinghpur district in Odisha, where more than 60% area is irrigated land (Planning and Convergence Department, Odisha, 2016). Agriculture/irrigation in the region sustains mainly on the monsoon season. Jagatsinghpur is developing very fast as an industrial hub of Odisha. Heavy withdrawal of groundwater are carried out in this district to fulfill the heavy requirement of water, which causes numerous water related issues such as contamination (salinity) of groundwater and progressive lowering of groundwater levels over the years. The need to solve the problem of the people motivated me to take up the present study on seawater intrusion in the Jagantsinghpur coastal aquifer system of Mahanadi river delta near Bay of Bengal in the Indian sub-continent.

1.5 OBJECTIVES

The major objectives of the present study are mainly outlined as,

(1) Identification of the causes of groundwater salinity in the coastal aquifer system in Jagatsinghpur coastal region.

(2) Estimation of groundwater recharge and factors for seawater intrusion in the Jagatsinghpur coastal aquifer system

1.6 ORGANIZATION OF THE THESIS

The work reported in the thesis has been synthesized and organized into following chapters.

Chapter 1 entitled **“INTRODUCTION”** describes the overall view of saltwater occurrence and factors, and major saltwater intrusion affected regions globally. It also incorporates the literature review, motivation and the major objectives.

Chapter 2 entitled **“LITERATURE REVIEW”** focusses on the research work and ideas of various researchers on hydrogeochemistry and groundwater modeling, which are relevant in studies on coastal aquifer system.

Chapter 3 entitled **“STUDY AREA”** presents the details of Jagtsinghpur coastal region, which include the physiography, geology, hydrogeology and soil types in the region.

Chapter 4 entitled **“METHODOLOGY”** includes methodology adopted for the present study, such as, groundwater sampling, laboratory analysis, collection of various hydrogeological parameters, and development of groundwater model.

Chapter 5 entitled **“RESULTS AND DISCUSSION”** discusses on the groundwater salinity in the Jagatsinghpur coastal region through geochemical evolution of measured chemical parameters. The results and discussion are described with major focuses on hydrogeochemistry and coastal aquifer modeling respectively as per the two major objectives of the work.

Chapter 6 entitled **“CONCLUSIONS”** summarizes the final findings based on the two main objectives set for the present thesis work, and concluded with a future scope of the study.

CHAPTER 2 LITERATURE REVIEW

2.1 HYDROGEOCHEMISTRY

Hydrogeochemical and isotopic studies are diagnostic tools to assess the groundwater quality and to understand hydrological and salinization processes in different coastal aquifer systems. Hence, it was applied globally such as, Zona Citricola (Mexico), Laizhou Bay (China), Fortescue Marsh (Australia), Rhone Delta (France), Buan-gun (Korea), Saturna Island (Canada) and Shean – Harod (Israel) (Rosenthal, 1987; Vengosh, and Rosenthal, 1994; Allen and Suchy, 2001; Lee and Song, 2007; de Montety et al., 2008; Skrzypek et al., 2013; Han et al., 2014; Ledesma-Ruiz et al., 2015). The groundwater salinization in coastal regions can be due to inter-aquifer mixing, pumping of saltwater, rock-groundwater interaction, paleo saltwater and anthropogenic contamination etc. (Han et al., 2014; Liu et al., 2015; Larsen et al., 2017). Groundwater in the Bay of Bengal coastal region of India show high chloride and strontium concentration with an indication of seawater mixing with groundwater (Basu et al., 2001) and groundwater discharge to the sea, which was inferred by studying the presence of nutrients and radon in groundwater (Moore, 2003; Michale et al., 2005; Debnath et al., 2017). This was designated as submarine groundwater discharge as opposite to that of seawater intrusion. Further, Debnath and Mukherjee (2016) estimated around 3.6 m^3 m^{-2} d^{-1} tidally induced groundwater discharge to Bay of Bengal with help of seepage meter. Mukherjee and Fryar (2008) developed a geochemical model with by taking different major cations and anions of deeper aquifers.

In previous studies, combination of ionic ratios, alongwith stable isotopes were used in shallow as well as deeper aquifers to understand seawater intrusion mechanisms (Allen and Suchy, 2001; Ghabayen et al., 2006; Lee and Song, 2007; de Montety et al., 2008; Wang and Jiao, 2012; Gurunadha Rao et al., 2013). The extent of seawater intrsusion process was studied by comparing the ionic ratios of seawater with collected groundwater samples (Rosenthal, 1987; Vengosh, and Rosenthal, 1994). Han et al. (2012) used chlorofluorocarbons (CFCs) and tritium for improved conceptual modelling of groundwater flow in the South Coast Aquifers of Laizhou Bay, China. ^3H and CFCs are crucial aids in estimation of the timing of seawater intrusion and time required for re-equilibration of the

saline/fresh groundwater interface (Abou Zakhem and Hafez, 2007) as they provide age/residence time. Geochemical and isotopic evidence from major ion and isotope composition (^{2}H, ^{18}O, ^{3}H, ^{14}C and ^{34}S) study of groundwater indicates paleo-seawater intrusion into the south coast aquifer of Laizhou Bay (Han et al., 2011). Similarly, stable isotopes of groundwater ($\delta^{18}O$ and $\delta^{2}H$) were used to trace the provenace of water, understand the recharge mechanisms and climate variability (Demlie et al., 2007; Clark and Fritz, 2013; Abu-Khader et al., 2018; Saldi et al., 2018).

Further, groundwater isotopes combined with chemistry is a useful tool for developing a reliable conceptual model of groundwater flow system in multi aquifer systems (Tsujimura et al., 2007; Han et al., 2011; Zhang et al., 2016). The coastal regions of India such as the Brahmani basin, Arani-Koratalaiyar river basin, South Chennai and the Godavari basin characterized by alluvial aquifers and river systems were mainly affected by seawater intrusion, which was explained by studying groundwater and isotope chemistry (Ramakrishnan et al., 2009; Gurunadha Rao et al., 2013; Kumar et al., 2013; Santha Sophiya and Syed, 2013; Soumya et al., 2013; Nair et al., 2015; Das et al., 2016; Raju et al., 2016). Gupta et al. (2005) studied $\delta^{18}O$, $\delta^{2}H$ and d-excess signatures of groundwater across India and suggested that the groundwater recharge was mainly attributed to local precipitation driven by NE and SW monsoon from Bay of Bengal and Arabian Sea respectively. Piper plot of hydrochemical data in coastal aquifer is useful in identifying ion exchange processes within the aquifer system (Appelo and Postma 2005, de Montety et al. 2008, Han et al. 2011, Wang and Jiao 2012) from recharge point to discharge point. Ionic ratios and correlation analysis are used as proxies to delineate the seawater intrusion into fresh aquifer system (Vengosh and Rosenthal 1994, Lee and Song 2007, de Montety et al. 2008, Rao et al. 2013). Iron oxide can be used as a geochemical barrier to prevent seawater by accumulation of certain dissolved chemical species carried by coastal seawater (Charette and Sholkovitz, 2002, Charlet et al. 2005).

2.2 GROUNDWATER MODELING

The landward movement of seawater due to density contrast is saltwater intrusion. It may be caused due to extended (or severe episodic) changes in coastal groundwater due to pumping, changes in land-use patterns, climate

variations or sea-level fluctuations (Adrian et al., 2013). According to Oude Essink, (2001), half of the population of the world resides along the shoreline and they commonly face the problem of saltwater intrusion The problem of saltwater intrusion is of prime concern in the scientific community and has drawn the attention of several researchers globally (Panday et al., 1993, Calvache and Pulido-Bosch, 1994, Stigter et al., 1998, Sherif, 1999, Das and Datta, 2001, Oude Essink, 2001, Post and Kooi, 2003, Arfib and De Marsily, 2004; Demirel, 2004, Bobba and Canada, 2009, Barlow and Reichard, 2010, Mondal et al., 2010, Werner, 2010, Walther et al., 2012, Morgan and Werner, 2014, Zhou et al., 2014, Cary et al., 2015, Sahoo and Jha, 2017, Baena-Ruiz et al., 2018). Mercer et al. (1980) and Essaid (1990) develop a simulation model based on sharp interface approach in which the transition zone is narrow in thickness and areal extent. The density dependent miscibility flow and transport approach models were developed (Huyakorn et al., 1987; Galeati et al., 1992; Das and Datta, 1995, 2000; Putti and Paniconi, 1995) which shows lateral as well as longitudinal extent of the transition zone. Giambastiani et al. (2007) observed that an increase in sea level of 0.9 m would increase the salt flux to bodies of surface water fed by groundwater by 44 % over present day values. Ferguson and Gleeson (2012) looked into the problem of saltwater intrusion in the United States and found that areas with low hydraulic gradient (<0.001) are more prone to seawater intrusion from sea level rise, whereas regions with large population densities are susceptible to seawater intrusion caused by incessant pumping. Various numerical codes are available to simulate density-dependent groundwater flow and solute transport. SEAWAT (Guo et al., 2002; Langevin, 2003) was used for coastal aquifers to predict the position of Freshwater Seawater Interface (Schneider and Kruse, 2006; Masterson and Garabedian, 2007; Lin et al., 2009; Praveena and Aris, 2010; Rozell and Wong, 2010; Sanford and Pope, 2010; Chang et al., 2011; Webb and Howard, 2011). SEAWAT iteratively pairs a variable density from groundwater flow model MODFLOW (McDonald and Harbaugh, 1988; Harbaugh et al., 2000) and the solute transport from MT3DMS (Zheng and Wang, 1999).

Seawater intrusion may be triggered by over-pumping along sensitive regions in the coastal aquifers. This leads to degradation of water quality within the aquifers Ghyben (1888) and Herzberg (1901) developed the first ever model of saltwater intrusion (Todd, 1959). There is a need for appropriate management for

assessing the maximum feasible pumping rates which protects seawater intrusion in coastal aquifers (Singh, 2013). Various groundwater issues such as assessment of fresh groundwater reserves, and prediction of seawater intrusion in response to groundwater exploitation have led to the development of these models (Volker and Rushton, 1982; Custodio and Bruggeman, 1987; Putti and Paniconi, 1995; Bear et al., 1999; Sadeg and Karahanoðlu, 2001). In order to represent the response of coastal aquifer system threatened by saltwater intrusion in Southern Turkey, Hallaji and Yazicigifl (1996) used steady-state and transient finite-element simulation models. Finite-difference methods are used to generate the hydraulic response equations of the groundwater basin for each aquifer, that incorporates different parameters like freshwater and saltwater heads, the location of the interface, and the pumping and recharge schedules (Finney et al., 1992). The problem of saltwater intrusion in the Yun Lin basin, Taiwan was modeled using influence coefficient methods and projected Lagrangian algorithms (Willis and Finney, 1988). Reichard and Johnson, (2005) successfully accessed saltwater intrusion activities in Montebello fore bay and checked the salt water intrusion by adopting artificial recharge in spreading ponds, by imposing restrictions on pumping, installing seawater-barrier injection wells and delivering imported surface water instead of pumping (Reichard and Johnson, 2005). In order to simulate the seawater intrusion in coastal aquifers, Das and Datta (2001) adopted an approach using the density-dependent miscible flow and transport modelling.

As climate change has great effects on ground water recharge, models are developed to use the water intrusion as a proxy to monitor the sea level fluctuation by global climate change. A three-dimensional numerical model of density-dependent groundwater flow coupled with solute transport was developed for the Richibucto region of New Brunswick for the investigation of eustatic changes and climate change (Green and MacQuarrie, 2014), in compliance with the recent refinement to projections of climate change (Intergovernmental Panel on Climate Change, 2007). This led to a boost in the number of studies investigating the effects of climate change on seawater intrusion (Taylor et al., 2013). In order to investigate the influence of deterministic changes in boundary conditions for conceptually simple coastal aquifers , most of the studies encompassed analytical or numerical models (Green and MacQuarrie, 2014). Loáiciga et al. (2012) used a numerical model to quantify seawater intrusion and test the effects of sea-level

rise near Monterey, California and concluded that the major cause driving seawater intrusion in the area was groundwater extraction.

Bobba, (2009) carried out an extensive study near the Godavari Delta in India through numerical simulations and deciphered that the seawater in the surficial aquifer increased substantially by a sea-level rise of 0.5 m. The pre-event salinity can also be a result of remnant salinity partially entrapped within the formations that might have been influenced by earlier tsunamis or cyclonic storms or long-term sea transgressions associated with pre-historic sea-level rises (Riedel et al., 2010; Singh, 2014). The experiences in the field of water management in India have shown that lowering in levels of groundwater, waterlogging and salinity in different parts of the country are the primary repercussions of indiscriminate and injudicious use of water resources. Taylor, (1959) divided various stratigraphic units into eight water provinces, from which five occur in east coast of India and opined that the coastline of Odisha state of India holds a strategic position in studying the phenomena of saltwater intrusion.

Approximately 3 million people in the western part of Odisha are facing acute drinking water crisis owing to large-scale deforestation, unplanned use of irrigation water, and low participation by people in the management of natural resources (Rejani et al., 2008). Moreover, overexploitation of groundwater in certain parts of the densely populated coastal Odisha has resulted in declining groundwater levels and seawater intrusion (Panda et al., 2007). The Kathajodi-Surua Inter-basin within the Mahanadi deltaic system was studied by Mohanty et al. (2012) for in-depth hydrologic and hydrogeologic investigations and explored the possibility of enhanced and sustainable groundwater supply. In order to effectively simulate and study the salinity structure, velocity profile, flow and circulation pattern of the Mahanadi Estuary, a numerical model was developed by Rao et al. (2002). Radhakrishna, (2001) studied the regional subsurface saline/freshwater interface structure through self-potential log analysis and suggested ideas for building up appropriate well fields and for sustainable developmental programs for drinking-water and irrigation systems in the Mahanadi delta region. The ASR-wells (Aquifer Storage and Recovery) (Holländer et al., 2009) may prove handy in such a scenario where they are able to infiltrate water into an aquifer and later extract water as per demands. Most of the coastal basins have become victims to low

groundwater levels and seawater intrusion as in Balasore groundwater basin of Odisha in eastern India (Rejani et al., 2003). A non-linear transient hydraulic management model and a linear optimization model in conjunction with the two-dimensional finite difference flow simulation model was developed for the Balasore groundwater basin (Rejani et al., 2008) to manage groundwater resources in this coastal basin. Another two-dimensional groundwater flow and transport model for the coastal basin was devised by Rejani et al., 2009 for the coastal basin using Visual MODFLOW for simulation of salient pumping strategies under existing agricultural practice. The simulation modeling is also helpful for efficient management of groundwater involving minimization of seawater intrusion and sustainable groundwater utilization on a long-term basis. These numerical models were conducted to study the effect of fresh water discharge from the Mahanadi River on the surge response along the Odisha coast on account of the super cyclone in October 1999, which led to severe flooding of the coastal and delta regions of Odisha (Dube et al., 2000)

CHAPTER 3 STUDY AREA

3.1 INTRODUCTION

Odisha state is situated along the eastern coast of India. The state experiences natural calamities such as flood, drought and cyclone almost every year. Out of 47 years (1961 – 2008), 37 years recorded various natural calamities (Odisha State Disaster Management Authority, 2008). Odisha is an agrarian state where more than 85% of population are dependent on agriculture for their livelihood (Planning and Convergence Department, 2016) . Because of uneven rainfall and its irregular distribution, reliance on groundwater resource usage has gradually been increasing to meet the water demand for agriculture, domestic and industrialization purposes

Jagatsinghpur district, which constitutes a part of the Mahanadi delta, is one such natural disaster prone coastal districts of Odisha. Almost all blocks of Jagatsinghpur coastal district were severely affected by the super cyclone, with wind speed of above 200 km/h on October 29, 1999 (Nayak et al., 2001). Some villages such as, Ersama, Kujang and Balikuda were mostly submerged due to the tidal wave (height > 7m) of Bay of Bengal and this super cyclonic storm brought devastation to human life, livestock, residence and property (Nayak et al., 2001; Chhotray and Few, 2012).

3.2 PHYSIOGRAPHY AND CLIMATE

Jagatsinghpur is one of the six coastal districts characterized by a total geographic area of 1668 km^2 and a population of more than one million (Office of the Registrar General and Census Commissioner, India 2011). The length of coastal line of this region is approximately 50 km along SW-NE direction. Jagatsinghpur coastal area is also a deltaic region bounded by Bay of Bengal along east direction and two rivers i.e. the Mahanadi River is flowing from west to east direction and the Devi River is flowing from north-northwest to south-southeast direction. The region is mainly influenced by tropical monsoon climate with annual average rainfall 1436 mm, and the main source of rain is south-west monsoon (Fig. 3.1). The maximum and minimum temperature in the area is 38 ^{0}C and 12 ^{0}C respectively, mostly characterized by hot and wet summer (monsoon)

(Naik, 2018). Approximately 80% of the total precipitation occurs during kharif season (June to September). The study area is a part of deltaic region, and it consists of thick sediments deposited by the rivers with very gentle land slope towards the Bay of Bengal (Tyagi and Kumar, 2000).

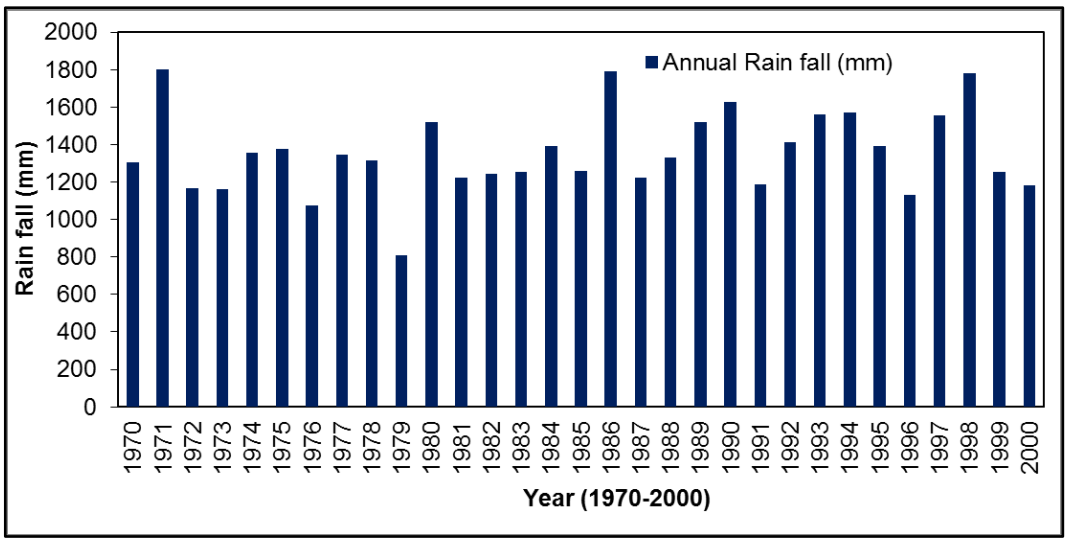

Figure 3.1 *Annual rainfall from1970 to 2000 (Indian Meteorological Department, Bhubaneswar)*

3.3 GEOLOGY AND HYDROGEOLOGY

The Jagatsinghpur deltaic region belongs to the Quaternary Formation, which comprises of recent alluvium sediments of flood plain deposits of the Mahanadi River and the Devi River in upper part of the study area. The deposits majorly consist of gravels, sand (fine to coarse grain), silt and clay (red, yellow and black) (Geological Survey of India (GSI), 2011) and is further classified into two parts (a) Lower delta formation and, (b) Upper delta formation (Fig 3.2). The Lower and Upper delta deposits consist of clay with fine sand and sandy silt, and silty clay respectively (Fig. 3.2), which are of middle to late Holocene age (GSI, 2011). The lower part of the study area lying close to the coast is characterized by low lying wet plains, tidal infected rivers, tidal creeks, swamps, ill drainage of land, non-development of levees (Mahalik et al., 1996; Naik, 2018). However, the natural levees are the only geomorphic features controlled by the Upper delta formation (Naik, 2018). The coastal tract acts as a good zone of groundwater availability, as very thick layer of sediments of varying sizes is present in this part of the study area. The aquifer system of Jagatsinghpur area is divided mainly into

two divisions, (i) shallow aquifer zone < 50 m thickness (ii) deeper aquifer zone 50-300 m thickness below ground level (CGWB, 2013).

3.3.1 Shallow aquifers

The shallow aquifers are to a depth of 50 m from land surface and consist of a mixture of sand and clay with little gravel at places (GSI, 2011) (Fig. 3.3). The thickness of the saturated sediments varies from 10 to 35 m (CGWB, 2013). Ground water in these aquifers usually occurs under water table condition. Dug wells and shallow tube wells are used to extract ground water from the aquifer. The dug wells are of very shallow depth and are recharged mainly from the local precipitation. Overall, both the zones supply water for irrigation. There are many shallow tube wells for domestic use in the area particularly in the eastern part by tapping 3 to 6 m zone within 30 to 50 m depth (CGWB, 2013). The hydraulic conductivity for unconfined aquifer varies from 8 m/day to 57 m/day in Mahanadi deltaic region (Sahoo and Jha, 2017).

3.3.2 Deeper aquifers

The depth of the deeper aquifer ranges from 50 to 300 m below ground level (bgl) (Fig. 3.3). In the major part of the study area, the depth of the borehole is confined to 300 m (CGWB, 2013). The boreholes show considerable variation in granularity and thickness. There is a sequence of alternating clayey and sandy layer with occasional presence of thin arenaceous materials (Mahalik, 2000). Adequate amount of fresh groundwater of varying thickness occurs at different depths. As the alluvial deposit is a good repository of ground water, it is exploited by installation of deep tube wells across the study area.

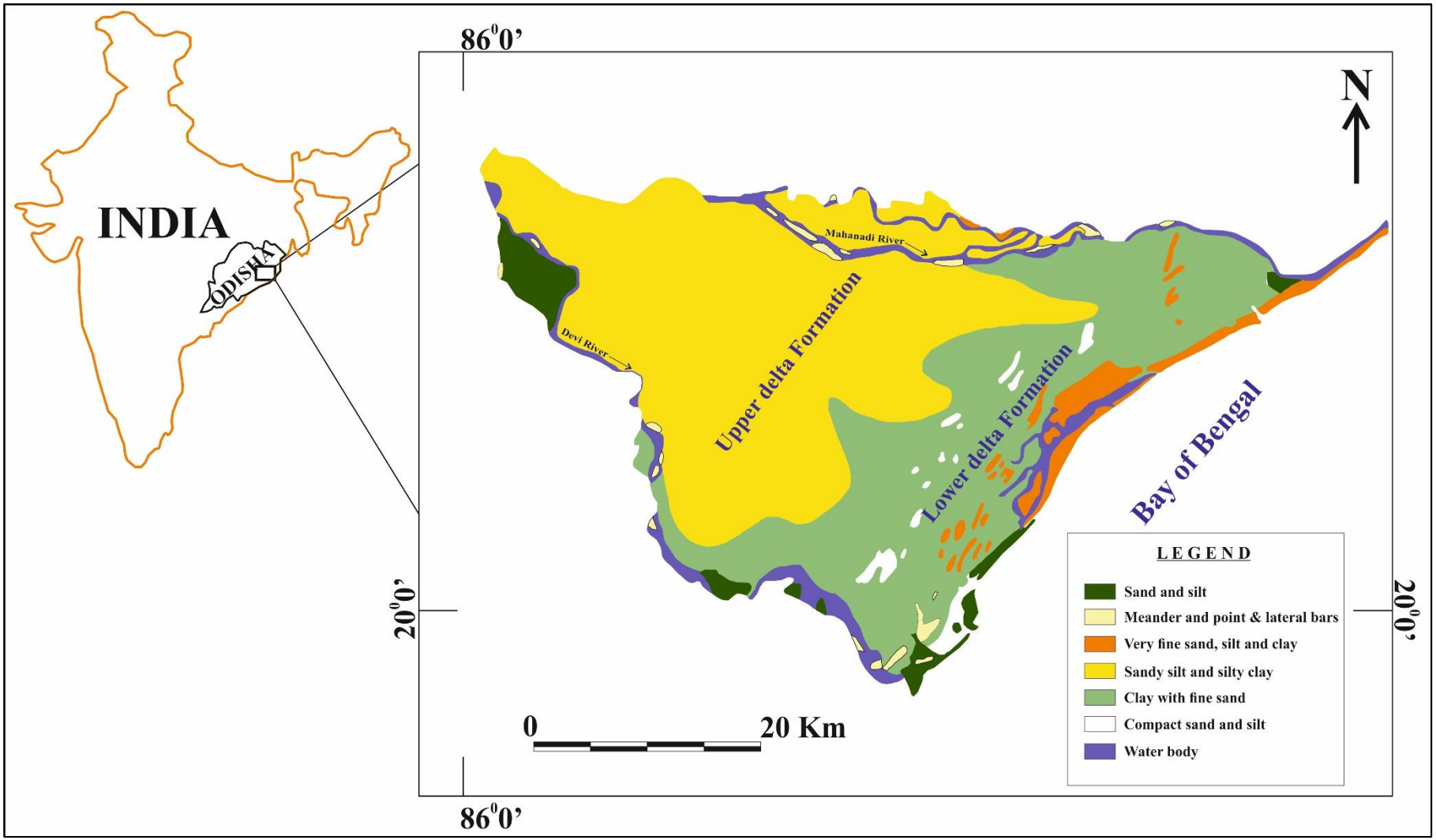

Figure 3.2 *Geological (the Upper delta formation and the Lower delta formation of the Mahanadi deltaic region) and hydrogeological (sand, silt, and clay) map of the study area (modified after, Geological Survey of India, 2011)*

Table 3.1 Hydrogeological parameters from different locations (CGWB, 2013)

Sl. No.	Location	Type	Depth (m) bgl	Depth of T/W	Hydro-chemical profile	Zone Tapped (m)bgl	Swl (m) bgl.	Yield (lps)	Drawdown (m)	T (m^2/day)	S
1.	Kujang	OW	374.08	142	0-340 F to B	98-140	-	-	-	-	-
2.	Balikuda	EW	299.50	80.0	0-85 F 85-299 S	48-62	2.15	38	4.77	5082	-
3.	Borikina	EW	367.68	-	0-80 F 80-190 S 190-209 B to S 209-254 S 254-325 B toF	-	-	-	-	-	-
4.	Machagon	EW	612.14	98.76	0-100 F 98-492 S	31-51, 80-97	1.55	56	3.93	9360	-
5.	Ersama	EW	609.62	291	0-137 B 137-312 F 312-600 S	184-189 203-208 226-232 257-267 279-289	0.676 (agl)	56	13.02	388	$2.5x10^4$
6.	Jagatsinghpur	OW	74.60	70.0	0-74.6F	50-68	-				
7.	Paradeep	EW	430.76	290.0	0-18 No data 18-23 S 230-260 B 260-288 288-320 B+F 320-392 S	273-288	-				
8.	Sahara	EW	303.0	127	0-303 F to B	18-25 76-93 115-125	0.10	69	4.08	2110	

Note: OW=Observation well, **EW** = Exploratory well, **bgl**=below ground level **agl** = above ground level, **SWL**=Static water level, **T/W** = Tube well, **T**= Transmissivity (m2/day), **S**= Storage co-efficient, **F**= Fresh water, **B**= Brackish water, **S**= saline water

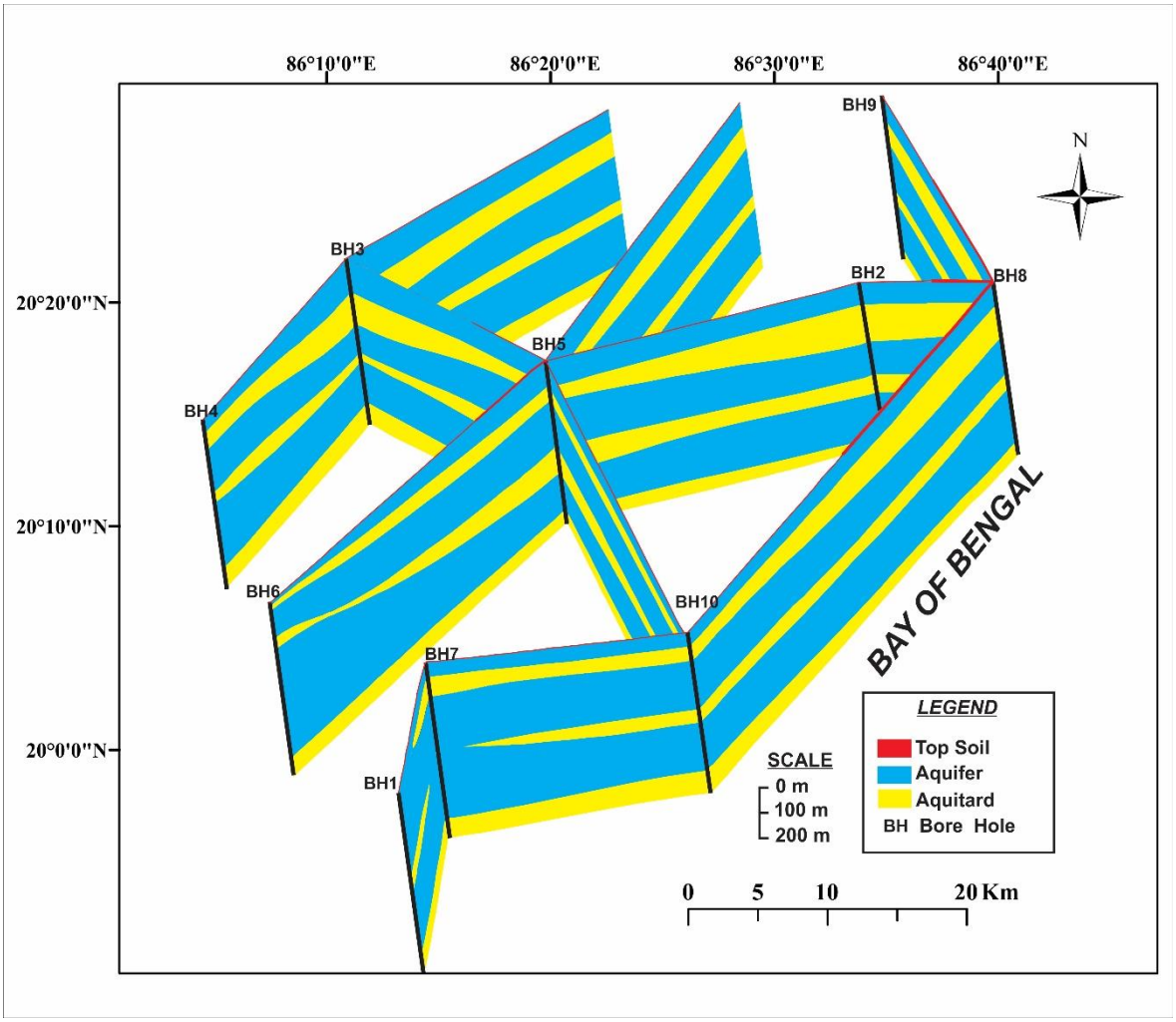

Figure 3.3 *Fence diagram with alternate layers of aquifer and aquitards (Data Source CGWB 2013)*

3.4 SOIL TEXTURE TYPE

The distribution and types of different soils in the study area depend on the physiographic and lithologic variations. Based on texture, the soils have been classified as coarse grained, medium grained and fine grained (Fig. 3.4).

The study area consists of approximately 90% fine to coarse textured soil, which include deltaic alluvial soils. The deltaic soils are chemically deficient in phosphate (P_2O_5) and nitrogen (N) (CGWB, 2013). In the north eastern and south eastern part of the study area, very small amount of medium textured soil of alkaline nature are observed to occur

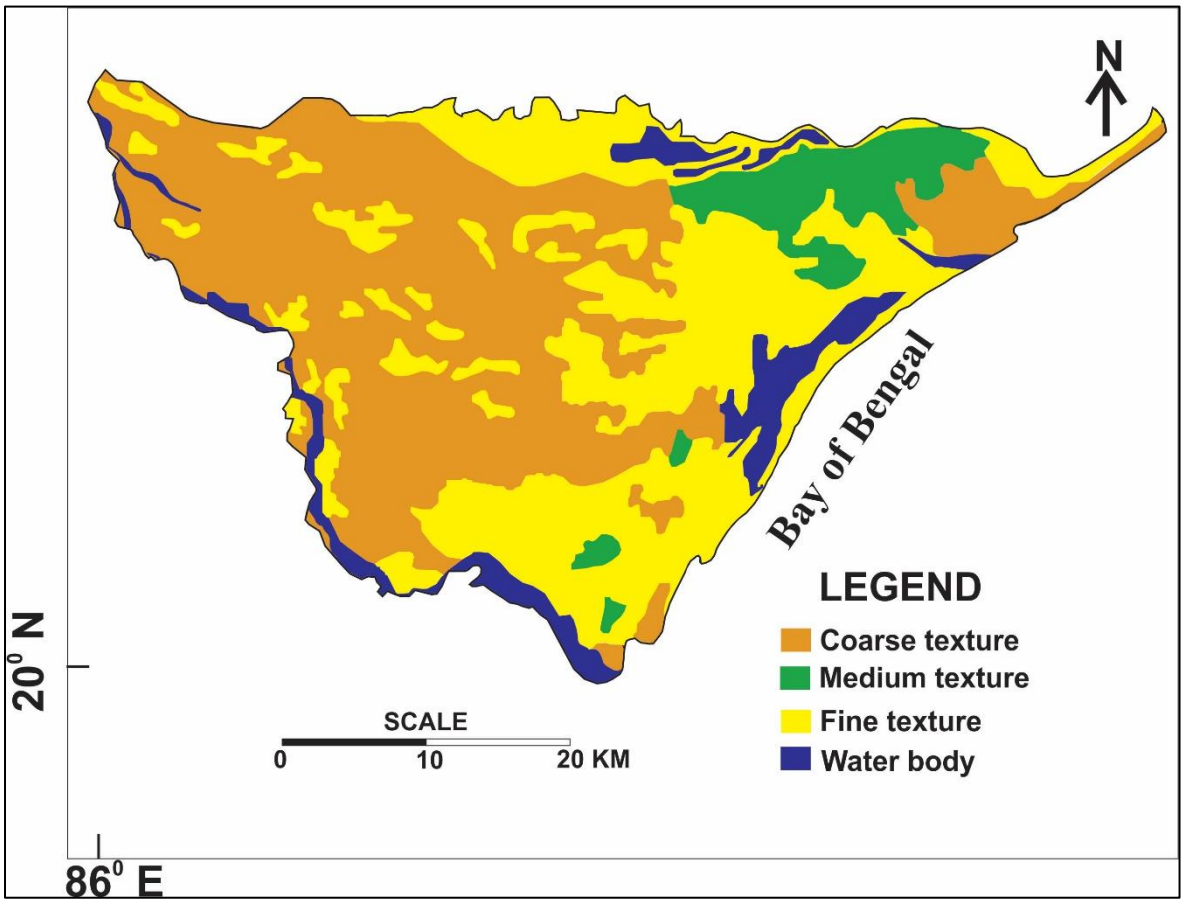

Figure 3.4 *Map showing different types of soil textures (National Remote Sensing Centre, India)*

3.5 LAND USE AND LAND COVER

Land use and land cover map reveals that more than 90% of the study area is crop land (Fig. 3.5). The villagers of this rural area depend on agricultural activity for their livelihoods. The study area is surrounded by two rivers, which act as sources of water along with groundwater. It also includes beach dune, beach and beach plains which are suitable for human settlement because of availability of fresh water at a shallower depth (Naik, 2018). Along the NE direction, the land use pattern suggests that urbanization due to Paradeep port is increasing.

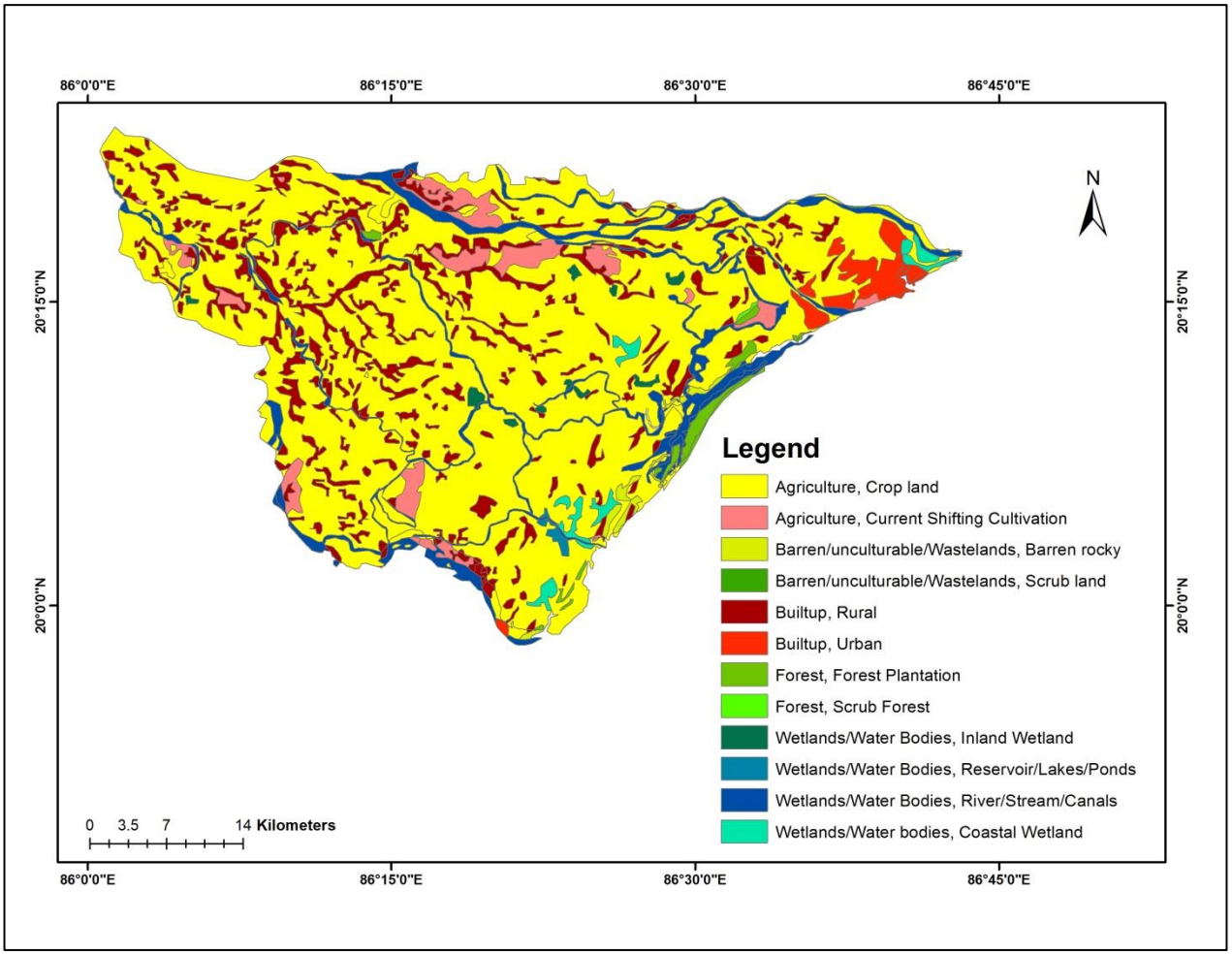

Figure 3.5 *Land use and land cover map (2005-2006) (Bhuvan thematic layers, NRSC, India)*

4.1 INTRODUCTION

To achieve the two major objectives of the present study, the methodology followed is shown in Fig. 4.1. It included field work, in which groundwater sampling, analysis and collection of data were carried out. A conceptual model was prepared based on lithological data and other relevant data. The process of saltwater intrusion in the coastal aquifer was assessed by development of a numerical model using visual MODFLOW.

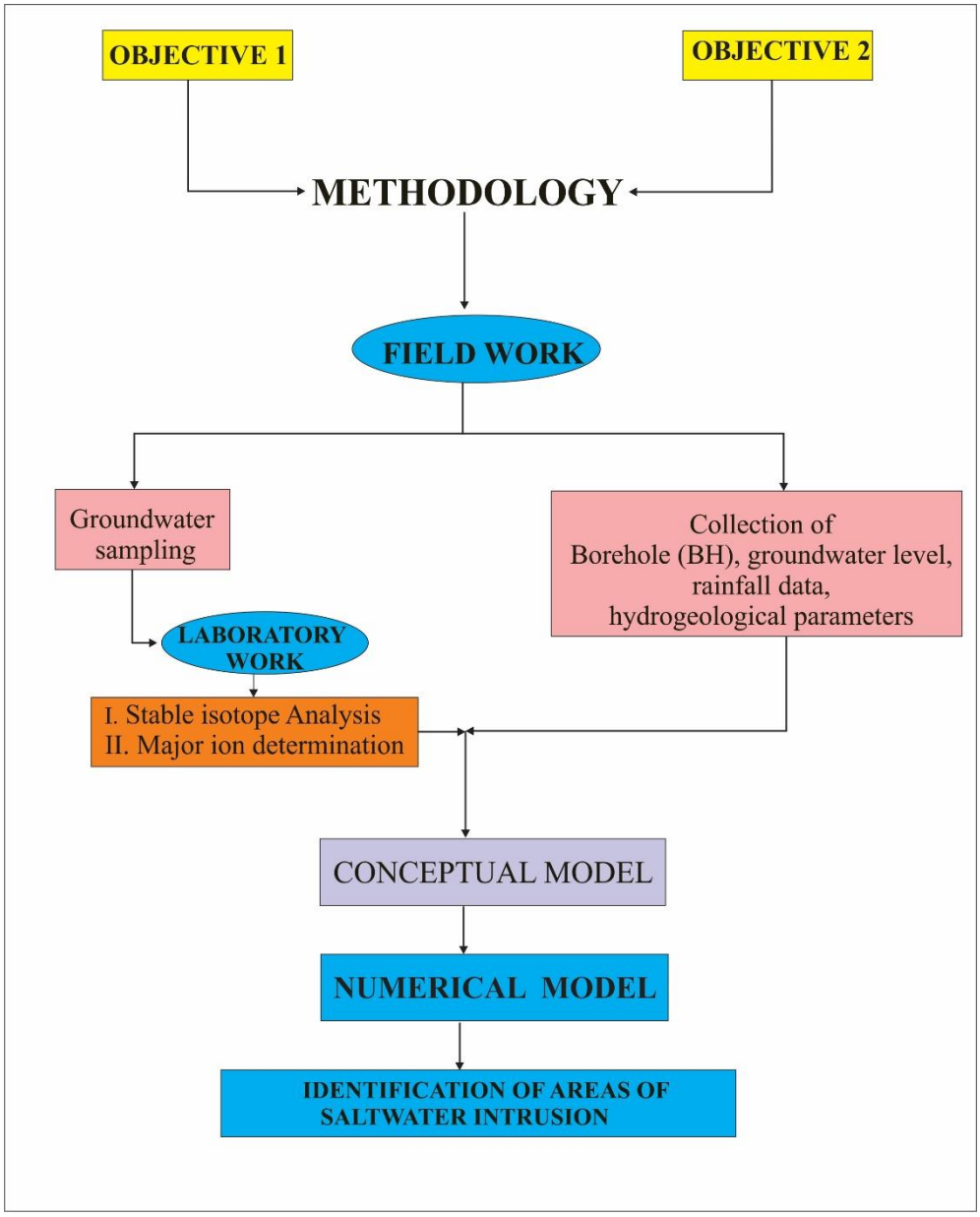

Figure 4.1 *A Flow chart of methodology for the present study*

4.2 FIELD STUDY

Groundwater samples from selected dug wells and hand pumps were collected (Fig. 4.2). The sample stations A1, A2, A3, A4, A5 (A), A5 (B), A6, A8, A11, A12, A14, A15, A17, A18, A20, A21 and A28 are located in the Lower region of the delta and the remaining sites are located in the Upper region of the Mahanadi delta.

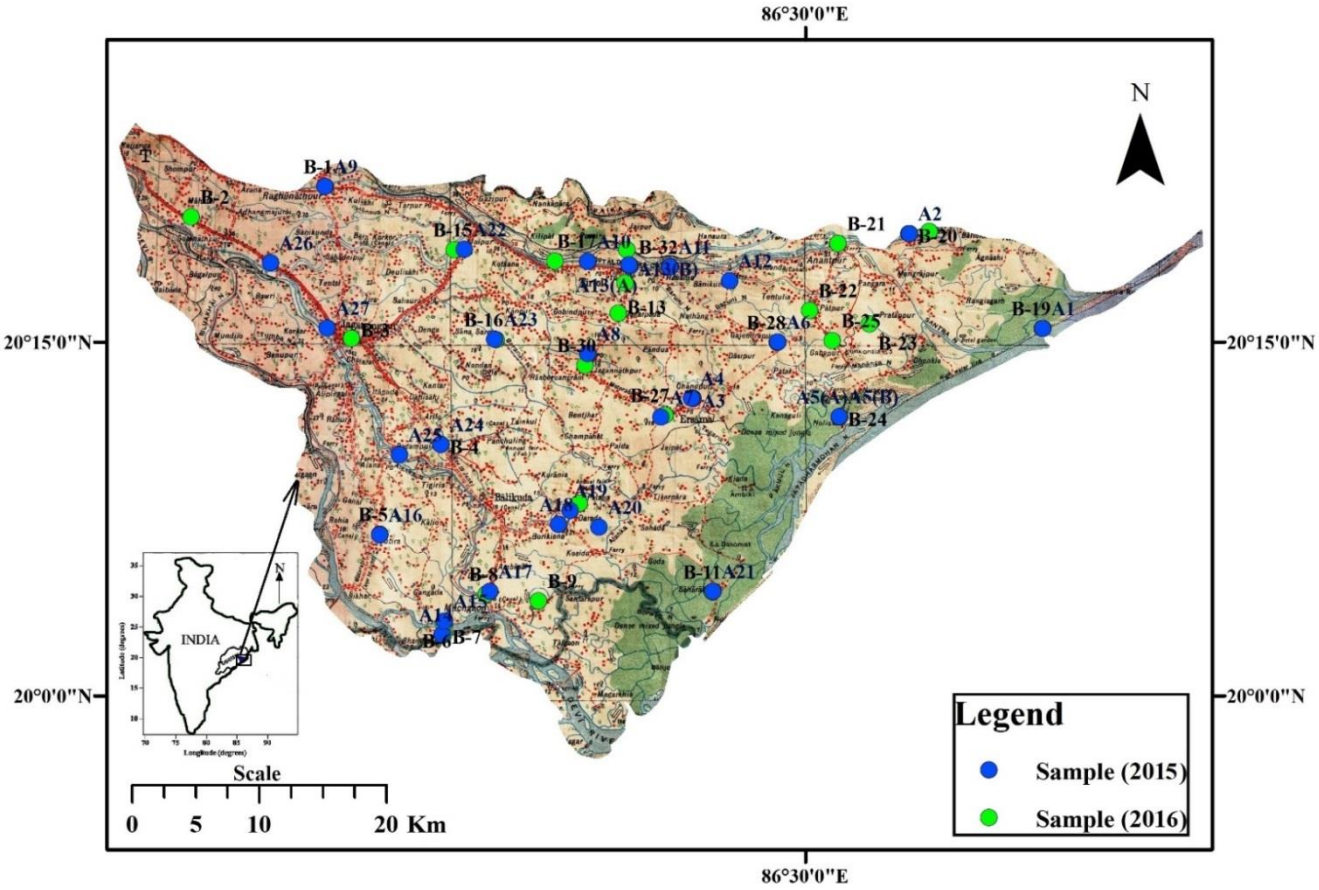

Figure 4.2 *Sampling locations for different periods during 2015 (post-monsoon) and 2016 (pre-monsoon)*

In situ measurements of on-field parameters such as pH, Temperature (℃) and Electrical Conductivity (EC in µS/cm) were carried out with the help of HACH HQ40d portable meter. The groundwater samples were collected in 500 ml laboratory pre-cleaned polyethylene bottles and filtered in field by using 0.45 µm filter papers for major cations and anions analysis.

Figure 4.3 *Field photographs showing a) collection of surface water sample, b) collection of groundwater sample from hand pump c) measuring of field parameters d) metal buckets show reddish brown stains due to excess iron content.*

4.3 WATER ANALYSIS

For major cations (Ca^{2+}, Mg^{2+}, Na^{+} and K^{+}) analysis the water samples were preserved in laboratory pre cleaned mild acid washed polyethylene bottles and the samples after in situ measurements were acidified to pH ~ 2 with ultrapure 6 N HNO_3. Alkalinity of samples was measured in field by titration (gran plot) using H_2SO_4 (0.22 N) during sampling. These water samples were preserved at 4 ℃ in a refrigerator until analysis. The concentration of ions was determined by using Ion Chromatograph model Dionex ICS – 5000+ at the Nuclear Hydrology Laboratory of National Institute of Hydrology (NIH), Roorkee, India. In this laboratory, anions and cations were measured using an ion chromatograph (IC) (Dionex ICS-5000) with AS11-HC and CS-16 columns respectively. Errors in mass-charge balance of groundwater samples were observed to be < 5% except in two groundwater samples with mass-charge imbalance of 5-6%

For isotopic analyses, the samples were stored in 10 ml polyethylene bottles, which were sealed air-tight. The stable isotopic analysis of collected samples was carried out at the Nuclear Hydrology Laboratory of National Institute of Hydrology (NIH), Roorkee. Dual inlet isotope ratio mass spectrometer (DIIRMS) was used to measure $\delta^{2}H$, whereas continuous flow isotope ratio mass spectrometer (CFIRMS) was used to measure $\delta^{18}O$. The water samples were equilibrated with CO_2 and H_2 to measure $\delta^{18}O$ and $\delta^{2}H$ values respectively by using the standard technique (Epstein and Mayeda, 1953). The system was calibrated to determine the $\delta^{18}O$ and $\delta^{2}H$ composition by IAEA standards Vienna standard mean ocean water (VSMOW), Greenland ice sheet precipitation (GISP) and standard light Arctic precipitation (SLAP) (Sengupta and Sarkar, 2006; Rai et al., 2014) having precision ± 1.0 ‰ and ±0.1 ‰ for $\delta^{2}H$ and $\delta^{18}O$ respectively.

4.4 CALCULATION OF SATURATION INDEX (SI)

PHREEQC Version 3 (Parkhurst and Appelo, 2013) has been used to calculate the saturation index of carbonate minerals. In carbonate minerals calcite, dolomite and gypsum have been taken into account as different phases for seawater intrusion study (Han et al., 2011). Minimal reaction-path can be developed using PHREEQC for pairs of wells located along regional groundwater flow direction with pumping at quasi-current rates (Mukherjee et al., 2007).

4.5 DEVELOPMENT OF MODEL

4.5.1 Conceptual model

A conceptual model (Fig. 4.4) consisting of shallow top aquifer was developed for the groundwater flow system of Jagatsinghpur based on lithological data, boundary conditions and groundwater level data. As the main aim of the present study was to analyze saltwater intrusion through quantification of net recharge in the top unconfined coastal aquifer due to rainfall, river seepage and irrigation return flow, only a single unconfined aquifer was considered up to a depth of 50 m. After preparing a conceptual model, it was translated into a numerical model with the help of Visual MODFLOW software package

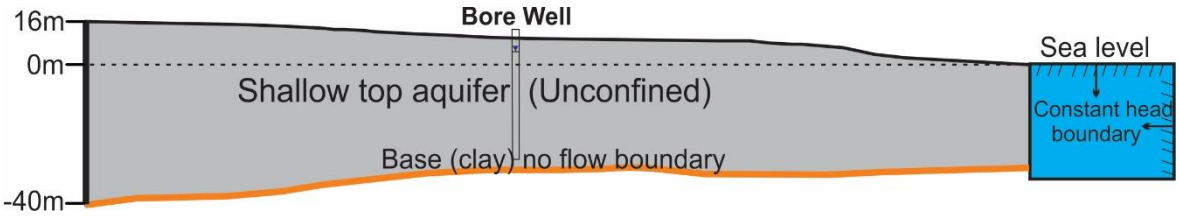

Figure 4.4 *Conceptual model consisting of single layer*

4.5.2 Numerical model

The groundwater flow simulation was carried out by Visual MODFLOW, which integrates the modular three dimensional finite difference groundwater flow code (McDonald and Harbaugh, 1988). Several numerical codes have been used to simulate groundwater flow both in local and regional groundwater system (Yidana and Chegbeleh, 2013). The groundwater flow equation (Eq.4.1) is used in MODFLOW to understand the groundwater flow in three different directions (Anderson and Woessner, 1992)

$$\frac{\partial}{\partial x}\left(K_x \frac{\partial h}{\partial x}\right) + \frac{\partial}{\partial y}\left(K_y \frac{\partial h}{\partial y}\right) + \frac{\partial}{\partial z}\left(K_z \frac{\partial h}{\partial z}\right) = S_s \frac{\partial h}{\partial t} - R \qquad (4.1)$$

Where K_x, K_y and K_z are hydraulic conductivity in three different directions; S_s, h and R represents specific storage, hydraulic head and sink or source respectively. Hydraulic head value does not change with time period under steady state condition. This condition expresses as (Eq. 4.2).

$$K_x \frac{\partial^2 h}{\partial x^2} + K_y \frac{\partial^2 h}{\partial y^2} + K_z \frac{\partial^2 h}{\partial z^2} = 0 \qquad (4.2)$$

Visual MODFLOW has a number of solvers such as Preconditioned Conjugate Gradient (PCG), Strongly Implicit Procedure package (SIP), Slice Successive Over Relaxation package (SOR), WHS solver for Visual MODFLOW package (WHS) and Geometric Multigrid solver (GMG) for numerical equation for groundwater flow simulation purposes. In the present study, WHS solver package with Bi-Conjugate Gradient Stabilized (Bi-CGSTAB) accelerator was used to solve the partial differentiation equations through iterative procedures.

4.5.3 Model discretization

The model study area was divided into 9394 cells with 77 rows (I=77) and 122 columns (J=122) and each cell consisted of 600 m × 600 m square blocks (Fig. 4.5). The modeled layer thickness varied approximately from 30 m to 50 m in the study area. The study area consists of 4632 active and 4762 inactive cells as shown in Table 4.1. The layer elevation and ground elevation data was imported to Visual MODFLOW through ASCII file.

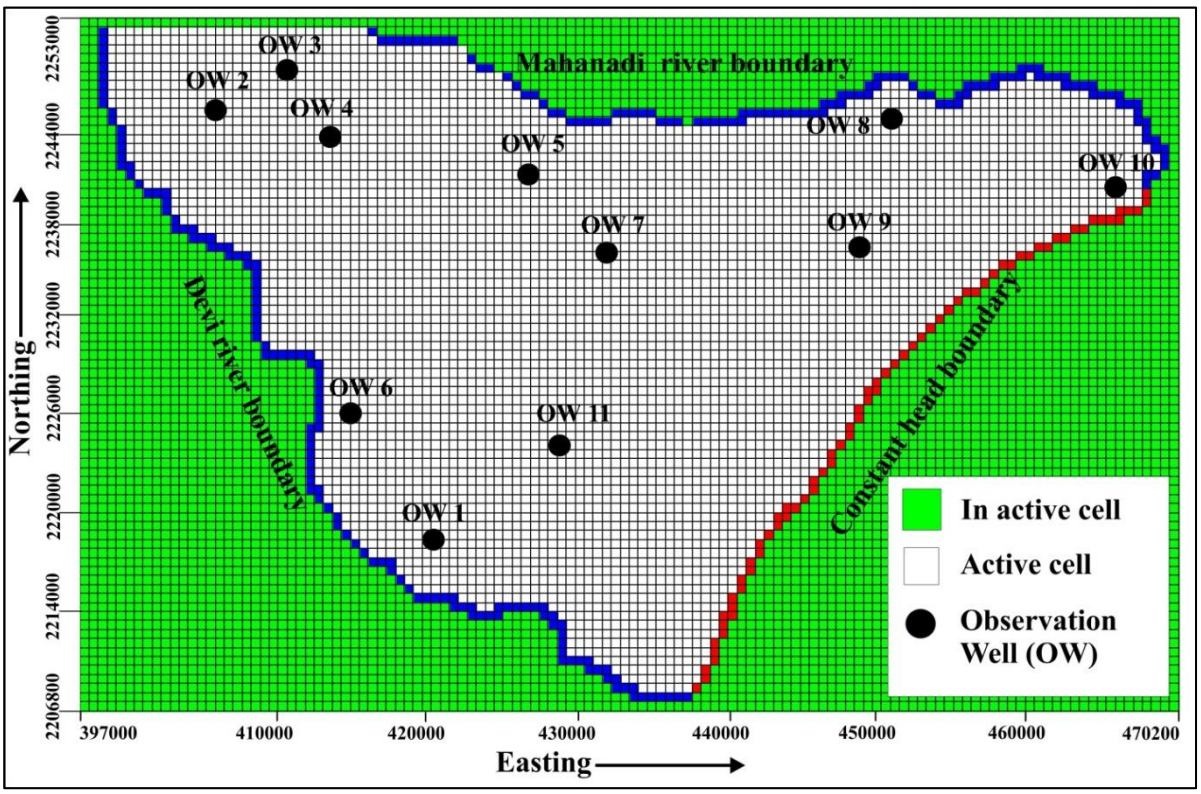

Figure 4.5 *Map with grid cells, observation wells and boundary condition*

Table 4.1 Model input parameters

Sl. No.	Parameters	Inputs
1.	Cell	
1.1	Active	4632 White Cells- (600 m X 600 m)
1.2	Inactive	4762 Green Cells- (600 m X 600 m)
2.	Model Boundaries	
2.1	Rivers (RIV)	Mahanadi River (W to E) Devi River (NNW to SSW)
2.2	Constant Head	Head = 0 m (Bay of Bengal - SW to NE)
2.3	Recharge	Variable
2.4	Evapotranspiration	Rate = 1400 mm/ year Extinction Depth= 3.0 m
3.	Layer	
3.1	Layer No.	1
3.2	Layer Type	Unconfined
4.	Aquifer Parameters	
4.1	Hydraulic Conductivity (K)	Kx=Ky= 40 to 45 m/d Kz=4 to 4.5 m/d
	Specific Yield (Sy)	5% to 7%
5	Wells	
5.1	Observation Wells	11 nos.
	Hydraulic Head	0.7-15 m
6.	Aquifer Stresses	Data for individual pumping wells not available, the same has been included in net recharge
7.	Simulation Period	
7.1	Steady State	1st Jan'04 (1day)
7.2	Transient State	2004 to 2009

4.5.4 Initial heads

Hydraulic head data of 11 different observation wells were collected from Central Ground Water Board (CGWB). The hydraulic head varied from 0.7 m near the sea coast to 15 m away from the shore line. For groundwater flow simulation, 1st day January 2004 was taken as initial time period and four different time periods of head data (from year 2004 to 2009) were used for both calibration and validation of the model (Annexure I). The head data was categorized as post-monsoon (Rabi) for January, pre-monsoon for April, monsoon for August and post-monsoon (Kharif) for November.

4.5.5 Boundary conditions

The Visual MODFLOW simulates the groundwater flow followed by different types of boundary conditions. In Jagatsinghpur coastal aquifer system, two types of boundaries were used (Fig. 4.6). Along the eastern side of the study area, Bay of Bengal was considered as constant head boundary or Dirichlet boundary (Datta et al., 2009). Two large perennial rivers i.e. the Mahanadi River and its distributary the Devi River flowing along the two sides of the study area was considered as Cauchy boundary or head dependent flux boundary. The river conductance value were determined from (Eq. 4.3) (Rejani et al., 2008).

$$C_{RIVER}=\frac{K_r \times L \times W_r}{B} \qquad (4.3)$$

where K_r= hydraulic conductivity of the river bed (m/day), L= length of the reach/grid size (m) W_r= width of the river (m) and B=thickness of the river bed (m). The river bed conductance of two rivers were i.e. 30,000 to 35,000 m^2/day (CGWB, 2013).

4.5.6 Hydrogeological parameters

The model domain was classified into 3 hydraulic and specific yield zones for the single unconfined aquifer system, which belongs to the alluvial formation of the Mahanadi delta (Fig 4.6). The horizontal hydraulic conductivity (K_h) of ZONE I, ZONE II and ZONE III were taken different because of geomorphic and lithological variations within the study area.

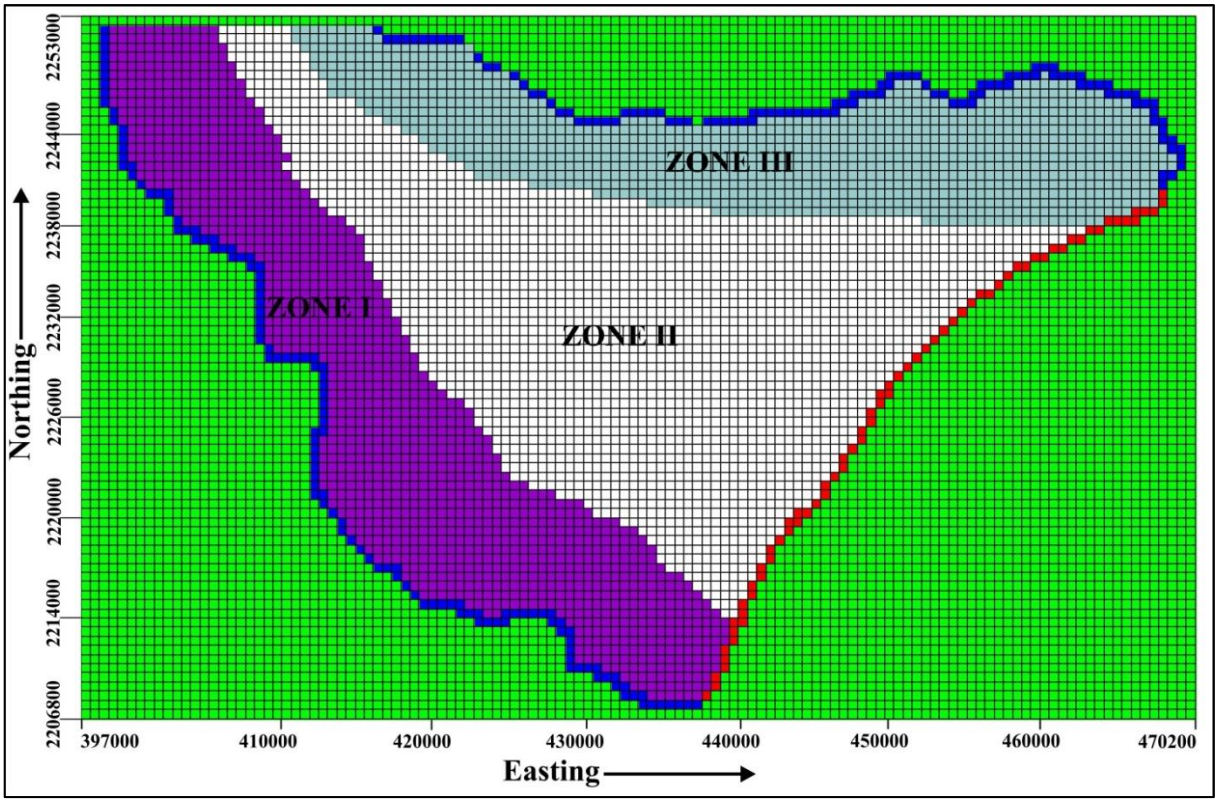

Figure 4.6 *Map showing three different zones of hydraulic conductivity and specific yield*

As the water table was very close to the ground surface, large amount of groundwater may be lost through evapotranspiration process. Hence, the evapotranspiration data was taken into consideration for groundwater simulation model. Further, the study area was divided into 11 different recharge zones in the form of Thiesen polygons (Yidana and Chegbeleh, 2013) in which monthly recharge were assigned (Fig. 4.7). In groundwater simulation model, the recharge was manually optimized to minimize the head difference between observed head and calculated head (Datta et al., 2009).

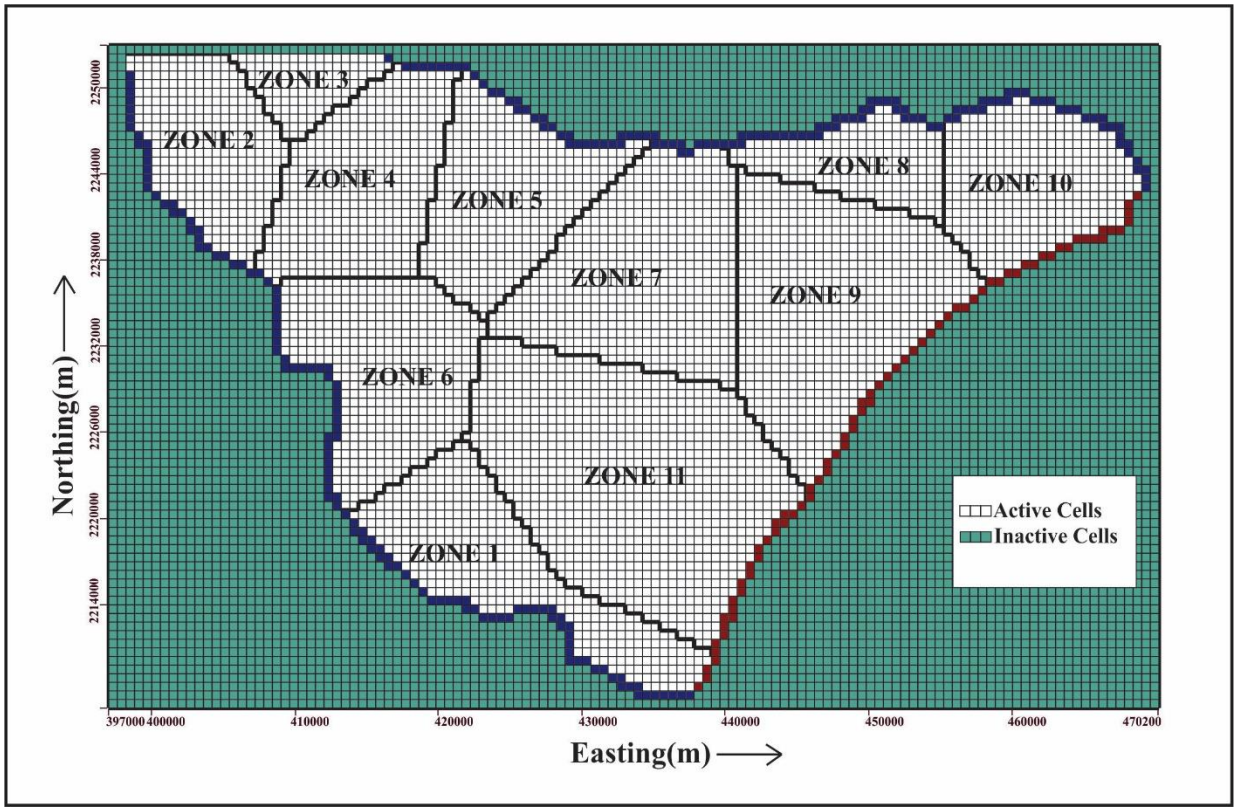

Figure 4.7 *Different recharge zones with different recharge values based on rainfall*

CHAPTER 5 RESULTS AND DISCUSSION

5.1 HYDROGEOCHEMISTRY

5.1.1 Chemical composition

The hydrochemical analysis of groundwater samples in the study area showed a wide range of variation (Table 5.1). The electrical conductivity (EC) varied from 146 µS/cm in NW to 33900 µS/cm in SE part in the Mahanadi deltaic region. The highest EC value was recorded in groundwater sample (A5 (B)) near to the coast of Bay of Bengal (Fig. 5.1), indicating the mixture of fresh groundwater and saline water, whereas low EC values were observed in many groundwater samples located away from the sea coast. The pH ranged from 6.7 to 7.0 and the average groundwater temperature was 19.8^0 C

The maximum concentration of sodium (286.45 meq/l), calcium (67.79 meq/l), magnesium (117.50 meq/l), potassium (18.33 meq/l), chloride (404.50 meq/l) and sulphate (32.86 meq/l) were observed in A5 (B) sample, which is presumably affected by seawater intrusion as it is located very close to Bay of Bengal. Similarly, the low concentration of sodium (0.47 meq/l), calcium (0.34 meq/l), magnesium (0.13 meq/l), potassium (0.03 meq/l), chloride (0.12 meq/l) and sulphate (0.01 meq/l) was observed in different wells located far away from the sea coast

The pie diagrams of ions in groundwater is shown in Fig. 5.1. The groundwater samples (A9, A22, A26 and A27) show higher percentage of Ca^{2+} (24 - 29%) compared to Na^{+} (10 - 16%) among cations; whereas among anions, the percentage of HCO^{-}_{3} (31 - 43%) far dominates Cl^{-} (4 - 16%).

Table 5.1 Chemical composition of groundwater

Sample ID	Type of well*	EC (µS/c)	pH	Cl^- (meq/l)	HCO_3^- (meq/l)	NO_3^- (meq/l)	SO_4^{2-} (meq/)	Ca^{2+} (meq/l)	Mg^{2+} (meq/l)	Na^+ (meq/l)	K^+ (meq/l)	NICB in %	$\delta^{18}O$ (‰)	δ^2H (‰)
A 1	SW	447	7.55	0.53	3.96	0.11	0.44	1.85	1.80	1.71	0.24	5.3	-6.87	-45.42
A 2	DW	1475	7.35	5.09	10.30	0.22	ND	1.66	5.26	9.09	0.68	-3.3	-3.65	-27.17
A 3	DW	3300	7.16	35.57	2.00	ND	1.68	10.97	8.24	16.23	0.29	4.7	-3.05	-20.29
A 4	DW	3500	6.9	40.06	2.50	ND	1.52	12.00	13.33	18.78	0.26	-0.3	--	--
A 5 (A)	SW	291	7.37	0.58	2.90	ND	0.07	1.41	1.17	0.76	0.11	1.4	-5.88	- 41.03
A 5 (B)	DW	33900	6.79	404.50	2.38	ND	32.86	67.79	117.50	286.5	18.33	-5.4	-1.86	-10.79
A 6	DW	7880	7.07	82.80	2.00	ND	3.52	17.23	19.33	52.17	0.93	-0.8	-2.65	-15.06
A 8	DW	3010	7.23	29.29	8.20	ND	0.26	3.06	3.99	30.76	0.56	-0.8	-3.95	-26.65
A 9	DW	180	7.28	0.36	1.90	ND	0.01	1.08	0.54	0.61	0.08	-0.9	-3.50	-26.34
A 10	DW	451	7.55	0.81	4.20	ND	0.40	0.34	0.13	5.42	0.07	-4.8	-4.00	-31.22
A 11	SW	5010	7.55	49.29	10.10	ND	5.79	1.02	4.57	54.34	0.84	3.5	-3.86	-24.27
A 12	DW	9340	7.03	128.57	3.50	ND	5.84	32.45	35.50	57.61	0.94	4.3	-3.09	-18.15
A13(A)	DW	3270	7.8	34.23	5.92	ND	1.19	0.60	1.30	35.70	0.22	4.4	-2.77	-16.26
A13(B)	SW	494	7.24	2.48	3.50	ND	0.17	2.09	1.35	2.89	0.14	-2.5	-4.10	-26.40
A 14	SW	4540	7.15	36.44	8.20	ND	2.72	5.16	8.73	36.27	0.83	-3.7	-4.29	-27.05
A 15	DW	694	7.48	3.26	3.53	ND	0.57	0.36	0.45	7.12	0.18	-4.8	-3.77	-27.12
A 16	DW	374	7.21	1.34	2.57	ND	0.03	0.53	0.51	2.83	0.12	-0.6	-4.83	-29.88
A 17	DW	424	7.33	1.21	4.00	ND	0.14	0.35	0.31	4.79	0.19	-2.6	-4.75	-33.88
A 18	DW	1729	7.63	4.99	4.40	ND	1.36	1.31	5.61	5.08	0.40	-2.9	-4.75	-30.87
A 20	SW	4500	7.4	52.46	6.10	ND	1.71	7.69	13.78	36.61	6.95	-3.8	-3.40	-22.43
A 21	DW	386	6.7	0.84	1.23	0.20	0.30	0.55	0.41	1.37	0.15	1.8	-5.08	-32.81
A 22	DW	146	6.92	0.12	1.50	ND	0.08	0.82	0.36	0.57	0.03	-2.3	-2.67	-20.43
A 23	SW	409	7.65	0.67	4.31	0.03	0.19	1.09	0.83	3.18	0.09	0.1	-5.64	-34.45
A 24	SW	334	7.58	1.07	3.00	ND	0.04	0.35	0.32	3.32	0.10	0.2	-4.83	-34.24
A 25	DW	403	7.46	0.79	3.97	ND	0.09	0.56	0.43	4.34	0.06	-5.3	-4.58	-30.69
A 26	SW	454	7.26	1.55	3.00	0.03	0.17	2.80	1.18	0.95	0.04	-2.3	-4.98	-33.81
A 27	DW	178	6.98	0.36	1.80	ND	0.09	1.00	0.50	0.47	0.11	3.9	-4.53	-36.86

***Note*: SW** = Shallow Well; **DW** = Deep Well, **ND**=Not Detectable, **NICB**= Net Inorganic Charge Balance

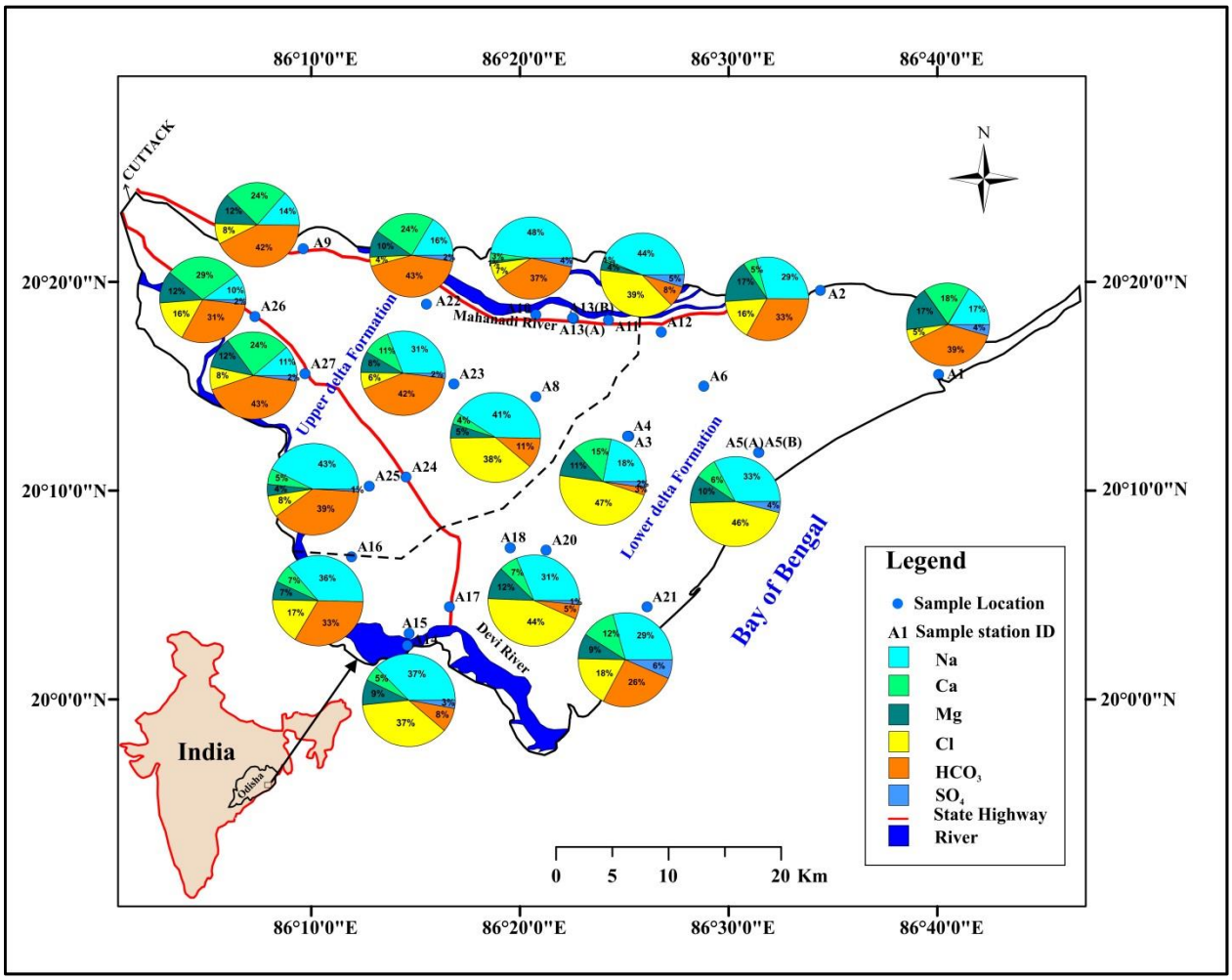

Figure 5.1 *Major ionic concentration in percentage*

5.1.2 Hydrochemical facies

The different hydrochemical facies are shown in Piper diagram (Piper, 1944) as in Fig. 5.2. Accordingly, the study area has been classified into several water types, such as Na-Ca-HCO_3, Ca-HCO_3, Na-Cl, Na-Cl-HCO_3, Na-Mg-Ca-Cl and Ca (Na, Mg)-HCO_3-Cl (Fig. 5.2) (Mukherjee and Fryar, 2008). Different chemical composition of groundwater is due to various chemical processes such as, hydration, hydrolysis, ion-exchange and oxidation-reduction reactions (Rosenthal, 1987). The Ca-HCO_3 water type was observed in groundwater samples A1, A5 (A), A9, A22, A23 and A27 and are considered to be fresh groundwater with Ca^{2+} and HCO^{-}_3 content predominately in the upper part of the coastal aquifer system (Appelo and Postma, 2004). The groundwater samples, A25 and A10 show Na-Ca-HCO_3 type of water (Fig. 5.2) and are also fresh groundwater unaffected by salinization process. Another group of groundwater samples (A15-17 and A24) shows Na-Cl-HCO_3 water facies, whereas some

groundwater samples (A13B, A18, A21 and A26) are of mixed water types (Fig. 5.2). The other samples are saline to highly saline with high chloride content and EC, and are categorized as Na-Cl and Na-Mg-Ca-Cl hydrochemical facies (Fig. 5.2).

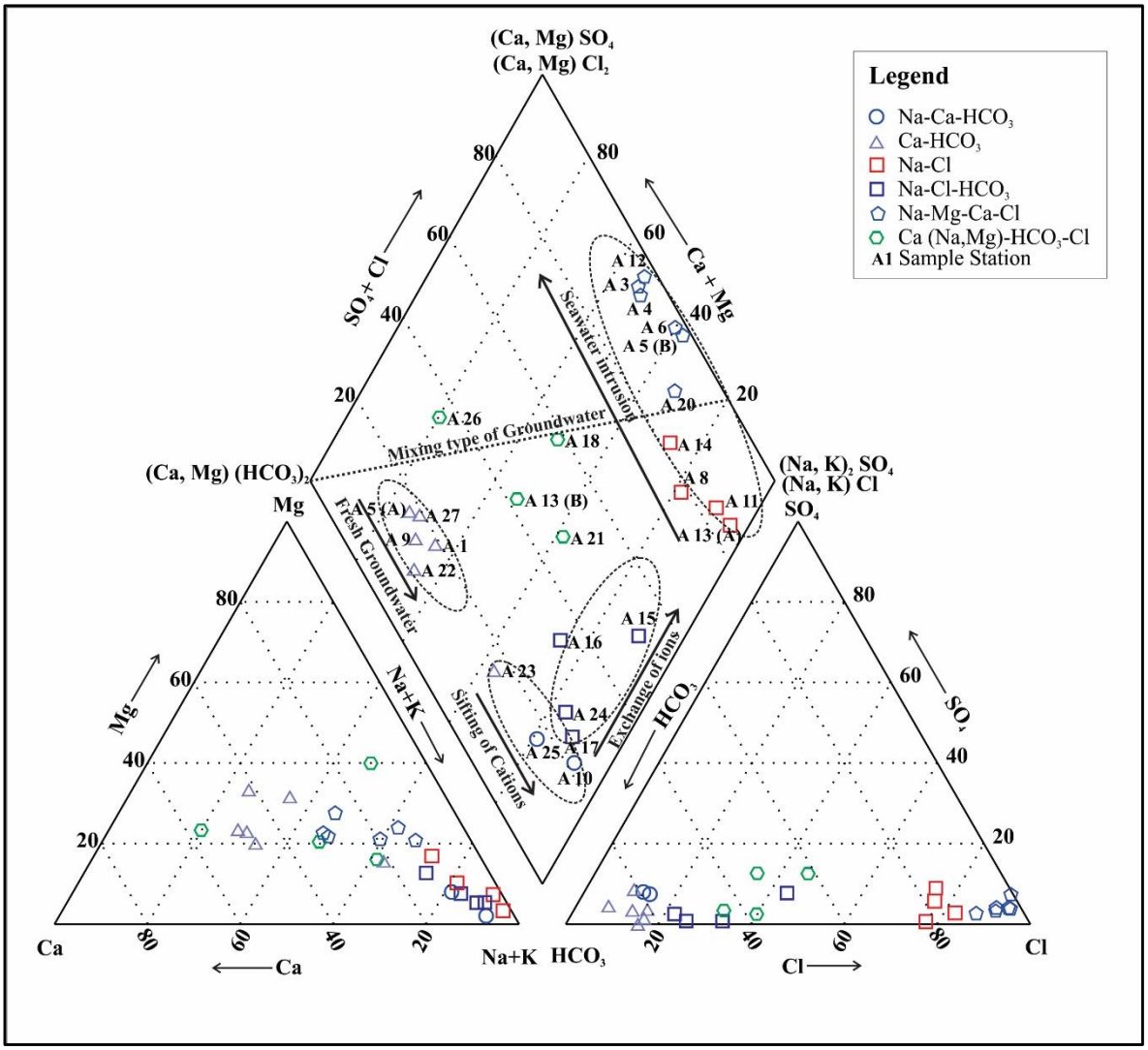

Figure 5.2 Piper plot with variation in hydrochemical facies

To interpret the mechanism of seawater intrusion process, an ionic correlation was made (Fig. 5.3). The parameter EC is strongly correlated with chloride ion (Cl^-) with r = 0.997 (Fig. 5.3a), indicating that the groundwater in the study area has been affected by seawater. Similarly, chloride (Cl^-) shows positive strong correlation with major ions (Na^+, Ca^{2+}, Mg^{2+}, SO^{2+}_4 and K^+) with correlation coefficient (r) of 0.987, 0.991, 0.974, 0.978 and 0.914 respectively (Fig. 5.3 b, c, d, e and f). The strong correlation between Cl^- and cations implies that the

groundwater salinity in the coastal region is derived mainly from seawater, as chloride represents the end-member proportion of seawater due to its conservative nature (Pulido-Leboeuf, 2004; Ghabayen et al., 2006; de Montety et al., 2008; Huang et al., 2013).

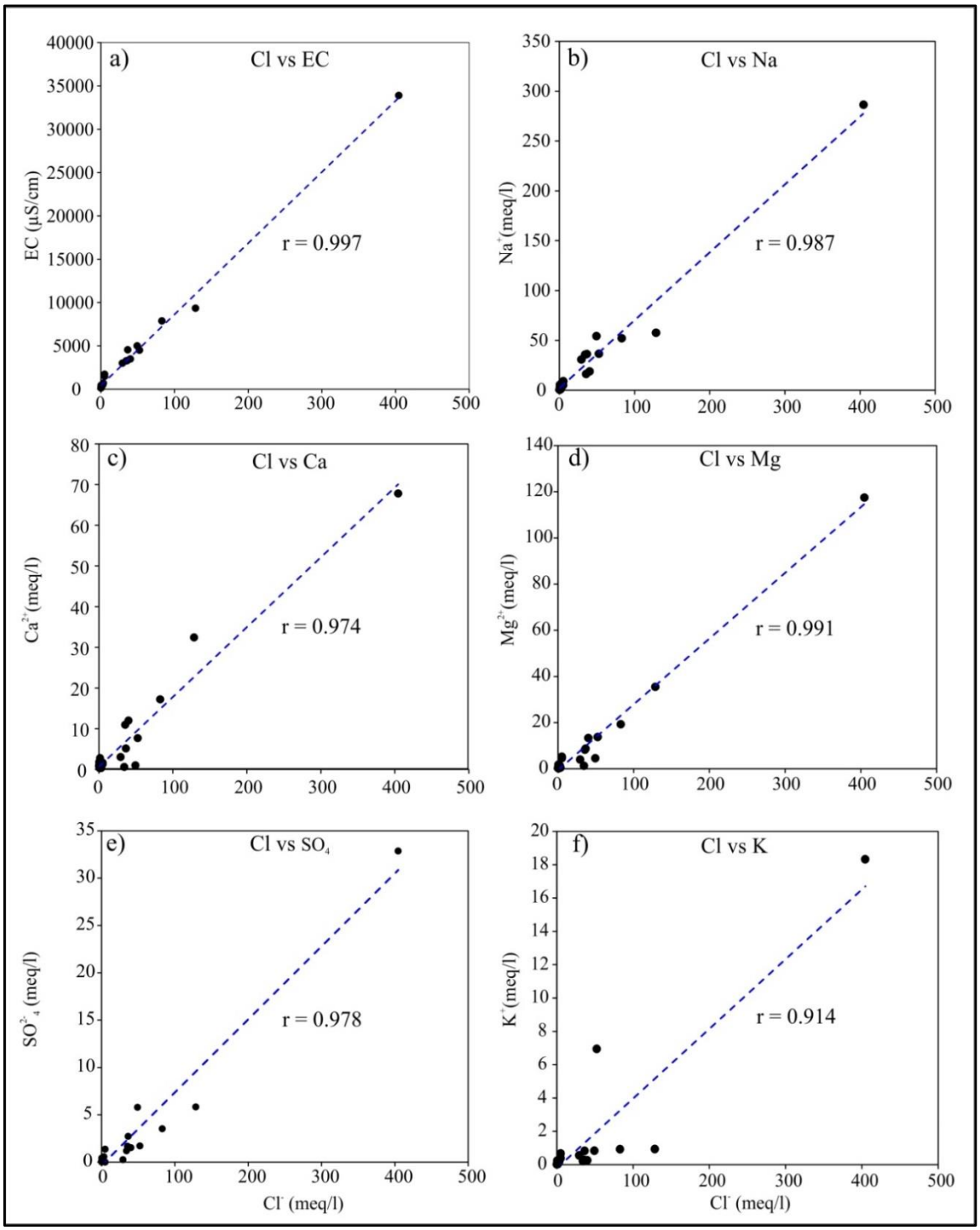

Figure 5.3 *Correlation showing strong positive correlation a) Cl Vs. EC b) Cl Vs. Na c) Cl Vs. Ca d) Cl Vs. Mg e) Cl Vs. SO_4 and f) Cl Vs. K*

Different molar ratios such as, Na^+ / Cl^-, HCO^-_3 / Cl^-, Mg^{2+}/ Ca^{2+}, SO_4^{2-}/ Cl^- and Ca^{2+}/ (HCO^-_3/ SO_4^{2-}) of groundwater samples were used to delineate the mixing between groundwater and seawater (Table 5.2). The average ratio of Na^+ / Cl^- ranges from 0.86 to 1.0 for water in hydrological cycle, whereas the ratio is 0.86 for seawater (Rosenthal, 1987; Vengosh, and Rosenthal, 1994; Stigter et al., 1998). The coastal aquifer system of the Mahanadi delta showed Na^+ / Cl^- ratio between 0.45 and 6.73 (average 2.01). The measured Mg^{2+} /Ca^{2+} ratio ranged from 0.37 to 4.47 with an average value of 1.29, which indicates the conversion of fresh groundwater to saline groundwater in the coastal region. Ratios in the ranges 0.5 - 0.7 and 0.7 - 0.9 imply that groundwater flows through limestone aquifer and dolomitic aquifers respectively (Rosenthal, 1987; Vengosh, and Rosenthal, 1994). HCO^-_3 / Cl^- molar ratio is generally used to determine the recharge region of the coastal aquifer system. The HCO^-_3 / Cl^- ranged from 0.019 to 12.35 with an average value of 2.6. The groundwater affected by seawater can be explained through the study of SO_4^{2-}/ Cl^- ratio (0-0.83), which provides key information about the origin of SO_4^{2-} due to various chemical processes such as sulfide oxidation, gypsum dissolution and mixing of seawater (Pulido-Leboeuf, 2004; Han et al., 2011). Ca^{2+}/ (HCO^-_3/ SO_4^{2-}) ratio, was used to understand the controlling factors on groundwater system in the present study. In calcareous aquifer system, the ratio of (Ca^{2+}/ (HCO^-_3/ SO_4^{2})) varies from 0.6 to 0.8, exceeding the ratio (0.34) of seawater (Rosenthal, 1987).

Table 5.2 Ionic ratios and saturation indices

Sample Station ID	Seawater fraction	HCO_3/Cl	Na/Cl	Mg/Ca	SO_4/Cl	Ca/ (HCO_3+SO_4)	SI Calcite	SI Dolomite	SI Gypsum
A 1	0.00	7.481	3.23	0.97	0.83	0.42	0.01	0.08	-2.51
A 2	0.01	2.022	1.79	3.18	0.00	0.16	0.08	0.74	Not available
A 3	0.06	0.056	0.46	0.75	0.05	2.98	-0.12	-0.31	-1.57
A 4	0.07	0.062	0.47	1.11	0.04	2.99	-0.30	-0.68	-1.60
A 5 (A)	0.00	4.984	1.30	0.83	0.11	0.47	-0.39	-0.79	-3.38
A 5 (B)	0.72	0.019	0.71	1.73	0.08	1.67	-0.10	0.15	-0.31
A 6	0.15	0.024	0.63	1.12	0.04	3.12	-0.17	-0.21	-1.30
A 8	0.05	0.280	1.05	1.30	0.01	0.36	-0.04	0.11	-2.85
A 9	0.00	5.276	1.69	0.50	0.02	0.56	-0.64	-1.42	-4.46
A 10	0.00	5.211	6.73	0.37	0.49	0.07	-0.67	-1.73	-3.21
A 11	0.09	0.205	1.10	4.47	0.12	0.06	-0.14	0.00	-2.11
A 12	0.23	0.027	0.45	1.09	0.05	3.47	0.17	0.45	-0.97
A 13 (A)	0.06	0.173	1.04	2.16	0.03	0.08	-0.29	-0.19	-2.86
A 13 (B)	0.00	1.411	1.17	0.65	0.07	0.57	-0.39	-0.90	-2.88
A 14	0.06	0.225	1.00	1.69	0.07	0.47	0.13	0.57	-1.72
A 15	0.00	1.083	2.18	1.26	0.18	0.09	-0.85	-1.54	-3.08
A 16	0.00	1.927	2.12	0.96	0.03	0.20	-1.05	-2.06	-4.05
A 17	0.01	3.311	3.96	0.89	0.12	0.08	-0.97	-1.94	-3.65
A 18	0.09	0.882	1.02	3.52	0.27	0.23	-0.16	0.30	-2.29
A 20	0.00	0.116	0.70	1.79	0.03	0.99	0.34	1.00	-1.83
A 21	0.00	1.466	1.63	0.74	0.36	0.36	-1.85	-3.78	-3.05
A 22	0.00	12.344	5.67	0.44	0.68	0.52	-1.36	-3.02	-3.42
A 23	0.00	6.440	4.75	0.77	0.29	0.24	-0.06	-0.16	-3.05
A 24	0.00	2.815	3.11	0.91	0.03	0.11	-0.78	-1.52	-4.21
A 25	0.00	5.042	5.52	0.78	0.11	0.14	-0.57	-1.20	-3.64
A 26	0.00	1.938	0.62	0.42	0.11	0.88	-0.21	-0.73	-2.73
A 27	0.00	4.951	1.30	0.50	0.24	0.53	-1.10	-2.45	-3.33

5.2 DISCUSSION

5.2.1 Ionic variation in groundwater

The major cation concentration showed an order of dominance of Na^+ > Ca^{2+} > Mg^{2+} > K^+ and the anions showed order dominance of Cl^- > HCO^-_3 > $SO_4{}^{2-}$. The groundwater samples (A9, A26, A27, A22, A10, A23, A24 and A25) from the Upper delta formation (Fig. 5.1) are mainly dominated by Ca^{2+}, Na^+ and HCO^-_3 ions (Table 5.1) and are considered as fresh groundwater. The groundwater samples from the Lower delta formation showed dominance of Na^+ and Cl^-. The analysis indicated the presence of both fresh groundwater and saline groundwater in two different formations of the Mahanadi delta. The upper part of the deltaic region consists of fresh groundwater with chemical composition of Ca^{2+} and HCO^-_3 and indicates the recharge area of the aquifer system (Han et al., 2015). As groundwater flows from upper part to lower part of the Mahanadi deltaic region exchange of ions is identified within the aquifer system. This results in cation exchange between Ca^{2+} and Na^+ and subsequently the concentration of Na^+ (31 - 48%) becomes high in comparison to Ca^{2+} (3 - 11%). Similarly, when further groundwater flows from the lower deltaic region to SE direction i.e. towards Bay of Bengal, the increasing concentration of Na^+ with Cl^- is observed in most of the groundwater samples. As, the groundwater samples A8, A4, A11, A14 and A20 have high concentration of Na^+ (18 – 44%) and Cl^- (37 – 47%) with low percentage of HCO^-_3 (3 – 11%), which suggests that the fresh groundwater has undergone mixing with saline water due to seawater intrusion process.

Cation exchange is a common process in the coastal region of the Mahanadi delta, in which seawater reacts with the ions of fresh groundwater to produce a new water type due to sweater intrusion process or mixing process. The groundwater of upper part of the Mahanadi deltaic region is of Ca-Mg-Na-HCO_3 water type with major concentration of Ca and HCO_3 ions in groundwater (Fig. 5.1 and Fig. 5.2). This hydrochemical facies shows two types of cationic exchange processes. Exchange between Ca^{2+} and Mg^{2+} derived due to the interaction of carbonate sediments of the Mahanadi River, where as the sodium released by clay layer supports the Ca^{2+} and Na^+ exchange process (Nadler et al., 1980), as explained by the following reactions (Eq. 5.1 and 5.2) (Martínez and Bocanegra, 2002; Appelo and Postma, 2004; Andersen et al., 2005)

$$Ca^{2+} + Mg^{2+} - X_2 \rightarrow Ca^{2+} - X_2 + Mg^{2+} \quad (5.1)$$

$$\frac{1}{2}Ca^{2+} + Na^{+} - X \rightarrow \frac{1}{2}Ca^{2+} - X_2 + Na^{+} \quad (5.2)$$

Where X is the natural exchanger. This results when clay releases Na^+ and Ca^{2+} is adsorbed by sediments. Ca-HCO_3 type of groundwater gradually converts to Na-Ca-HCO_3 type of water along the groundwater flow direction (towards SE) due to cation exchange process, which means the groundwater has undergone freshening with displacement of Ca^{2+} by excess of Na^+ content (Martínez and Bocanegra, 2002; Appelo and Postma, 2004; Han et al., 2011; Wang and Jiao, 2012).

$$Na^{+} + \frac{1}{2}Ca^{2+} - X_2 \rightarrow Na - X + \frac{1}{2}Ca^{2+} \quad (5.3)$$

$$Na^{+} + \frac{1}{2}Mg^{2+} - X_2 \rightarrow Na - X + \frac{1}{2}Mg^{2+} \quad (5.4)$$

Where X is the natural exchanger. Similarly the Na-Ca-HCO_3 type of water comes in contact with saline water and changes to Na-HCO_3-Cl type of water with addition of Na^+ and Cl^- ions derived from seawater. This hydrochemical facies is found to occur in the transition zone between the Upper delta formation and the Lower delta formation of the study area (Fig. 5.1 and Fig. 5.2). From this transition zone, the fresh groundwater gets affected by the salinization process, which indicates the mixing of saline water and fresh groundwater. Hence, ion exchange process is the controlling process for the evolution of groundwater chemistry in the present study. Gradually the Na-HCO_3-Cl type of water changing to Na-Cl type of water is observed in A8, A11, A13 (A) and A14. Then, Na-Mg-Ca-Cl types of water is deduced in A3, A4, A5 (B), A6, A12 and A20 samples having high chloride content and EC close to the coast of Bay of Bengal, suggesting that the fresh groundwater has undergone major ionic changes driven by seawater major ionic composition (Na^+, Mg^{2+}, Ca^{2+} and Cl^-) due to sea water intrusion process.

5.2.2 Evidence of seawater mixing process

The groundwater samples (A9, A22, A23, A25 and A27) of the Upper delta formation (Fig. 5.1) away from the coast of Bay of Bengal show molar ratio of Na^+ / Cl^- > 1, which indicate the occurrence of fresh groundwater. The Na^+ / Cl^- ratio of < 0.86 in some groundwater samples (A3, A4, A5 (B), A6, A12, A20 and A26) (Fig.

5.1), indicate encroachment of seawater into the coastal aquifer and likely occurrence of mixing of seawater and fresh groundwater (Lee and Song, 2007). The groundwater sample A5 (B) from deeper well (>200 meter) located close to the sea (Fig. 5.1) and shows Na^+ / Cl^- ratio of 0.71 with high Cl^- concentration, which is due to seawater intrusion (Stigter et al., 1998).

In addition to Na^+ / Cl^- ratio, Mg^{2+} /Ca^{2+} molar ratio is an important chemical parameter, which indicates the seawater and fresh water interface. Generally in coastal aquifer system, the fresh groundwater and seawater are dominated by Ca^{2+} and Mg^{2+} respectively (Mondal et al., 2010; Gurunadha Rao et al., 2013) due to diagenesis of carbonate minerals (Vengosh A. and Rosenthal, 1994). Several groundwater samples such as, A4, A5 (B), A6, A8, A12, A14 and A20 show Mg^{2+} /Ca^{2+} ratio between 1.09 and 1.79 with high chloride concentration and electrical conductivity and indicates the influence of Bay of Bengal on coastal aquifer system (Mondal et al., 2010). Some groundwater samples show higher ratio of Mg^{2+} /Ca^{2+} i.e. >2.0, which is due to abundance of Mg^{2+} over Ca^{2+} and similarly low ratio samples i.e. < 0.5 are more Ca^{2+} rich in groundwater (Rosenthal, 1987). High Mg^{2+} /Ca^{2+} ratio and low Na^+/ Cl^- molar ratio along with high chloride content (140 meq/l) in A12 location (Fig. 5.1), may be due to the presence of paleo seawater in the Mahanadi deltaic region during Holocene marine transgression period as observed by Larsen et al.(2017).

High HCO^-_3 / Cl^- molar ratio (> 4) observed in groundwater samples, A9, A10, A22, A23, A25 and A27; indicate fresh groundwater recharge in the study area. The ratio gradually decreases along the groundwater flow direction towards the Bay of Bengal. Low HCO^-_3 / Cl^- molar ratio (<0.06) was observed in groundwater samples of the Lower deltaic formation of the Mahanadi delta region, implying the mixing of seawater (molar ratio <0.0069) into the coastal aquifer system (Lee and Song, 2007). Low SO_4^{2-}/ Cl^- (> 0.3) ratio has been observed with low Cl^- content (Table 5.1 and 5.2) in upper part of the Mahanadi deltaic region, suggestive of microbial reduction of SO_4^{2-}in the system (Pulido-Leboeuf et al., 2003; Wang and Jiao, 2012). Whereas, low SO_4^{2-}/ Cl^- (< 0.2) along with high Cl^- content observed close to the coast in deeper well (Table 5.1 and 5.2), shows seawater mixing with fresh groundwater (Pulido-Leboeuf et al., 2003; Huang et al., 2013).

In the present study, Ca^{2+}/ (HCO^{-}_{3}/ SO_4^{2-}) ratio ranged from 0.06 to 3.47 with an average value of 0.81 i.e. most of the groundwater samples are fresh. The ratio > 1 in groundwater samples A3, A4, A5 (B), A6 and A12 with high chloride content, imply inflow of Ca-Chloride brine due to seawater intrusion activity (Rosenthal, 1987).

5.2.3 Saturation Indices (SI)

The aim to study saturation indices (SI) was to understand the different conditions of equilibrium, oversaturation and understauration between minerals and groundwater (Table 5.2). The groundwater samples were catagorized into two groups based on the Mg^{2+} /Ca^{2+} ratio and saturation indices (Fig. 5.4). The blue dashed circle (Fig. 5.4) shows that the saturation index with respect to calcite and dolomite was under saturated as SI < 0, which can be interpreted as dissolution of carbonate minerals in these groundwater samples (Pulido-Leboeuf, 2004; de Montety et al., 2008; Liu et al., 2015). Further, these groundwater samples (A9, A22, A23, A25 and A27) in the Upper delta formation of the coastal aquifer system were identified as Ca-rich as the Mg^{2+} /Ca^{2+} ratio is less than 1, which indicates the presence of fresh groundwater in the aquifer system unaffected by the seawater. The saturation index of calcite or dolomite of groundwater samples grouped in red dashed circle (Fig. 5.4) close to or above 0 or equilibrium line, is intepreted as saline groundwater with more Mg^{2+} content. This is due to mixing of fresh groundwater and saline water. The groundwater samples A4, A5 (B), A6 and A12 with Mg^{2+} /Ca^{2+} ratio >1, suggests Mg^{2+} has been derived from seawater and adsorbed by fresh groundwater with release of Na due to cation exchange process (Fig. 5.4). The Ca-rich fresh groundwater in the Upper delta formation converted into Mg-rich saline groundwater in the Lower delta region along the groundwater flow direction of the study area. All groundwater samples were undersaturated as the saturation index was negative with respect to gypsum (Table 4.2), which may be due to dissolution of gypsum from the saline salts and fertilizers used for agriculture activity.

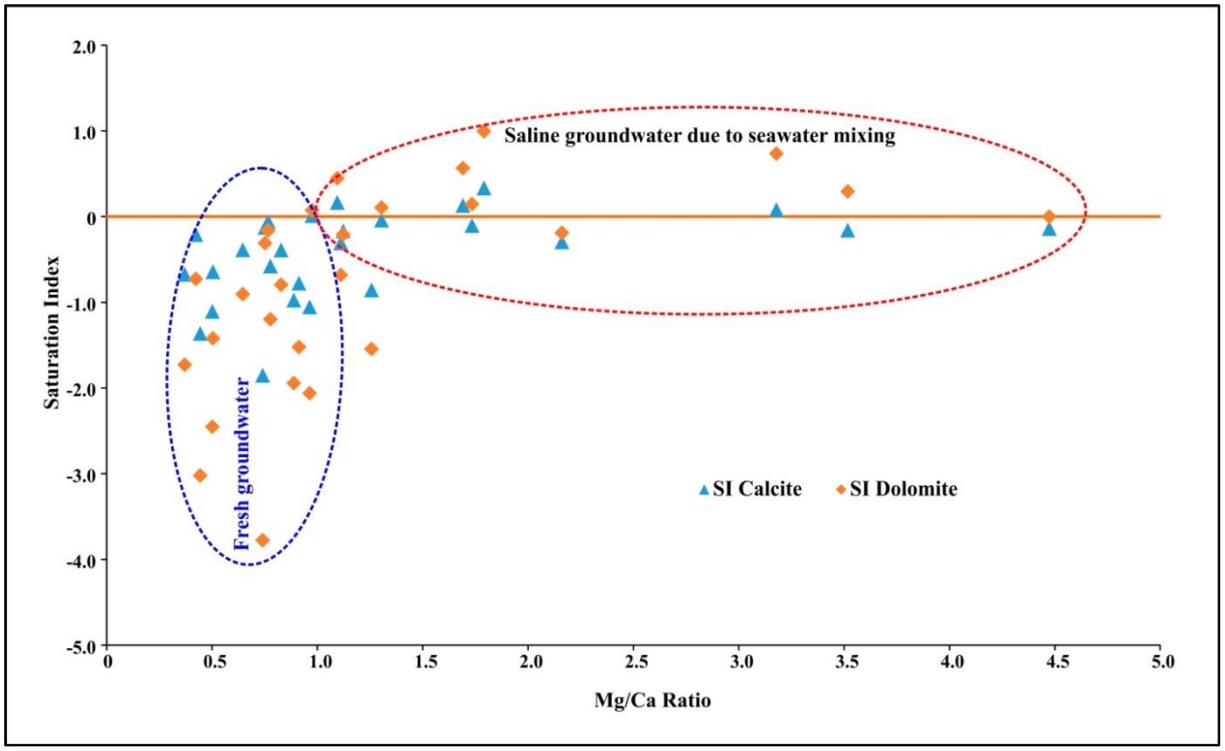

Figure 5.4 *Plot of Mg / Ca ratio and Saturation Index (SI). The samples within blue dashed lines are fresh groundwater (Mg / Ca < 1 and SI < 0) and the groundwater samples within the red dashed circle are saline (Mg / Ca >1 and SI > 1)*

5.2.4 Groundwater recharge and origin of saline water

Stable isotopic ($\delta^{18}O$ and $\delta^{2}H$) data were used to identify the possible sources of groundwater recharge from precipitation, river recharge and also to understand the process of groundwater salinization through dissolution of existing salts and seawater ingress. The $\delta^{18}O$ and $\delta^{2}H$ values of groundwater samples showed a wide range of variation i.e. for $\delta^{18}O$ between -1.86 $^{0}/_{00}$ and -6.87 $^{0}/_{00}$ and for $\delta^{2}H$ between -10.79 $^{0}/_{00}$ and -45.42 $^{0}/_{00}$ (Table 5.1). All groundwater samples plotted below the Global Meteoric Water Line (GMWL) equation ($\delta^{2}H = 8\ \delta^{18}O + 10$) (Harmon, 1961) as shown in Fig. 5.5a. The slope and intecept of regression line ($\delta^{2}H = 5.97\ \delta^{18}O + 0.412$) of groundwater data indicates local precipitation, which gets slightly evaporated before recharge. The deep saline groundwater samples close to sea coast showed enrichment in isotopic composition (Fig. 5.5a) due to mixing of seawater and fresh groundwater in the deeper aquifer (Wang and Jiao, 2012). Similarly, a positive correlation (Fig. 5.5b) between enriched $\delta^{18}O$ value and high Cl^{-} conetent in groundwater samples was also observed, supporting the

mixing process (de Montety et al., 2008; Han et al., 2011; Chandrajith et al., 2016). Another group of groundwater samples plotted on evaporation line (δ^2H = 5.18 $\delta^{18}O$ - 4.63) with depleted isotopic composition as shown in Fig.5.5a. The slope (5.18) suggestes that the shallow saline groundwater originates due to evaporation before infiltration and interaction with saline soil and sand of unsaturated zone (Clark and Fritz, 2013). The relationship between $\delta^{18}O$ and Cl^- indicate salinity in shallow aquifer system, which may have been derived from marine sediments during cyclonic event (Fig. 5.5c). The slope and intecept of regression line (δ^2H = 5.59 $\delta^{18}O$ – 6.7) of fresh groundwater data imply a combined effect of precipitation and evaporation in coastal region (Gupta and Deshpande, 2005) with higly depleted value of $\delta^{18}O$ and δ^2H which range beween -3.95 $^0/_{00}$ to -6.87 $^0/_{00}$ and -26.65 $^0/_{00}$ to -45.42 (Fig. 5.5).

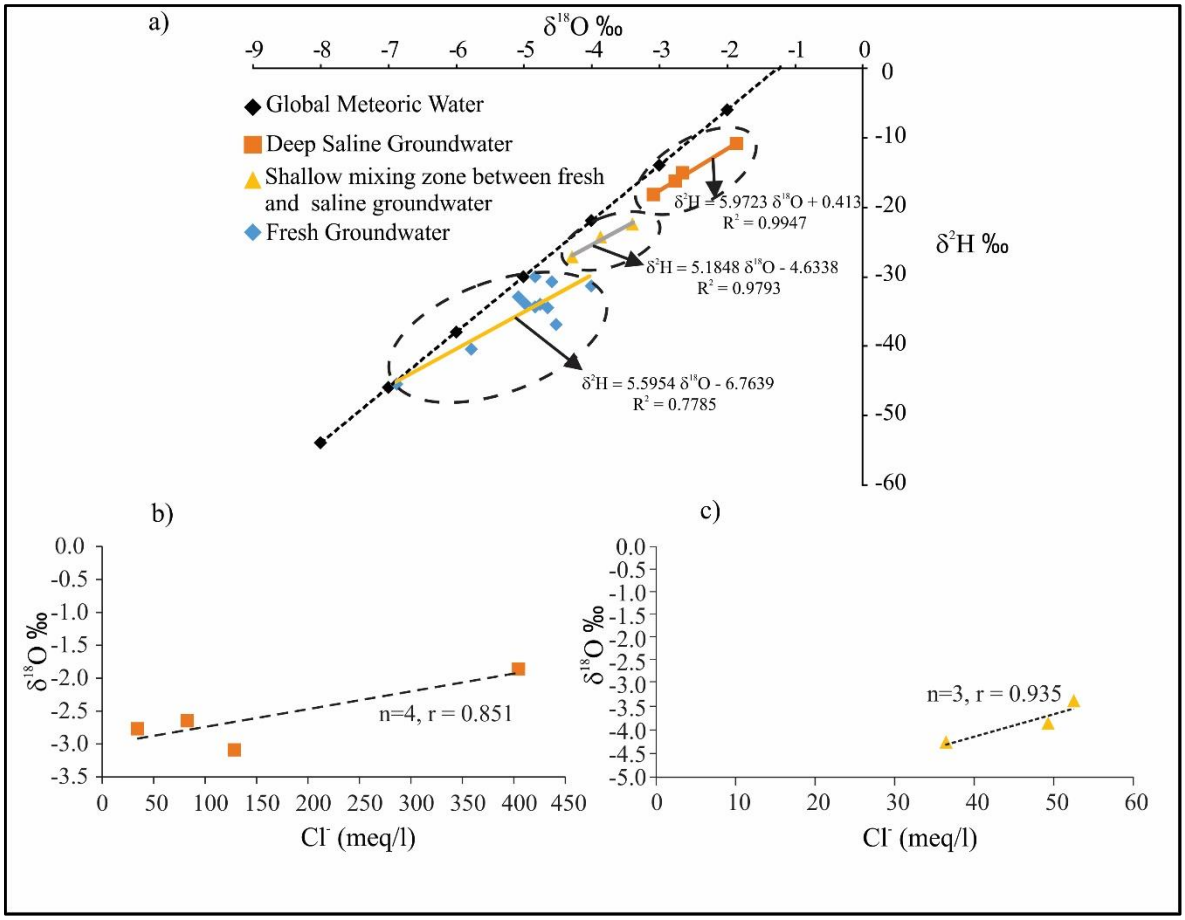

Figure 5.5 *a) $\delta^{18}O$ versus δ^2H values of groundwater compared with Global Meteoric Water Line (GMWL) Correlation graph $\delta^{18}O$ Vs. Cl, b) for deep saline groundwater, c) for shallow saline water*

5.2.5 Conceptual model of aquifer system

A conceptual model was developed to describe the hydrochemical changes along groundwater flow direction from NW to SE towards Bay of Bengal (Fig. 5.6). Groundwater water samples collected from four different wells (A27, A25, A5 (A) and A5 (B)) were used for this conceptual model to identify seawater intrusion in the coastal aquifer system. The depth of all deep wells (A27, A25 and A5 (B)) is approximately 210 m and the shallow well (A5 (A)) is 10 m depth below ground level (Fig. 5.6). The chemical composition of groundwater at station A 27 suggests the groundwater in deep well is Ca-HCO_3 type with minor constituents of Mg^{2+} and Na^{+}, which originates due to cation exchange process during flushing of groundwater in the aquifer system (Appelo and Postma, 2004; de Montety et al., 2008). The stable isotopic composition ($\delta^{18}O$ = -4.53 $^{0}/_{00}$ and $\delta^{2}H$ = -36.86 $^{0}/_{00}$) indicates that the groundwater is recharged by precipitation in Upper delta region (Fig. 5.6).

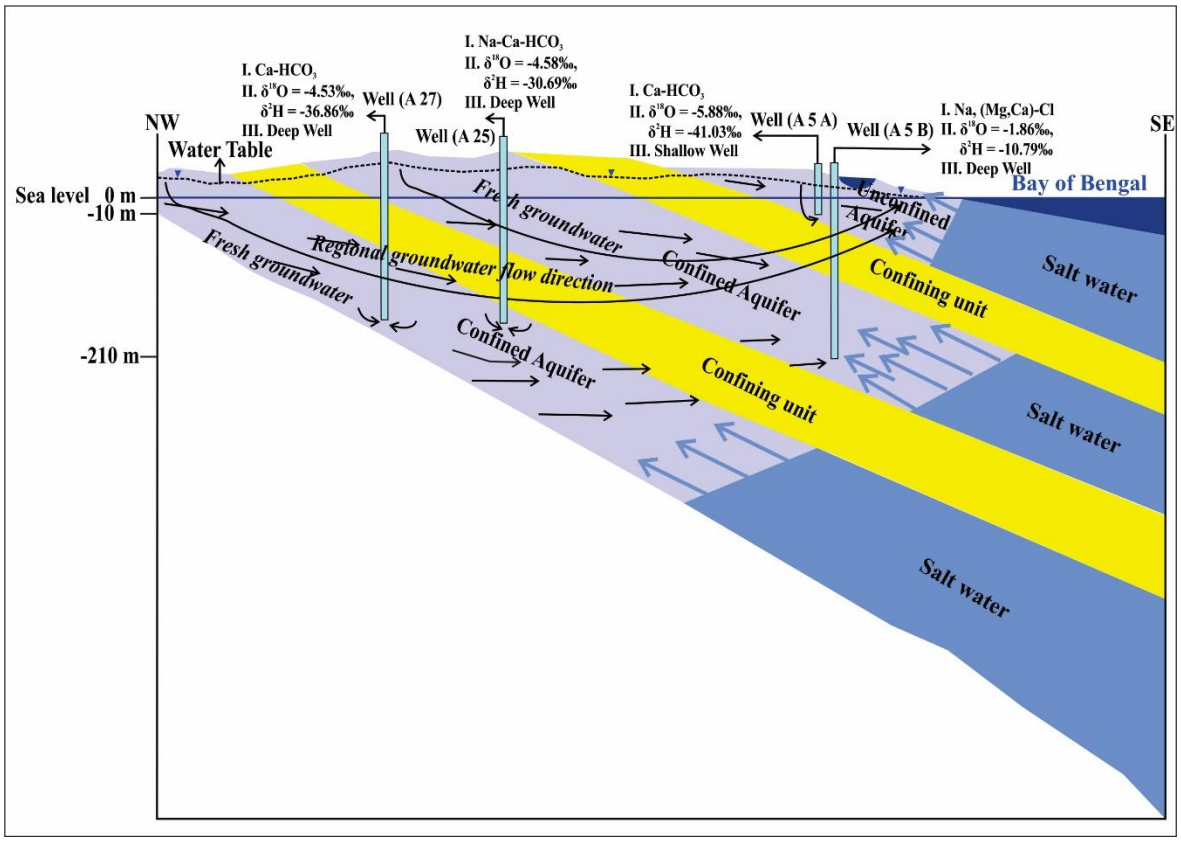

Figure 5.6 *Simple conceptual model to visualize hydrochemical evolution of groundwater away from Bay of Bengal. The different hydrochemical facies Na-Cl, Na-Ca-HCO_3 and Ca-HCO_3 in handpump wells A5 (B), A25 and A27 respectively show influence of seawater*

As the groundwater flows from the Upper deltaic region to Lower deltaic region chemical variation in groundwater was observed in a deep well (A25) (Fig. 5.6), in which the stable isotopic composition ($\delta^{18}O$ = -4.58 $^{0}/_{00}$ and $\delta^{2}H$ = -30.69 $^{0}/_{00}$) suggested the same source of recharge as that of the previous well. But the change of water facies from Ca-HCO_3 to Na-HCO_3 type by replacing Ca^{2+} and Mg^{2+} completely developed the freshening condition of groundwater (Martínez and Bocanegra, 2002; Appelo and Postma, 2004). This well is located in the middle part of the Mahanadi delta, which is considered as the transition zone between the fresh groundwater and saline groundwater (Fig.5.1). The deep well (A5 (B)) close to Bay of Bengal in the Lower delta showed highly saline groundwater of Na-Mg-Ca-Cl type with relatively enriched value of $\delta^{18}O$ = -1.86 $^{0}/_{00}$ and $\delta^{2}H$ = -10.79 $^{0}/_{00}$, which indicates the influence of seawater (Wang and Jiao, 2012). The groundwater sample collected from shallow well (A5 (A)) close to the sea coast is Ca-HCO_3 type and unaffected by seawater. Moreover, the highly depleted isotopic value ($\delta^{18}O$ = -5.88 $^{0}/_{00}$ and $\delta^{2}H$ = -41.03 $^{0}/_{00}$) suggested that the groundwater is immediately recharged by rainwater and prevented the seawater ingress (Fig. 5.6). A hydrochemical facies changing from Ca-HCO_3 in recharge area to Na,(Mg, Ca)-Cl in discharge area was also identified.

5.2.6 Quantification of seawater intrusion

The seawater fraction $(f_{seawter})$ in fresh groundwater was calculated by using conservative ion, Cl^- (Appelo and Postma, 2004).

$$f_{sea} = \frac{m_{cl^-sample} - m_{cl^-freshwater}}{m_{cl^-sea} - m_{cl^-freshwater}} \qquad (5.5)$$

Where $m_{Cl^-\,sample}$ the Cl^- concentration of collected groundwater sample, $m_{Cl^-freshwater}$ is the Cl^- concentration of freshwater and m_{Cl^-sea} is the Cl^- the chloride concentration of sea. By using Eq. 5.5, the seawater fraction was calculated, which showed a variation from 0 in NW region (away from the coast) to 0.72 in SE region (close to the sea coast) (Fig. 5.1). The groundwater samples (A3, A4, A5(B), A8, A11, A12, A13(A), A14 and A18) showed seawater fraction < 0.20 except A5(B) and A12 with seawater fraction 0.72 and 0.23 (Table 5.2), which suggested the occurrence of seawater in groundwater samples A5(B) and A12 was 72% and 23% respectively (Fig. 5.7). In most of the fresh groundwater samples (A9-10, A22-27) located in the Upper delta formation (Fig. 5.1), 0% of seawater was observed with negative saturation index (SI) with respect to calcite,

dolomite and gypsum indicating to dissolution of carbonate minerals (Fig.5.7a). As the groundwater flows from the Upper deltaic formation to the Lower deltaic formation, the proportion of seawater in fresh groundwater increased from 5% to 72% due to ingress of seawater. The SI of calcite and dolomite close to or above equilibrium line (Fig. 5.7a) suggested that the groundwater was salinized by mixing of seawater. Calcium enrichment in groundwater samples of Lower delta formation were due to cation exchange process and not due to carbonate dissolution (de Montety et al., 2008). The strong positive correlation between Cl^- content and seawater fraction (Fig. 5.7b) in groundwater samples is also an indication of mixing of fresh groundwater and saline water (Bear et al., 1999).

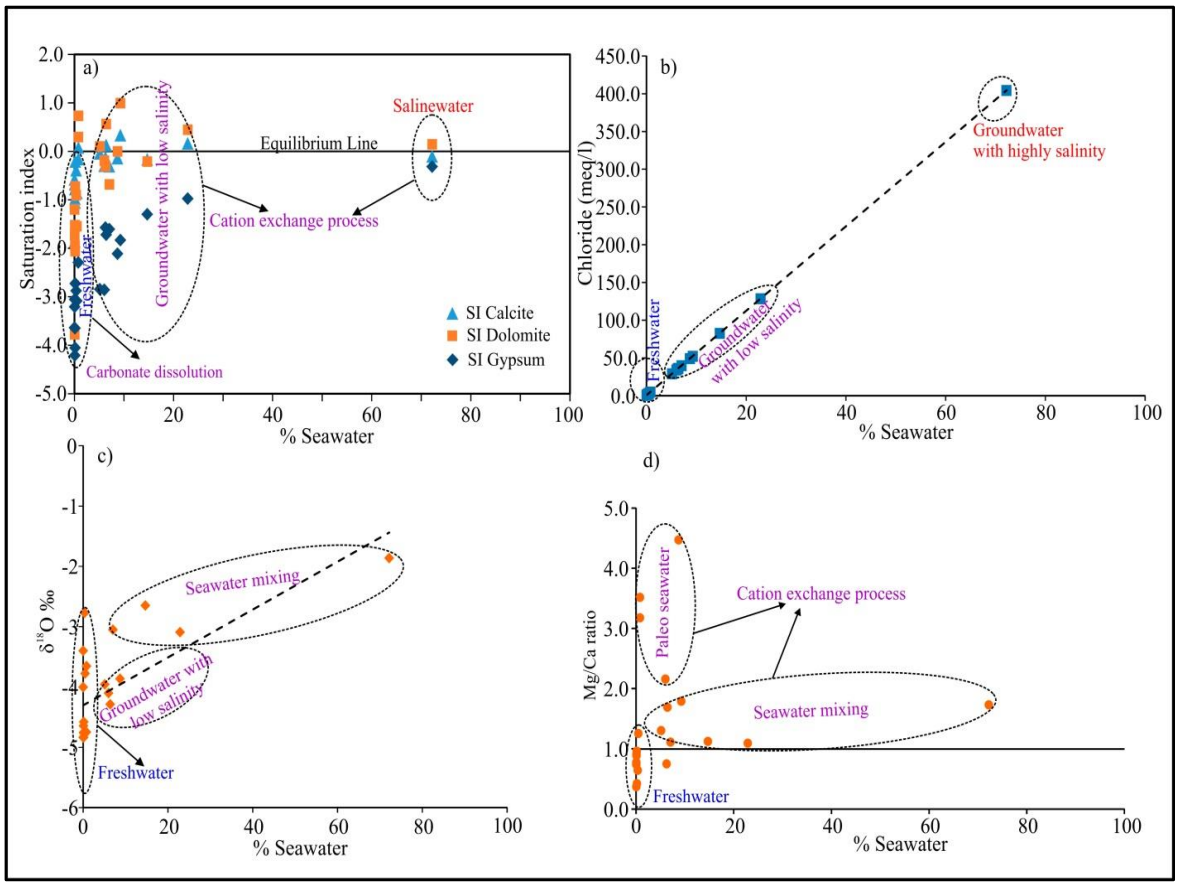

Figure 5.7 *Plotting of percentage of seawater Vs. a) saturation index with respect to calcite or dolomite or gypsum, b) chloride (Cl) concentration, c) $\delta^{18}O$ composition d) Mg / Ca ratio value*

The chloride content increased in samples (Fig. 5.7b) with an increase of seawater proportion from 0% (away from sea coast) to 72% (close to Bay of Bengal). Similarly, the influence of seawater on fresh groundwater was identified by isotopic studies (Fig. 5.7c), in which the deep well groundwater samples close to sea coast with > 10% of seawater showed enriched $\delta^{18}O$ value with range from -1.86 $^{0}/_{00}$ to -3.09 $^{0}/_{00}$. The shallow well groundwater with low salinity affected by marine sediments was driven by the cyclonic storms. They also significantly showed low depleted isotopic composition due to evaporation effect with some seawater fraction (< 0.1) (Fig. 5.7c). The Mg^{2+} /Ca^{2+} ratio of these groundwater exceeded 1 which was used as a proxy for mixing of seawater (> 2%) and groundwater (Pulido-Leboeuf, 2004). High Mg^{2+} /Ca^{2+} ratio (> 2) with a proportion of seawater < 15 % was identified in some groundwater samples (Fig. 5.7d), and suggested the influence of saline water on fresh groundwater. The salinization of groundwater is due to cation exchange process ($Mg^{2+} + Ca^{2+} - X_2 \rightarrow Ca^{2+} + Mg^{2+} - X_2$) in which Mg^{2+} replaced Ca^{2+} (Han et al., 2015). The samples located away from Bay of Bengal with high salinity (EC: 1500 µS/cm -5000 µS/cm) and chloride content (< 50 meq/l) are assumed to be the presence of paleo seawater in the coastal aquifer system (Larsen et al., 2017).

5.3 GROUNDWATER MODELING

5.3.1 Calibration and validation

Calibration is the process through which the calculated head value is subjected to match with the observed head value. The groundwater level data for the years 2004 and 2005 was used for calibrating the model. The observed hydraulic head varied from 0.7 m to 15 m in the Jagatsinghpur shallow unconfined aquifer system.

The steady state model was calibrated through trial and error method in which the unknown hydrogeologic parameters were adjusted to minimize the head difference between calculated head and observed head. The parameters were adjusted within the range measured by the pump tests carried out by CGWB (2013).

The hydraulic conductivty of the Zone-I, Zone-II and Zone-III was estimated to be 40 m/day, 42 m/day and 45 m/day respectively, whereas the corresponding

vertical conductivity (K_v) of the three zones were estimated to be 4 m/day, 4.2 m/day and 4.5 m/day respectively. The different specific yield values 0.05, 0.06 and 0.07 for three respective zones I, II, III (Table 5.3).

Table 5.3 Hydrogeological parameters used for calibration

ZONES	Horizontal Hydraulic Conductivity (K_h) m/day	Vertical Hydraulic Conductivity (K_v) m/day	Specific Yield
I	40	4	0.05
II	42	4.2	0.06
III	45	4.5	0.07

Subsequently, the model was run for 2 years from January 2004 to December 2005 under transient state condition to estimate the groundwater recharge. To measure the goodness of fit of the simulated head value with observed head data various statistical measures were used like the mean error (ME) (Eq.5.6), the mean absolute error (MAE) (Eq.5.7) and the root mean squared error (RMSE) (Eq.5.8) (Anderson and Woessner, 1992). After a calibration, then validation of model was done by taking the hydraulic head values from January 2006 to December 2009.

$$Mean\ Error\ (ME) = 1/n \sum_{i=1}^{n} (h_o - h_c)_i \quad (5.6)$$

$$Mean\ Absolute\ Error\ (MAE) = 1/n \sum_{i=1}^{n} [(h_o - h_c)_i] \quad (5.7)$$

$$Root\ Mean\ Squared\ Error\ (RMSE) = \sqrt{[1/n \sum_{i=1}^{n} (h_o - h_c)_i^2]} \quad (5.8)$$

Where h_o is the observed head value, h_c is the calculated head value and n is total number of observed data. A statistical analysis of calibrated model under steady state condition has been given in Fig. 5.8. The correlation coefficient value for steady state condition was 0.999, and the comparison graph also showed a good match between observed and calculated head (Fig. 5.9). Under transient state condition, the calibrated and validated model showed correlation between observed head and calculated head in the study area (Fig. 5.10 and Fig 5.12). The correlation coefficient values for calibrated and validated model were 0.994 and 0.988 respectively. In addition, the observed head matched with the calculated

head in different periods for both transient state of calibration (2004-2005) and validation (2006-2009) as shown in Fig. 5.11 and Fig. 5.13.

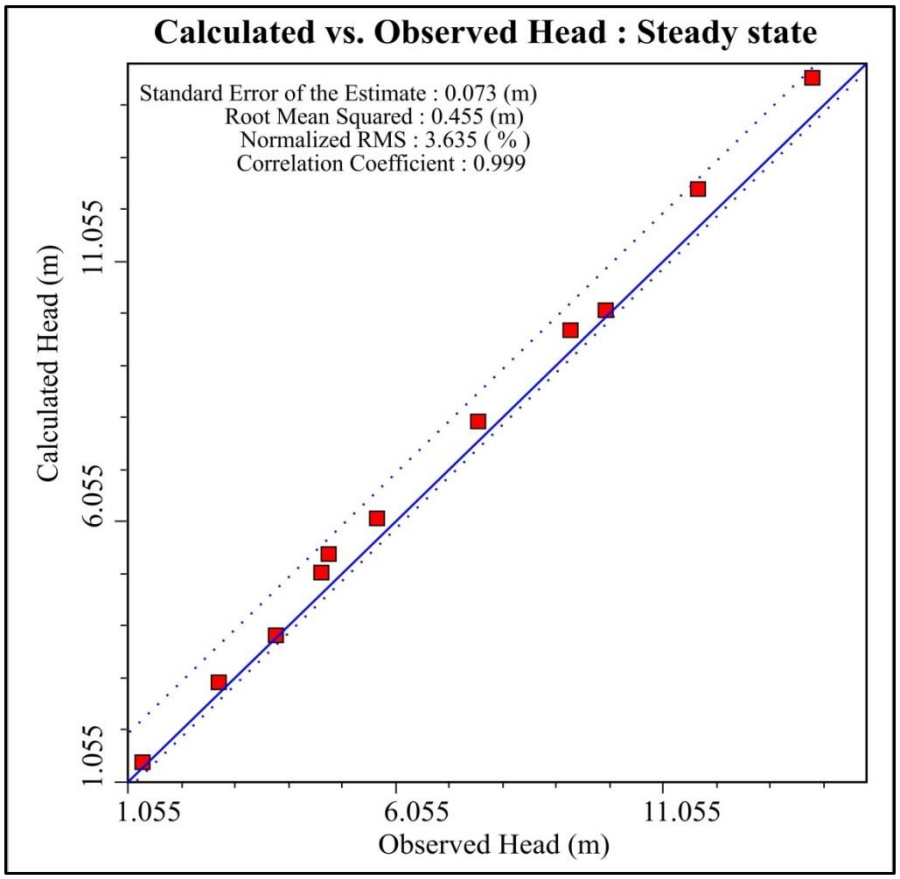

Figure 5.8 *Correlation plot between calculated head and observed head during calibration (2004-2005) of model under steady state condition*

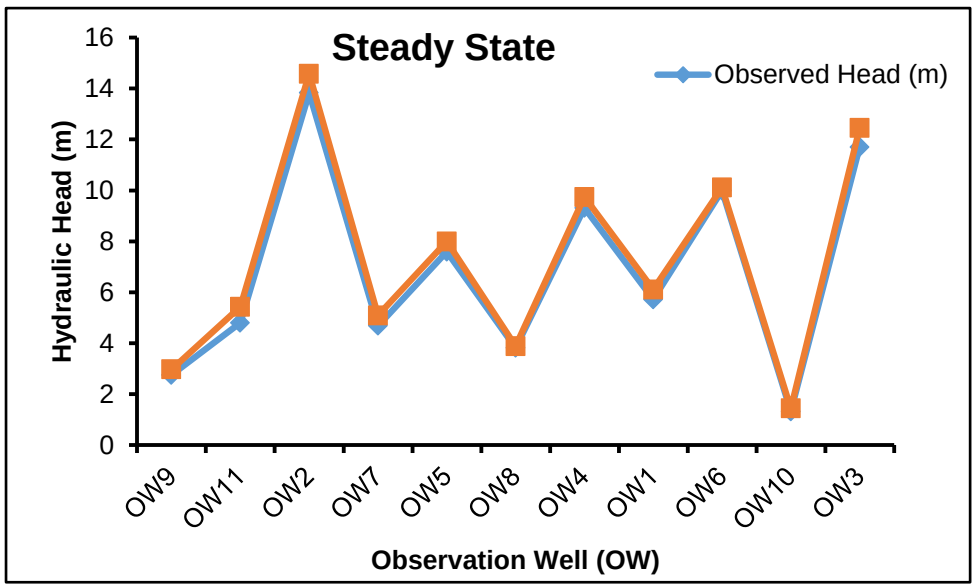

Figure 5.9 *Comparison graph between observed and calculated head (m) of different Observation Wells under steady state condition*

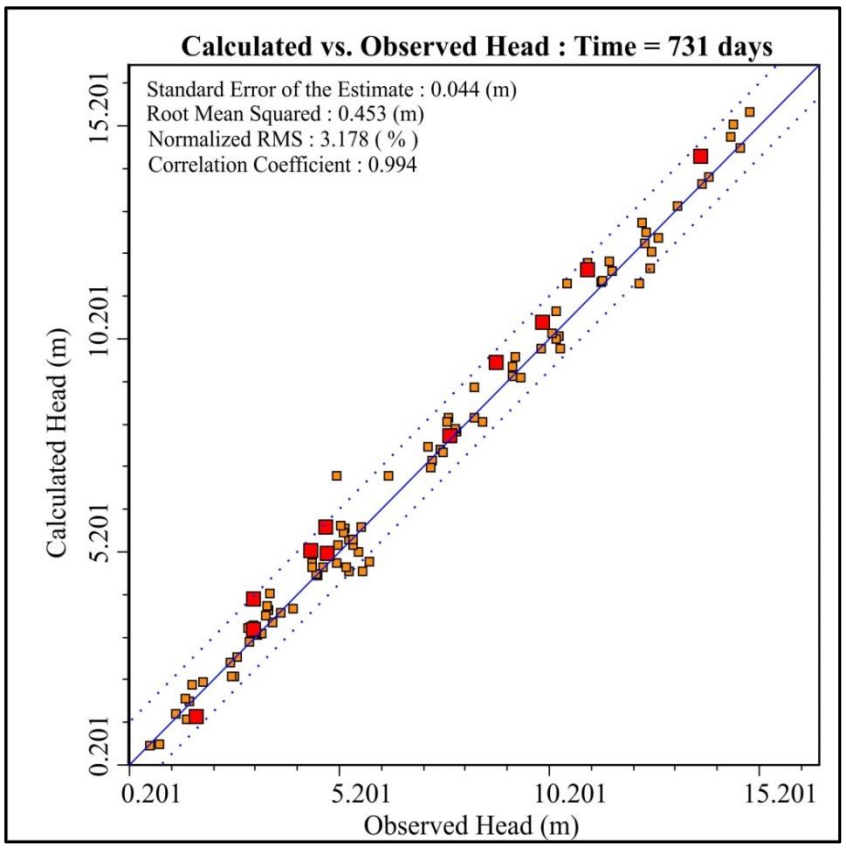

Figure 5.10 *Correlation plot between calculated head and observed head during calibration (2004-2005) of model under transient state condition*

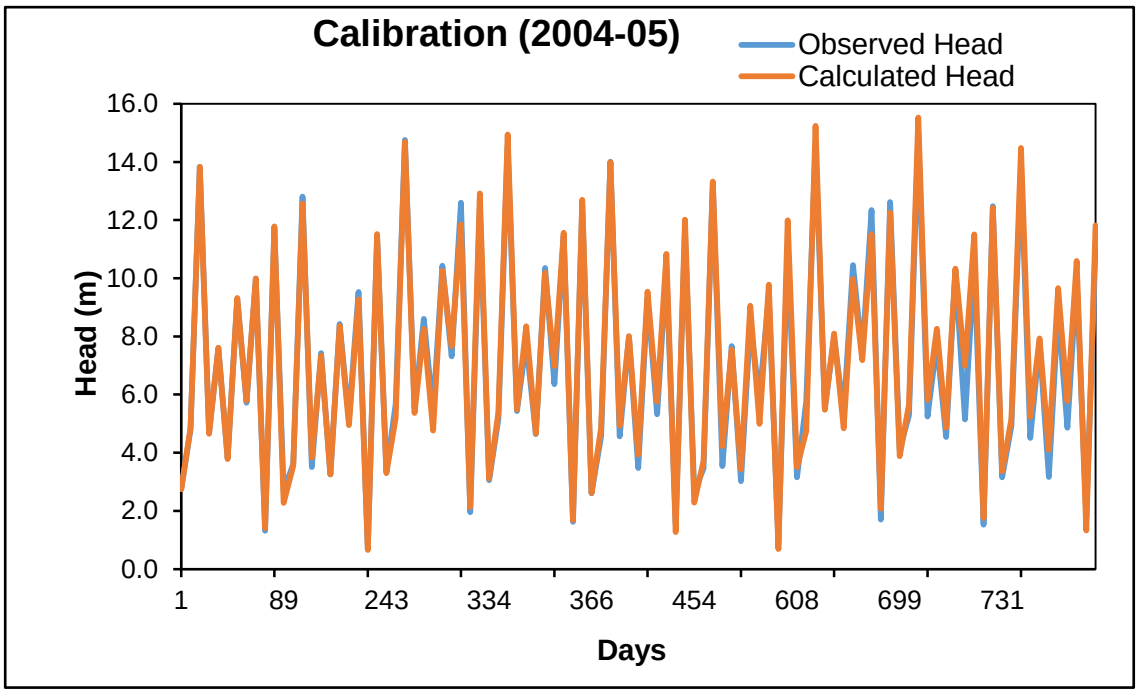

Figure 5.11 *Comparison graph between observed and calculated head (m) under transient condition*

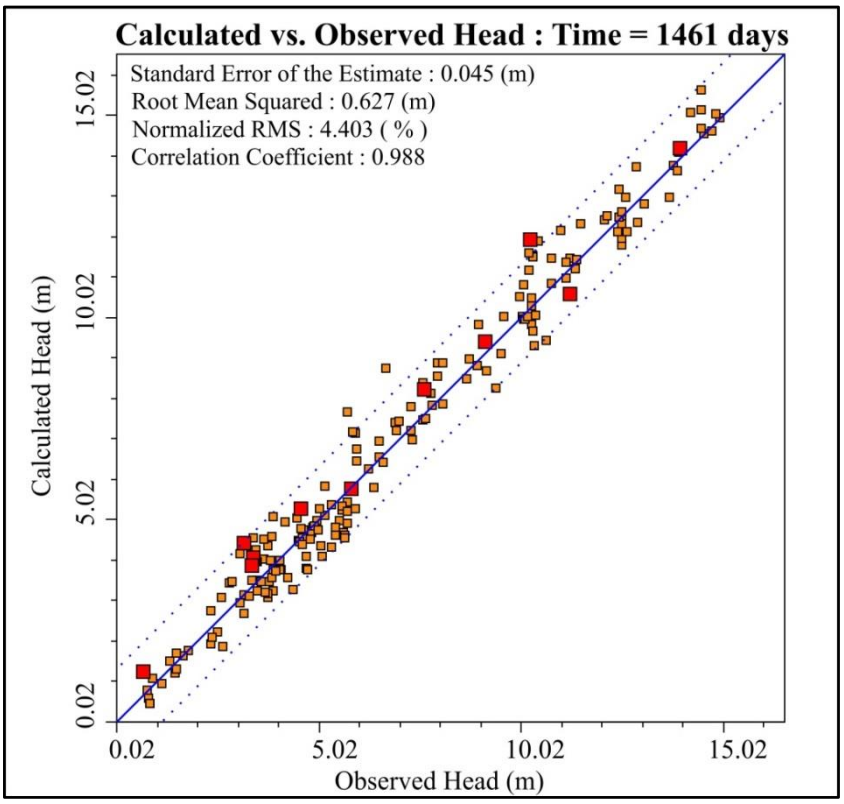

Figure 5.12 *Correlation plot between calculated head and observed head during validation (2006-2009) of model under transient state condition*

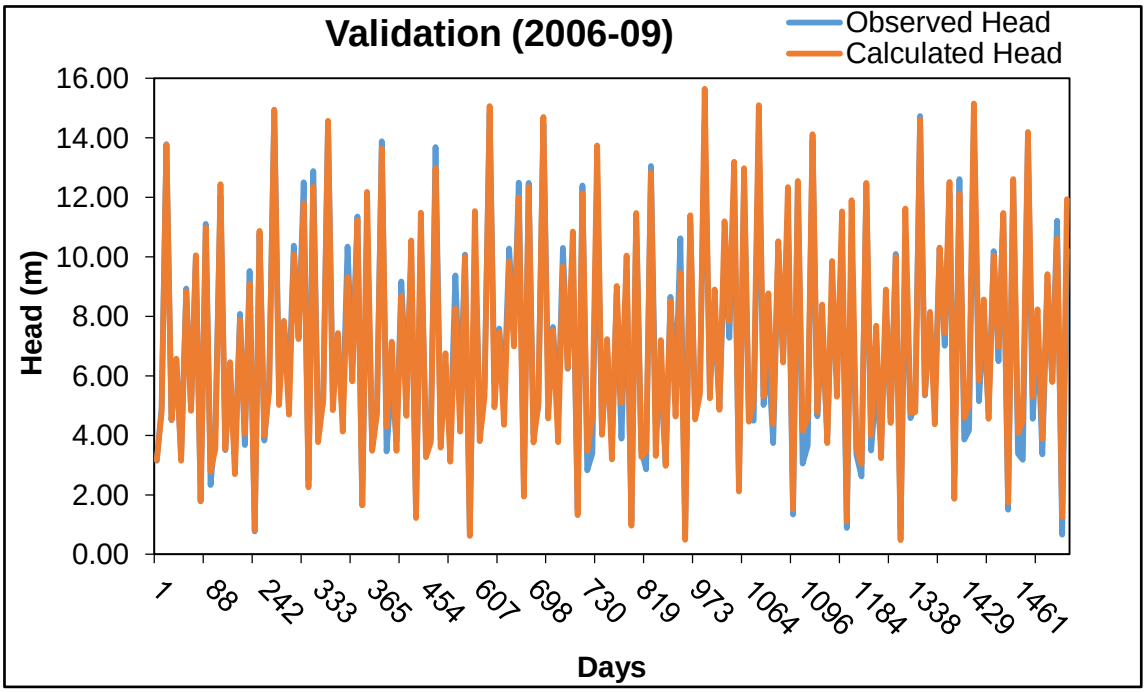

Figure 5.13 *Comparison graph between observed and calculated head (m) under transient condition*

5.3.2 Groundwater levels

The observation wells showed temporal and spatial variation in groundwater level in the Jagatsinghpur coastal district. Three different observation wells OW2, OW7 and OW10 located in different sites of the study area, indicated variation in hydraulic head at different times (Fig. 5.14a, b and c).

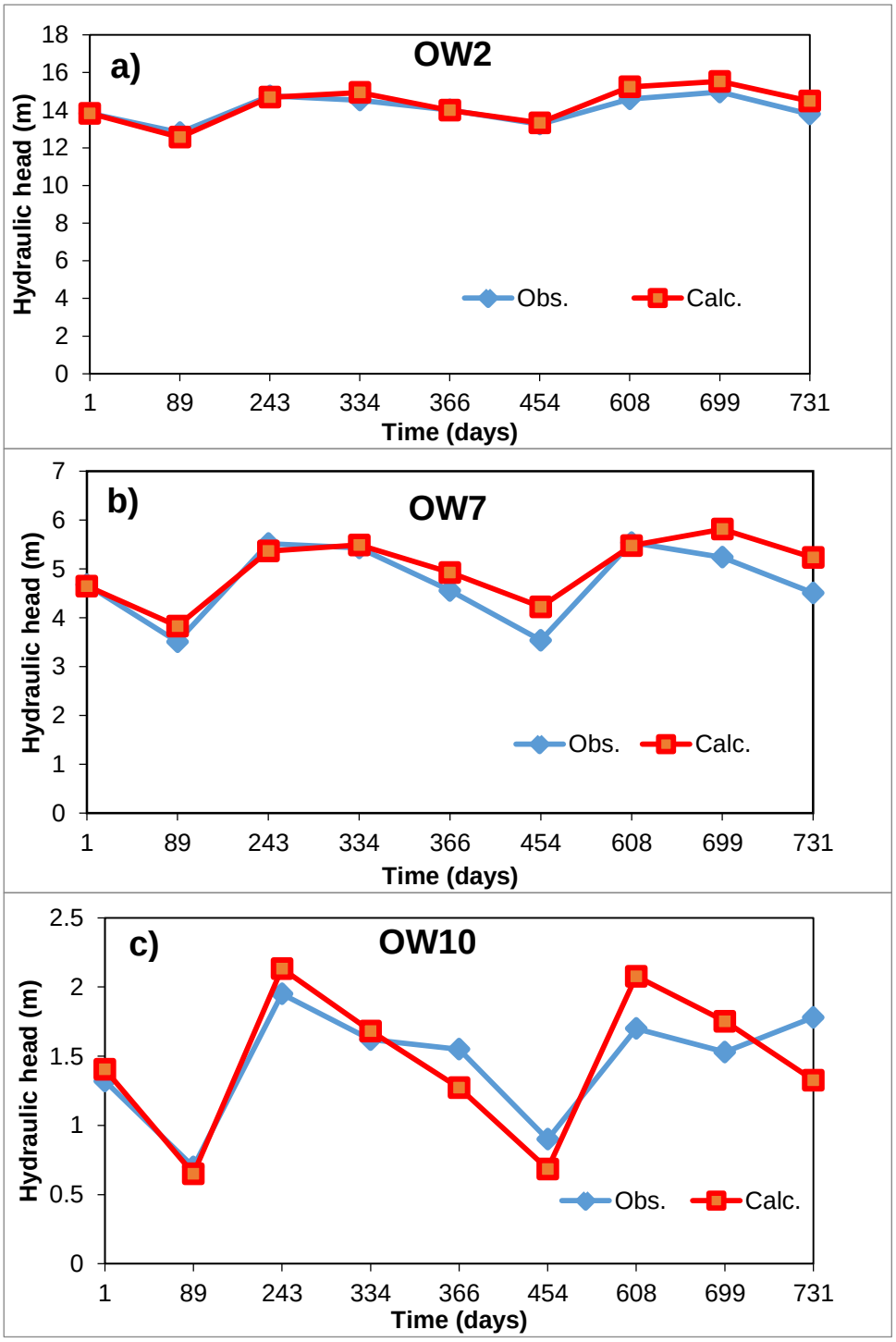

Figure 5.14 *Graph showing the hydraulic head variation at different times for different observation wells a) OW2 b) OW7 c) OW10 during calibration (2004-05)*

Observation well 2 (OW2) situated at the upper part of the study area, showed the maximum hydraulic head value, which ranged from 12 to 14 m. The OW7 located in the middle part of the study area with hydraulic head variation between 3.5 to 5.5 m, whereas, OW10 located close to the Bay of Bengal showed head value of less than 2.5 m. The well data revealed that the upper and lower parts of the study area are the recharge and discharge zones of the aquifer system respectively, (Fig. 5.14).Similar head variation was observed after validation of groundwater model.

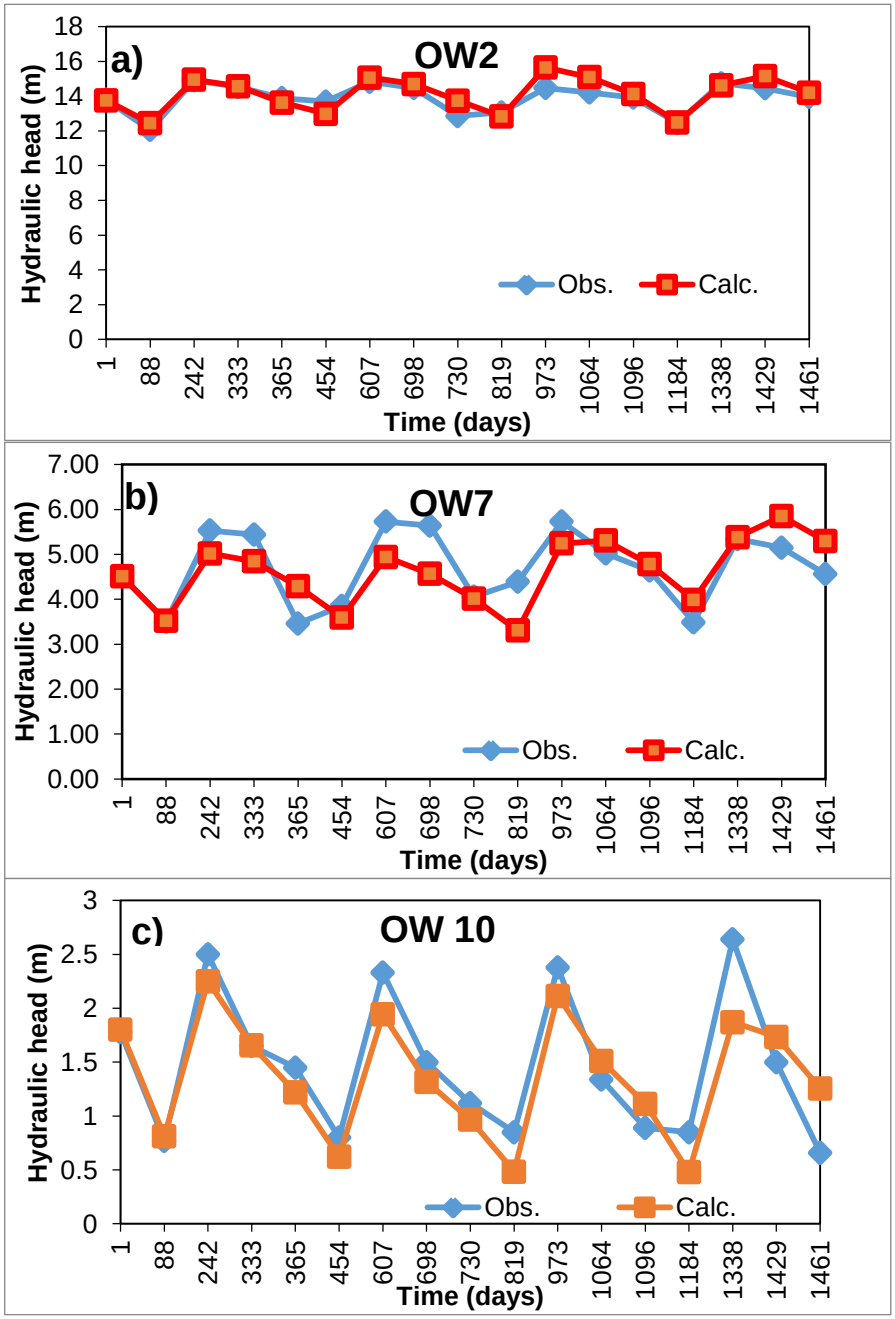

Figure 5.15 *Graph showing the hydraulic head variation at different times for different observation wells a) OW2 b) OW7 c) OW10 during validation (2006-09)*

5.3.3 Recharge zones

The study area was classified into eleven different recharge zones based on rainfall distribution, crop water requirement and groundwater abstraction for irrigation. The Zone 2 is located far away from the shoreline of Bay of Bengal, whereas the Zone 10 is located close to the Bay of Bengal. The two zones showed both positive and negative net recharge patterns, which depended on rainfall and groundwater abstraction. When there is rainfall (during monsoon period), quick recharge of groundwater is observed and the net recharge is positive (Fig. 5.16a). As soon as dry periods ensue (no rainfall event), the net recharge reduces and becomes negative as shown in Fig. 5.16b. This is due to more withdrawal of groundwater for domestic as well as agriculture purposes than rainfall recharge. In Jagatsinghpur coastal aquifer system, Zone 2 has high net recharge value (< 70 mm) as compared to zone 10 (< 20 mm), because of more rainfall recharge than groundwater abstraction occurs (Fig. 5.16a and b). However, the net recharge in zone 10 is low during monsoon period, though the rainfall is high. This may be due to high development of groundwater and low rainfall recharge.

This estimated recharge by calibration of modeling was applied for validation of model. It was showing the similar results in Fig. 5.17. In Zone 2, when the monthly rainfall was maximum (> 800mm) during monsoon, then the net recharge was < 60mm (Fig. 5.17a). Due to abstraction of groundwater the Zone 2 showed negative net recharge, as there was no rainfall event. In case of Zone 10, the net recharge was as low as it was during calibration (Fig. 17b). This implies that the net recharge in zone 10 is attributed to heavy pumping for domestic and agriculture purposes.

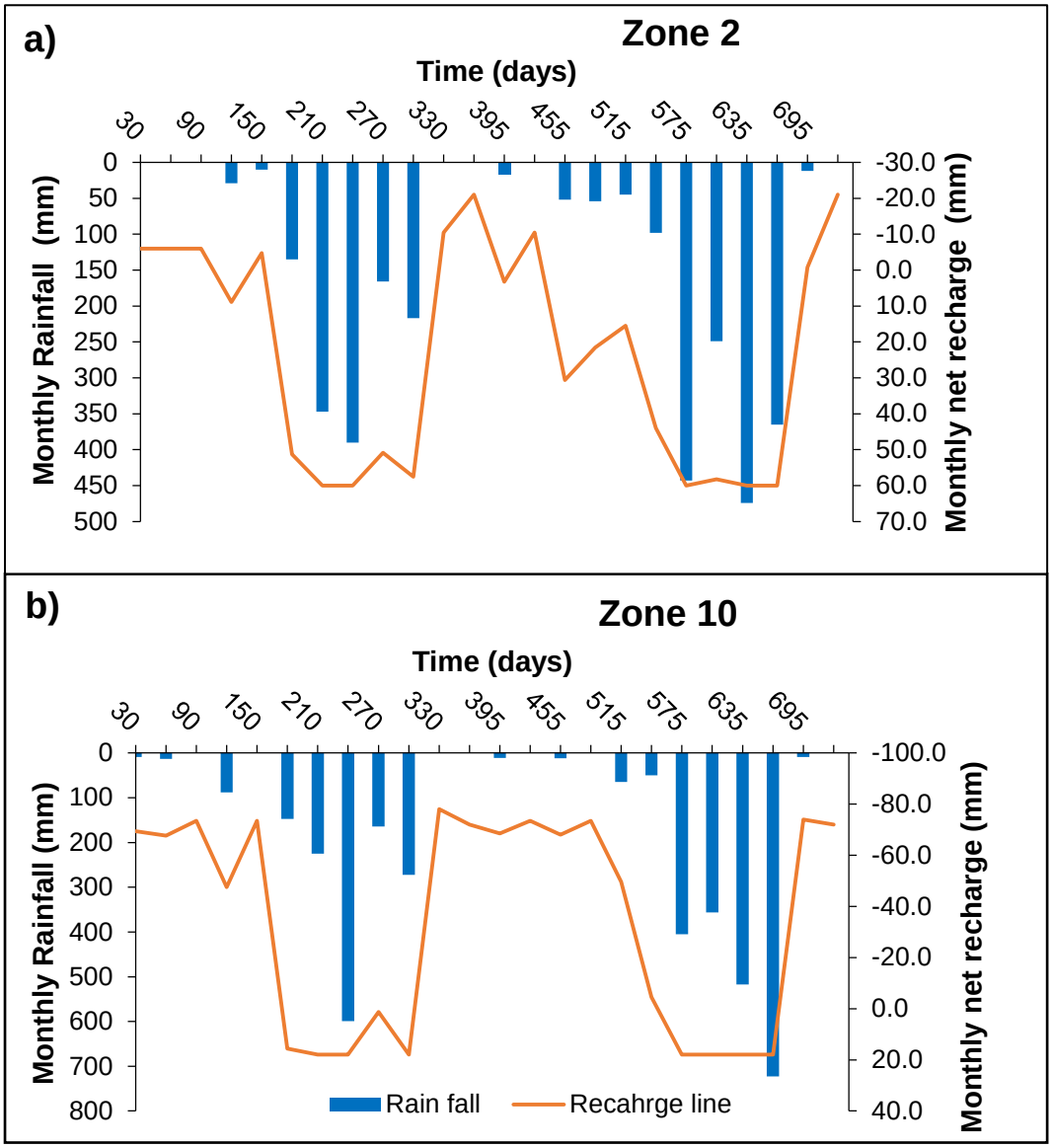

Figure 5.16 *Net recharge variation on the basis of monthly rainfall a) zone 2 with high recharge and low groundwater abstraction, b) zone 10 with low recharge and high groundwater abstraction (Calibration 2004-05)*

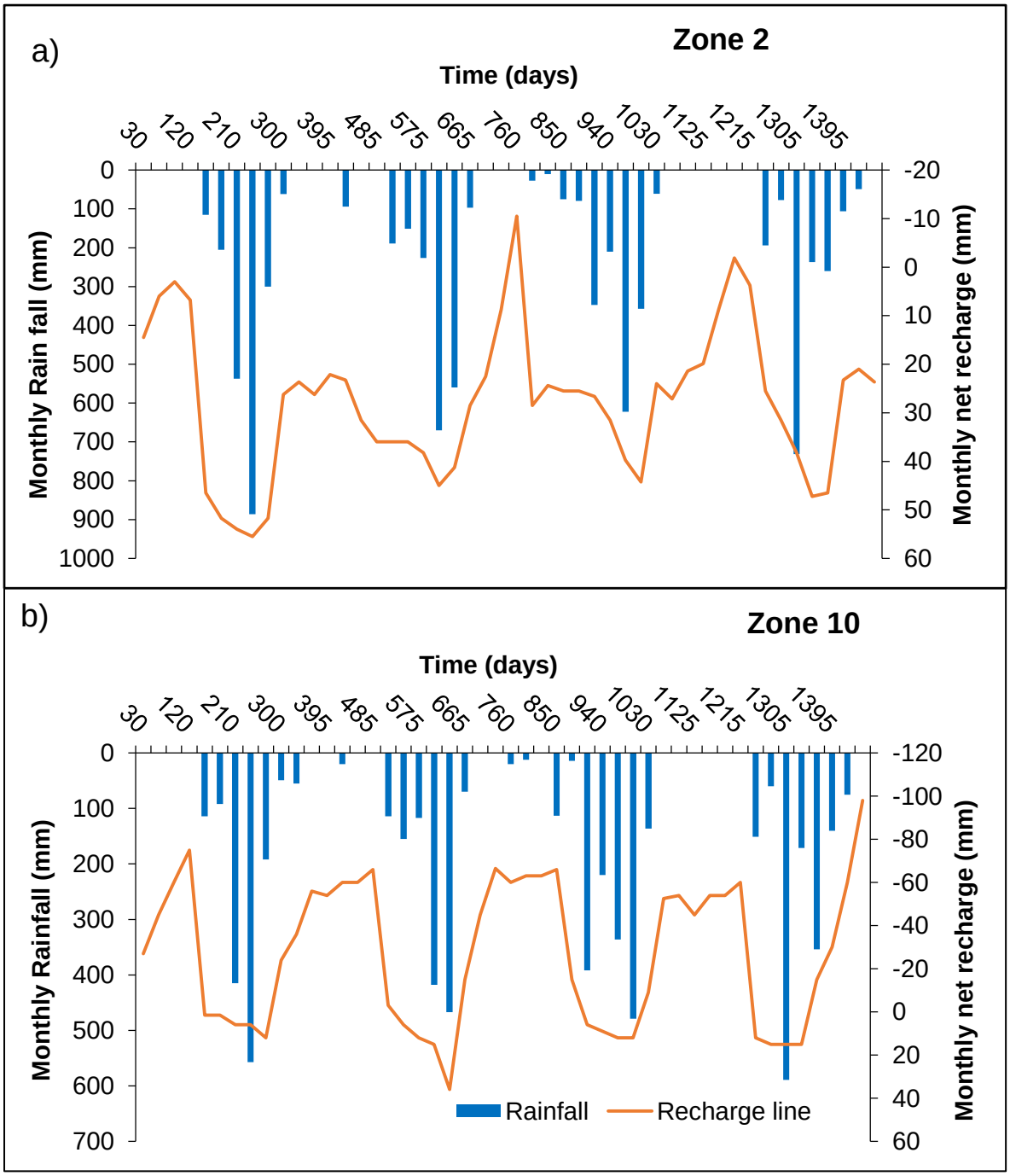

Figure 5.17 *Net recharge variation on the basis of monthly rainfall a) zone 2 with high recharge and low groundwater abstraction, b) zone 10 with low recharge and high groundwater abstraction (validation: 2006-09)*

5.3.4 Rainfall recharge

In present study, rainfall recharge was calculated for different zones (Fig. 5.18). The calculated recharge was assigned during calibration of groundwater model. After successful calibration, the same rainfall recharge factors were assigned during validation for different zones (Fig. 5.19).

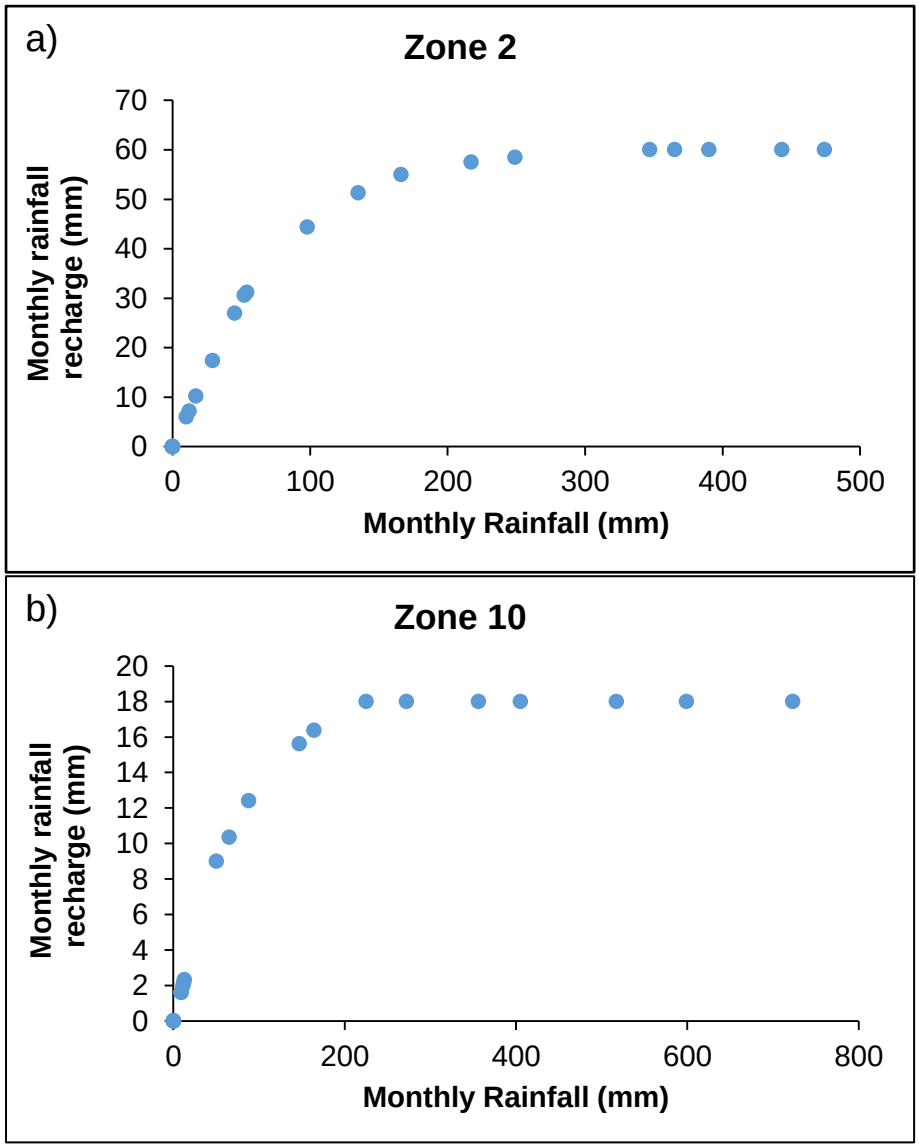

Figure 5.18 *Plot between monthly rainfall (mm) and monthly rainfall recharge (mm) a) Zone 2 with high rainfall recharge b) Zone 10 with low rainfall recharge (Calibration: 2004-05)*

Fig. 5.18 revealed the zone wise variation of rainfall recharge. The Zone 2 is located away from the sea coast with the highest rainfall recharge, whereas the Zone 10 located near the sea coast with low rainfall recharge. In both zones, the rainfall recharge increased with increase in rainfall. Gradually the two zones maintained a stability of recharge irrespective of high rainfall. The zone 2 showed a monthly maximum rainfall recharge of 70 mm, whereas the zone 10 showed less recharge of 18 mm (Fig. 5.18). Similarly, during validation the Zone 2 and Zone 10 showed the similar type of result, indicating that the rainfall recharge is not linear but becomes constant after a certain value (Fig. 5.19).

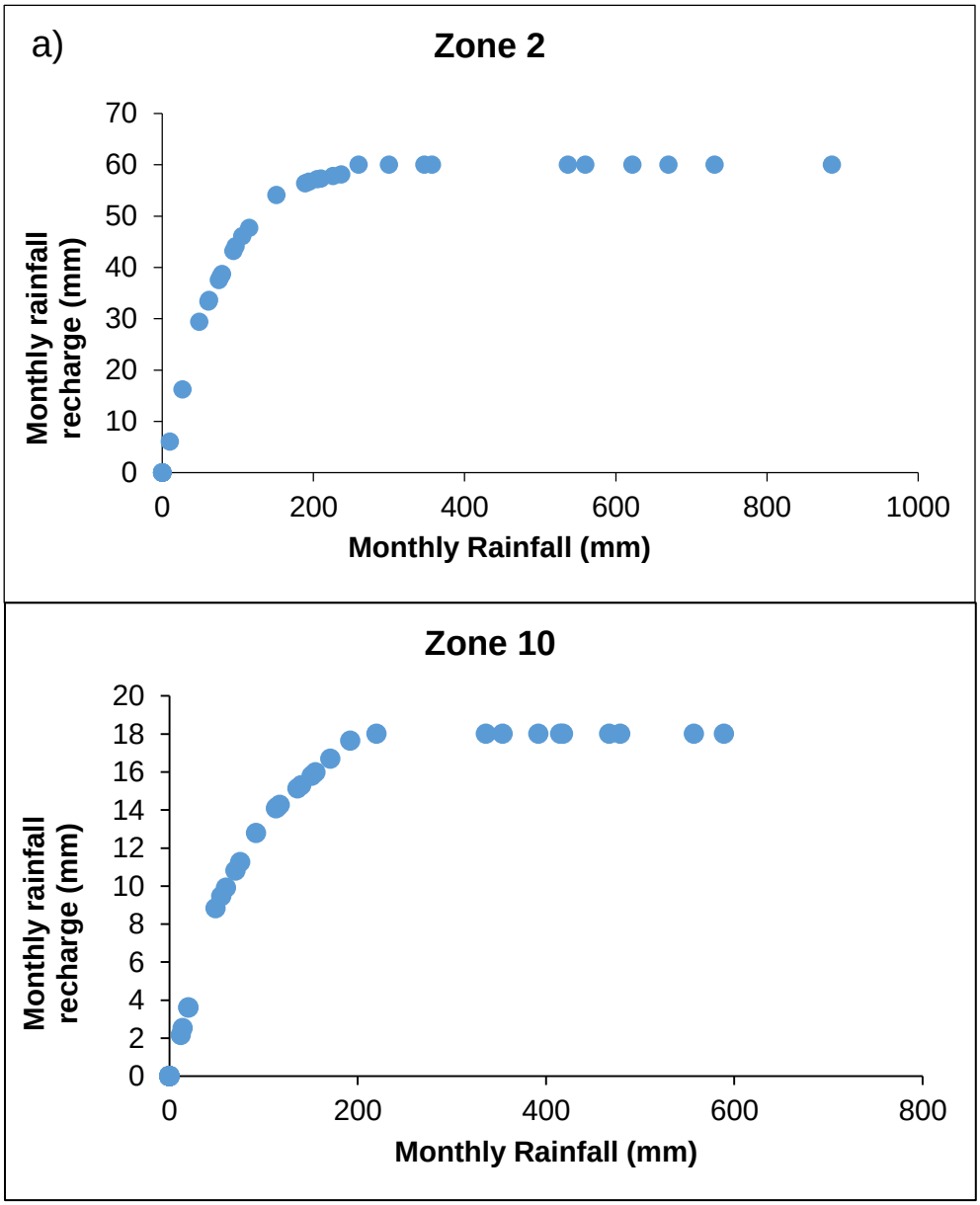

Figure 5.19 *Plot between monthly rainfall (mm) and monthly rainfall recharge (mm) a) Zone 2 with high rainfall recharge b) Zone 10 with low rainfall recharge (Validation: 2006-09)*

5.3.5 Parameter Estimation

The groundwater model parameters were also estimated by using Parameter Estimation Model (PEST) (Doherty, 2018). Knowling and Werner (2016) used PEST to minimize the weighted least squares objective function based on Tikhonov regularization. In the present study, the groundwater model was auto calibrated with the help of PEST module of MODFLOW to optimize the aquifer parameters (hydraulic conductivity and specific yield). The calibrated model showed a good correlation between the observed head value and calculated head value with correlation coefficient value of 0.993 (Fig. 5.20).

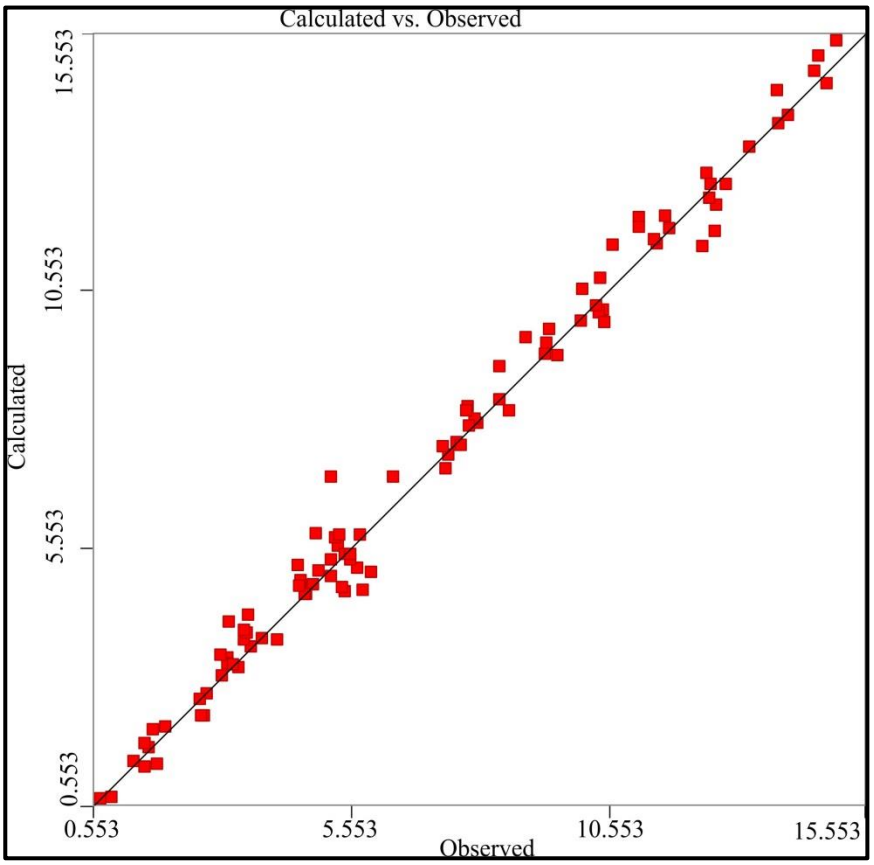

Figure 5.20 *Correlation plot between observed head and calculated head by PEST*

The automated calibrated (PEST) aquifer parameters (conductivity and specific yield) compared to the manual calibrated aquifer parameters are shown in in Table 5.4.

Table 5.4 Initial and PEST estimated aquifer parameters

Zones	**Initial Hydraulic parameters**		**PEST estimated parameters**	
	Hydraulic Conductivity (m/day)	***Specific Yield***	***Hydraulic Conductivity (m/day)***	***Specific Yield***
I	40	0.05	36.85	0.058
II	42	0.06	44.39	0.075
III	45	0.07	44.01	0.053

Uncertainty is the process through which the uncertainty on the estimated parameters is quantified to understand the risk associated with different groundwater management models (Delottier et al., 2017). In the present study, the estimated parameters such as hydraulic conductivity and specific yield by PEST tool were subjected to uncertainty analysis, which showed 95% confidence interval between 30.74 and 48.78 m/day for hydraulic conductivity, and 0.043 and 0.074 for specific yield (Table 5.5).

Table 5.5 Uncertainty analysis (95% confidence interval) by PEST

Zones	**Hydraulic conductivity (K) m/day**	**Specific Yield (S_y)**
I	30.746< K < 44.18	$0.046 < S_y < 0.074$
II	40.81 < K < 48.30	$0.048 < S_y < 0.076$
III	39.70 < K < 48.78	$0.043 < S_y < 0.067$

5.4 DISCUSSION

5.4.1 Interaction between aquifer and river

Both inflow from the rivers into the aquifer system and outflow from aquifer system to the rivers were observed in different time periods. The unconfined

coastal aquifer received water from rivers during pre-monsoon and post-monsoon period, whereas the excess amount of groundwater in the form of base flow discharge to the rivers were observed during monsoon season (Fig. 5.18a and 5.18b). The inflow from river boundary was estimated as 34 MCM during post-monsoon and pre-monsoon period in the years 2006 and 2007. In monsoon period, the unconfined coastal aquifer system supplied around 23 to 27 MCM of groundwater to the river system after irrigation (Fig. 5.21a and 5.21b). The deltaic aquifer system was mostly recharged by rainfall during the wet days. As depicted in Fig. 5.21c and 5.21d, the extraction of groundwater is different in different time periods. In post-monsoon time period withdrwal of groundwater was more than that of pre-monsoon period to provide water for post-monsoon crop, athough there was adequate availability of water in coastal areas to meet the monsoon period kharif crop (Mohanty et al., 2012; Rejani et al., 2008). The extracted groundwater for sustainibility of agricultural productivity and livelihoods in the post-monsoon season was estimated as approxmately 180 MCM in year 2006-07 (Fig. 5.21c and 5.21d). This implies that the heavy abstraction of groundwater for agriculture activity and other domestic uses declined the groundwater level of aquifer system, which resulted in river inflow into the aquifer sytem with river inflow of 33.92 MCM of water entering into this coastal aquifer due to pumpage of groundwater. During pre-monsoon time period the groundwater was extracted to fullfill the water demand for rabi crops, but the amount of water requrement was less than that of post-monsoon season. It was estimated by calculation that approximately 100 MCM of groundwater was pumped out for agricultural activity and other needs, which caused the inflow of water through river boundary. When there is groundwater stress, whether less or more, the river system gets affected.

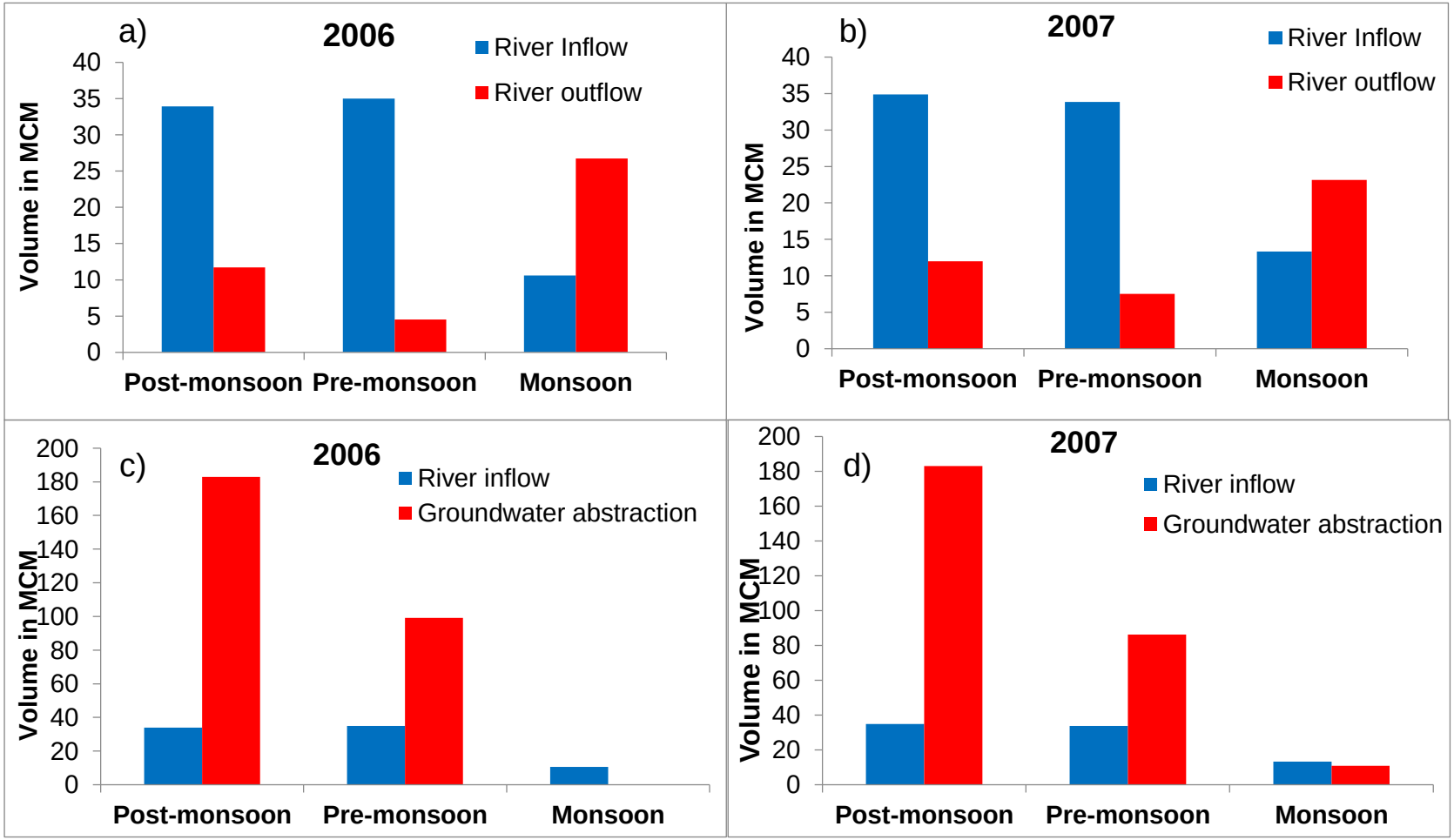

Figure 5.21 *River inflow to aquifer and outflow from aquifer in a) year 2006 and b) year 2007; river inflow into aquifer and groundwater abstraction c) in year 2006 and d) 2007*

The river-aquifer interaction showed a good correlation between river stage and the ouflow / inflow from river boundary (Fig. 5.22a and 5.22b). As the outflow from river boundary increased, the river stage also increased or vice versa. The estimated base flow of 7.81 MCM to the river caused highest river stage of 8 m in the month of August of monsoon period.

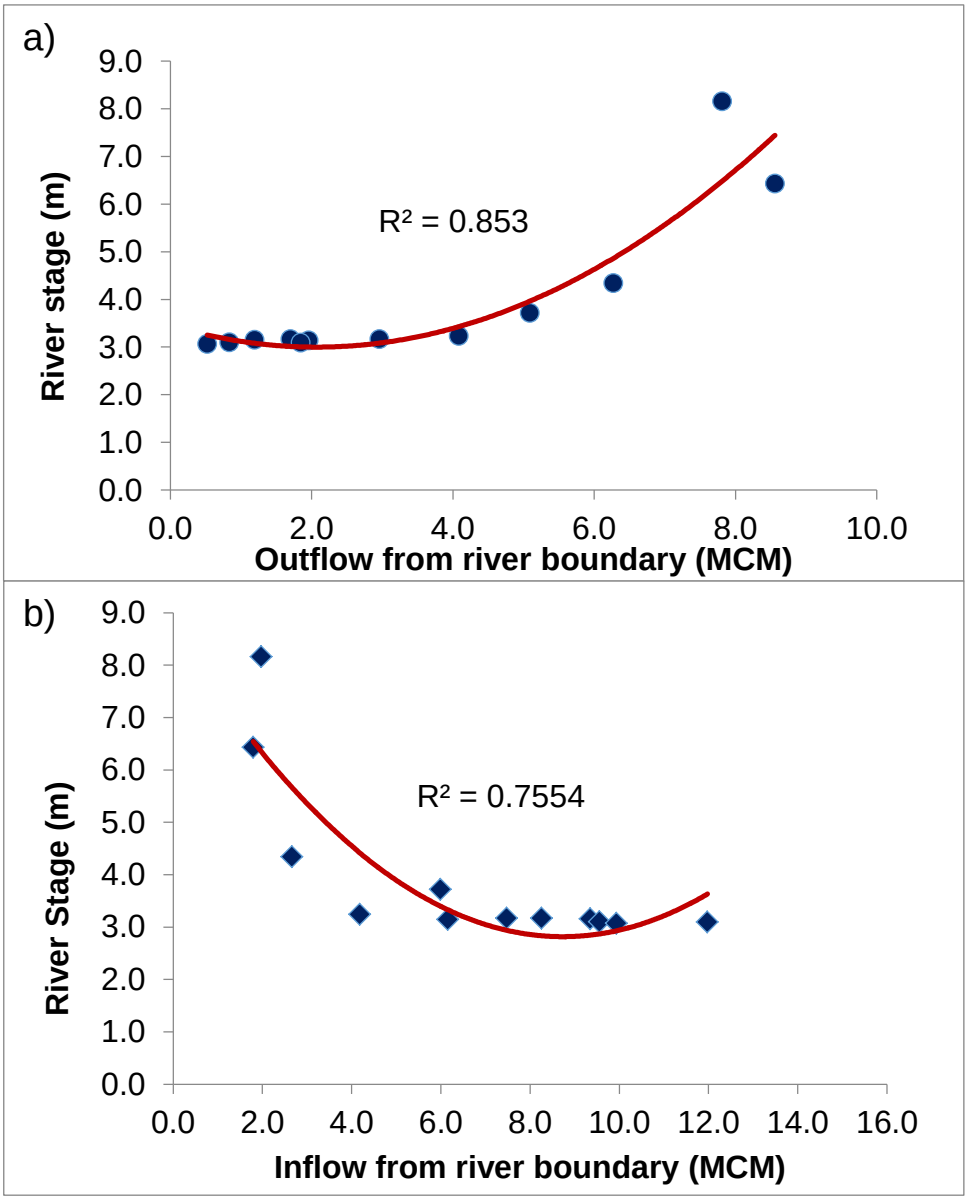

Figure 5.22 *A regression line between the river stage and groundwater volume a) the river stage Vs.outflow from the river boundary b) the river stage Vs. inflow the river boundary*

the inflow from river boundary to aquifer system during pre and post-monsoon time caused declination of river stage from 8 m to 3 m. According to the present estimation, approximately 10 MCM of water from river system entered into the aquifer syetm during this season, which showed the influence of groundwater flux on the river stage and a good interaction between river and the coastal aquifer system (Mohanty et al., 2012).

5.4.2 Groundwater level fluctuations

A spatio-temporal variation in groundwater level was observed in the present study in this coastal aquifer system. The Jagatsinghpur coastal area showed a head variation between 0.7 m to 15 m with an avarage head of 6 m. There was a rise in hydraulic head in all observation wells during monsoon period as compared to pre-monsoon period with an average rise of 1.84 m. This implies that the shallow aquifer of this coastal region gets recharged quickly due to rainfall events, which is also a good indication for sustainable groundwater management. The observation well (OW 6) situated away from the coastal tract of the study area showed the highest hydraulic head rise of 3.07 m. The lowest hydraulic head rise of 0.75 m was observed in observation well (OW 9), which is close to the Bay of Bengal. This spatial variation in hydraulic head rise depends on the rain fall intensity, type of soil and land use patterns. Groundwater stress was observed during pre-monsoon time period due to heavy abstraction of groundwater for irrigation and domestic use purposes, which resulted in decline in groundwater levels for 1 and 89 days as shown in Fig 5.23a and b. In case of monsoon and post-monsoon time period (243 days and 334 days), the hydraulic head increased from place to place, suggesting that the groundwater was being mostly recharged by rainfall and regained intermittently (Fig.5.23c and d). The close contour lines in the upper part of the study area showed the presence of high hydraulic gradient with high groundwater movement (Morgan et al., 2012; Sahoo and Jha, 2017) with a sluggish movement in the lower reaches (Fig. 5.23). The general groundwater flow direction is towards the Bay of Bengal i.e. in South East direction. However, theThe general groundwater flow direction is towards the Bay of Bengal i.e. in South East direction is maintained.

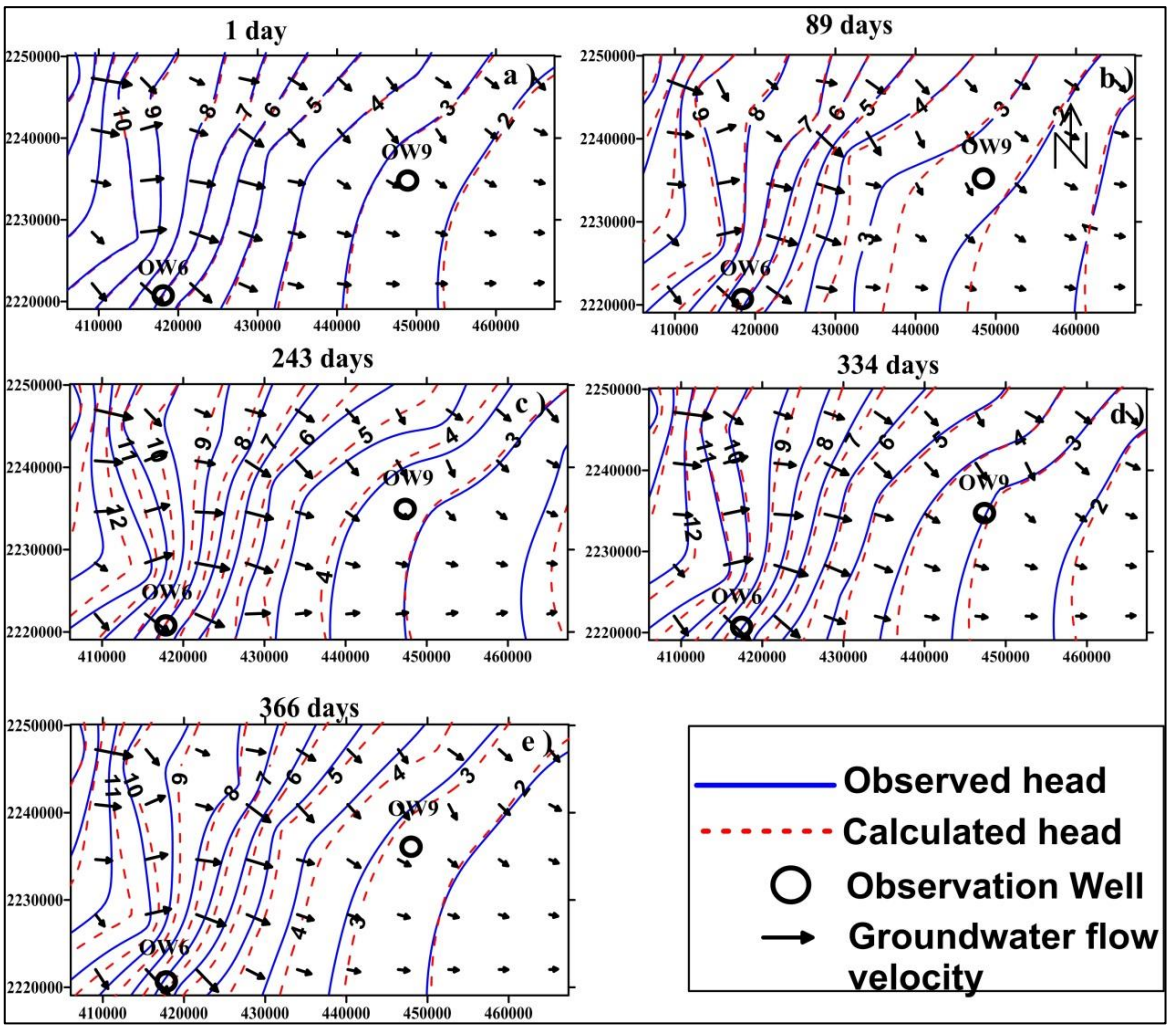

Figure 5.23 *Spatial and temporal variation of hydraulic head (m) in the study area*

5.4.3 Groundwater recharge

In the present study area, rainfall, seepage from the riverbed and irrigation returnflow were observed to be the major sources of groundwater recharge. Groundwater recharge estimation plays a vital role for optimal development and efficient management of fresh groundwater resource in costal areas (Callahan et al., 2012). Modelled recharge rates varied across recharge zones and from year to year due to large variation of rainfall over the simulation period. The temporal and spatial distribution of annual rainfall from year 2004 to year 2009 varied from 875 mm to 1229 mm. The average net recharge (rainfall recharge – groundwater draft) in the area varied from 247.89 to 262.63 million cubic meter (MCM) in year 2006-2007. The net recharge in post-monsoon is estimated to be less than that of pre-monsoon and monsoon period (Fig. 5.24). Approximately 6 to 15 MCM of water recharged the aquifer system during post-monsoon period, whereas 33 to 54 MCM

of water percolated into the aquifer system in pre-monsoon period. At the same time, a large extraction of groundwater led to less net recharge in post-monsoon season. As compared to the post and pre-monsoon season, the coastal aquifer system got recharged by rainfall which was estimated to be between 180.26 and 223.08 MCM.

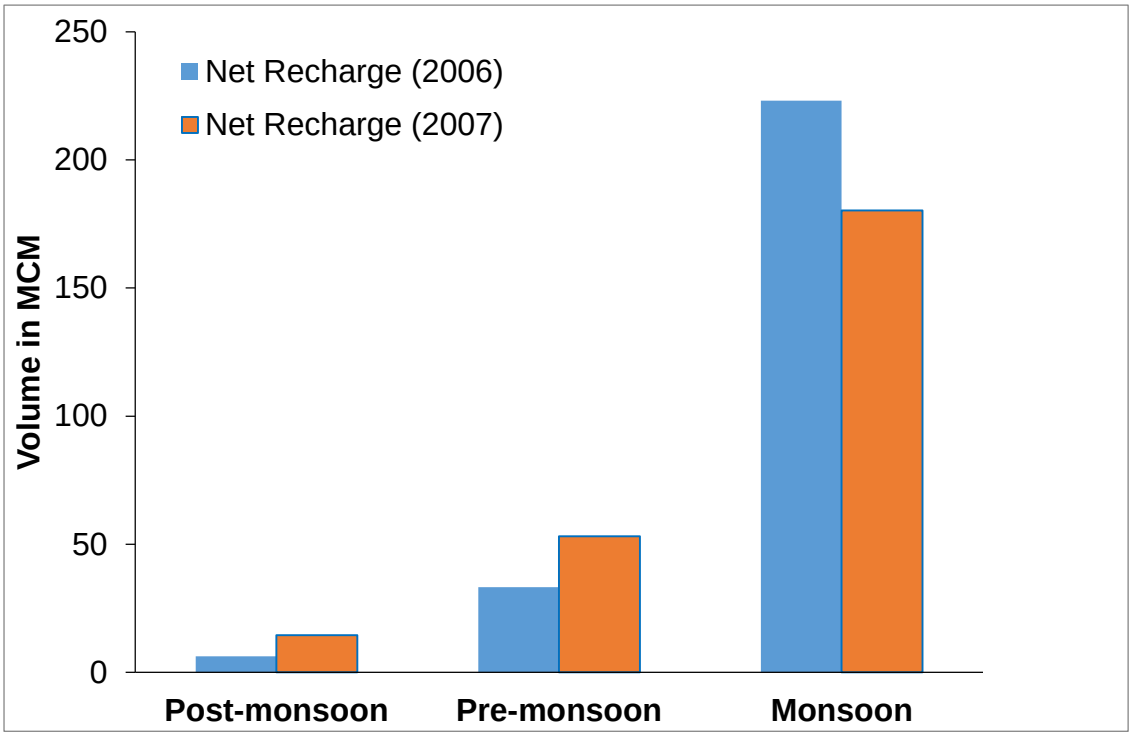

Figure 5.24 *Estimated net recharge in the study area in different time periods for year 2006-2007*

5.4.4 Saltwater intrusion

The saltwater intrusion effect has been identified in the lower part of the study area, which is close to the sea. This study is based on inflow from constant head boundary due to groundwater abstraction and depletion of hydraulic head during the non-monsoon time. In the groundwater model, estimated outflow and inflow from the Bay of Bengal indicated seawater intrusion in some areas. From the validation results, year 2006 and 2007 were considered for interpretation of seawater intrusion into the aquifer system. During pre-monsoon period of year 2006 and 2007, the inflow from the constant head ranged from 5.17 MCM to 5.36 MCM, whereas 1.94 MCM to 1.97 MCM of groundwater were discharged to the Bay of Bengal. The limited supply of groundwater was unable to prevent the

seawater ingress during pre-monsoon time and resulted in saltwater intrusion near the seacoast. However, the outflow or discharge of groundwater ranging from 3.76 to 4.84 MCM exceeded the inflow during monsoon season and prevented landward migration of seawater. This suggest that groundwater recharge is one of the important parameters to reduce the influence of seawater intrusion in shallow coastal aquifer system.

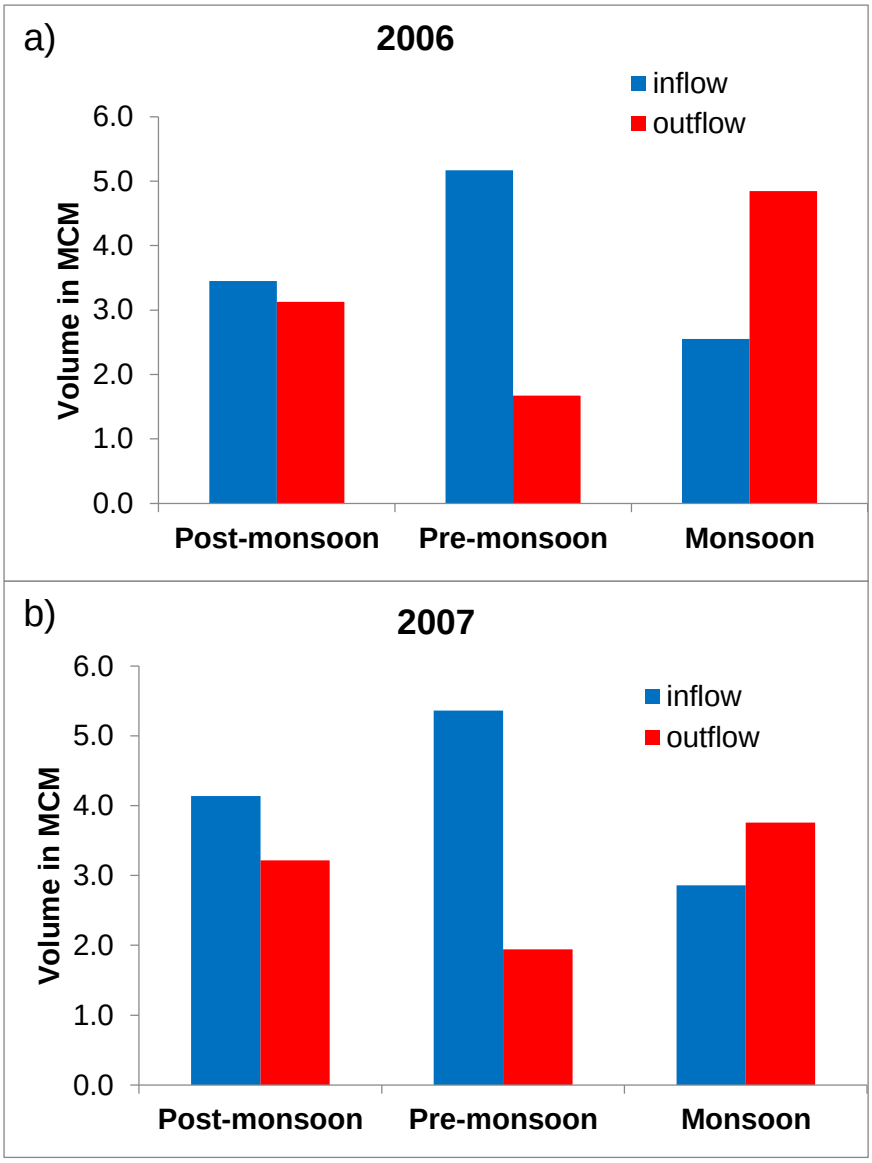

Figure 5.25 *Estimated inflow from Bay of Bengal during pre and post-monsoon time and outflow towards Bay of Bengal during monsoon time a) for year 2006 b) for year 2007*

The influence of seawater intrusion has been observed in the NE and Southern part of the study area during non monsoon time (1day,89 days and 365 days) as indicated by the reverse flow direction of groundwater (Rejani et al.,

2008) as shown in Fig. 5.25. As soon as monsoon commences, groundwater recharge takes place, leading to outward flow of groundwater from land when rainfall is high. The north-eastern part of the study area is affected by saltwater intrusion as the depletion of hydraulic head has been observed throughout the year (Fig. 5.26). During day 1, the head value was 6 m below mean sea level (MSL), and then it declined to 8 m below mean sea level (MSL) during pre-monsoon or dry time i.e. 89 days. Once again, the head value regained to its original position i.e. 6 m below sea level. The Paradeep port located in the north eastern part of study area (Fig. 3.5) has also an industrial and urbanization built up. The increasing water demand for domestic and agricultural activity declined the groundwater level and caused seawater intrusion. The observation wells OW8, OW9, OW10 and OW11 are located close to the sea coast (Fig. 5.26). The groundwater abstraction and reduction in recharge in Jagatsinghpur coastal aquifer caused decline in hydraulic head at different times. In addition, the decline in hydraulic head accounted for seawater intrusion as shown in Fig. 5.17.

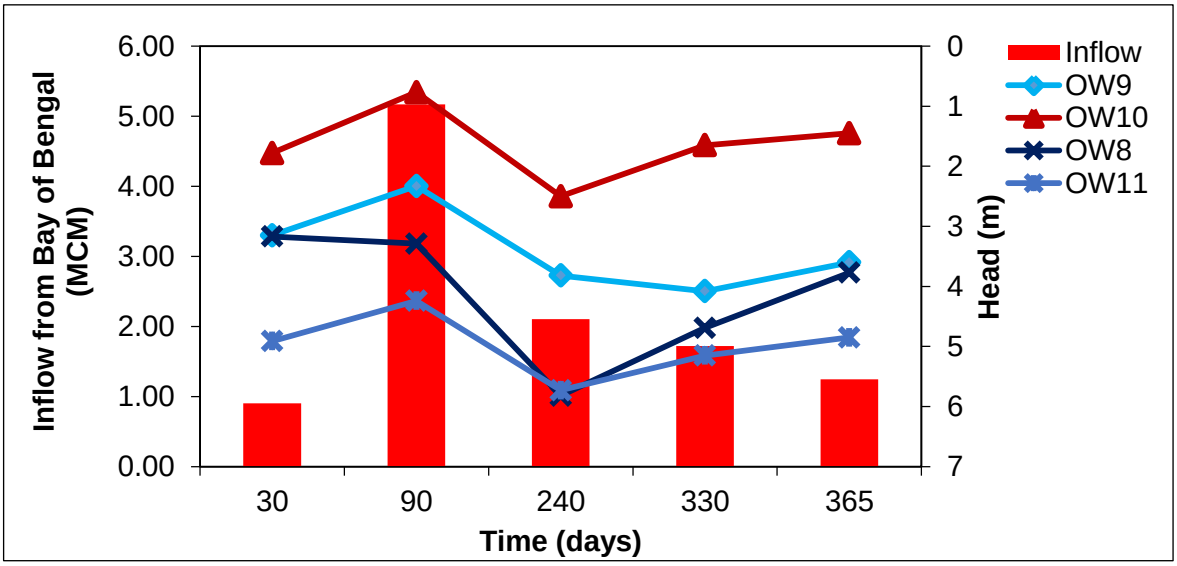

Figure 5.26 *Map showing variation in head value of observation wells (OW8-OW11) near seacoast causes inflow from constant head boundary.*

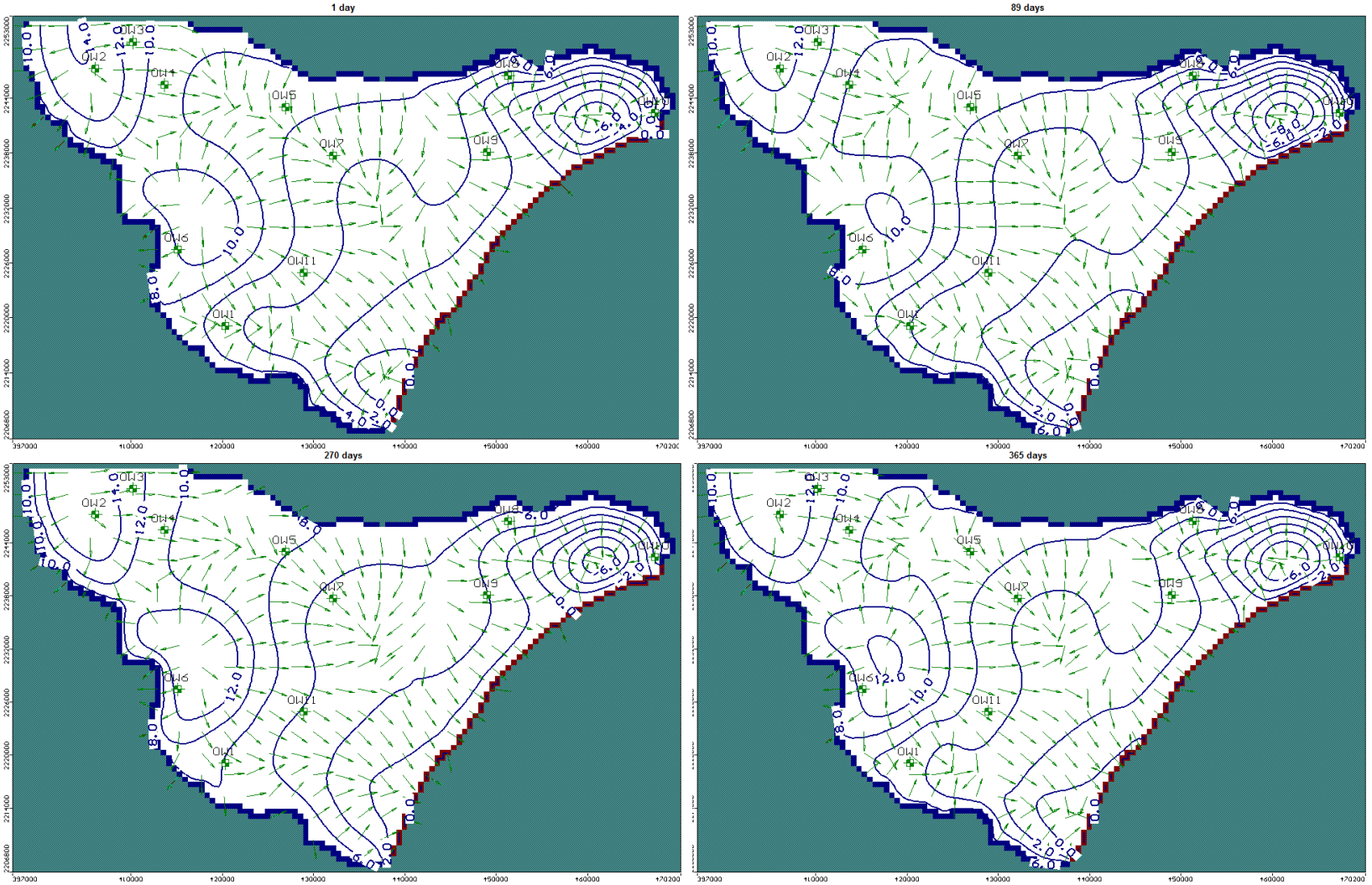

Figure 5.27 *Groundwater flow direction with changing of hydraulic head in different time periods (1 day, 89 days, 270 days and 365 days) of year 2006.*

6.1 CONCLUSIONS

The present study on saltwater intrusion modeling in Jagatsinghpur coastal aquifer was approached with two main objectives and the conclusions inferred thereby are:

6.1.1 Objective 1

Identification of the causes of groundwater salinity in coastal aquifer system in Jagatsinghpur coastal region

6.1.1.1 Conclusion

- For the first time, hydrochemical analysis and isotopic evidences were used to identify the seawater signature in the coastal aquifer system of the Mahandi delta, Bay of Bengal.
- Groundwater in the upper part of the Mahanadi deltaic region is Ca-HCO_3 type with less concentration of Mg^{2+} and Na^{+}, suggesting dissolution of carbonate minerals in the aquifer system.
- The hydro-chemical facies gradually changed from Ca-HCO_3 type to Na-Ca-HCO_3 type along the groundwater flow direction, where Ca was exchanged by Na.
- The groundwater in the lower part of the delta was characterized as Na-Cl and Na, (Mg,Ca)-Cl types of water with moderate to high salinity. The ionic ratios like Na^{+} / Cl^{-}, HCO^{-}_3 / Cl^{-}, Mg^{2+}/ Ca^{2+}, SO_4^{2-}/ Cl^{-}, Ca^{2+}/ (HCO^{-}_3/ SO_4^{2-}) were interpreted to understand the salinization process.
- The chemical evolution of groundwater suggested that the groundwater in the lower part of Mahanadi delta was affected mainly by seawater intrusion. The ratio of Mg^{2+} /Ca^{2+} less of than 1 and SI < 0 in most of the groundwater samples of the Upper delta formation of the study area concluded that the groundwater in the aquifer system is Ca-rich. In contrast, the interpreted Mg^{2+} /Ca^{2+} ratio value (>1) and SI (>1 and close to 0) suggested the occurrence of Mg-rich groundwater in the Lower delta formation of the study area, which is due to the mixing of sea water and fresh groundwater.

- The saline groundwater in deeper aquifer was derived from seawater and the source of salinity is characterized by mixing of seawater and fresh groundwater, which was supported by the enriched stable isotopic composition and its good positive correlation with chloride content.
- The conceptual model based on groundwater chemistry revealed that the groundwater in deep well very close to sea coast was highly contaminated by seawater ingress with 72% of seawater, while the shallow well remained unaffected by seawater. The groundwater in the lower delta formation is more vulnerable in both quality and quantity than the upper delta formation

6.1.2 Objective 2

Estimation of groundwater recharge and factors for seawater intrusion in the Jagatsinghpur coastal aquifer system.

6.1.2.1 Conclusion

- For the first time, a groundwater model was developed to estimate and understand the dynamics of groundwater recharge in the delta region of Jagtsinghpur in Odisha state along the Bay of Bengal in India.
- The simulated heads matched with the observed heads and showed that the groundwater flow direction in the area was mainly towards southeast (SE) direction, i.e., towards the Bay of Bengal.
- Under steady state condition, the RMSE and correlation coefficient values are 0.455 m and 0.999 respectively, which means the model was well calibrated before further validation process.
- RMSE values for calibrated and validated model are 0.453 m and 0.627 m respectively under transient state condition, whereas the respective correlation coefficient values for calibrated and validated model are 0.994 and 988.
- The horizontal hydraulic conductivity and the specific yield values in the study area varied from 40 m/day to 45 m/day and 0.05 to 0.07 respectively.
- The aquifer parameters (hydraulic conductivity and specific yield) estimated by PEST tool and by trial and error method were very close

to the initial and lie within the range of parameters estimated by pump test.

- Uncertainty analysis at 95% confidence level indicated the range of hydraulic conductivity between 39.70 and 48.43 m/day.
- The shallow coastal aquifer was influenced by the river system. The estimated groundwater abstraction (180 MCM) led to inflow from the river during non-monsoon time. Further, the excess amount of groundwater as base flow during monsoon period recharged the river. This phenomenon had also affected the river stage, in which the out flow from river boundary caused an increase of river stage. A decline of river water level occurred as heavy extraction of groundwater was carried out for agricultural purposes.
- The temporal and spatial groundwater level variation was mainly controlled by rainfall and gradient in this deltaic aquifer system. The zone wise recharge distribution reveals that the zones near the sea coast received less rainfall recharge as compared to the zones away from the Bay of Bengal. However, the groundwater pumping in zones close to sea coast was observed to be more than that of zones present away from the Bay of Bengal.
- Depletion in hydraulic head due to over pumping in the coastal aquifer system resulted in seawater ingress. It is estimated that the inflow from Bay of Bengal ranged from 5.17 MCM to 5.36 MCM.

6.2 FUTURE SCOPE

The work done in this thesis can be extended for further future work with multi aquifer system and various flow conditions. Due to lack of available data of other aquifers, the present modeling technique could not be applied for multi aquifers. As seawater intrusion is the main concern in this region, chemical transport modeling needs to be developed in detail and management strategies implemented keeping various climate change and utility scenarios.

BIBLIOGRAPHY

Abou Zakhem, B., Hafez, R., 2007. Environmental isotope study of seawater intrusion in the coastal aquifer (Syria). **Environmental Geology** 51, 1329–1339.

Abu-Khader, M.M., Shawaqfeh, A.T., Naddaf, Z., Maity, J.P., Bhattacharya, P., 2018. Radon in the groundwater in the Amman-Zarqa Basin and related environments in Jordan. **Groundwater for Sustainable Development** 7, 73–81.

Adepelumi, A.A., Ako, B.D., Ajayi, T.R., Afolabi, O., Omotoso, E.J., 2009. Delineation of saltwater intrusion into the freshwater aquifer of Lekki Peninsula, Lagos, Nigeria. **Environmental Geology** 56, 927–933.

Adrian, D.W., Bakker, M., Vincent, E.A.P., Alexander, V., Lua, C., Behzad, A., Sim, C.T., Barry, D.A., 2013. Seawater intrusion processes, investigation and management : Recent advances and future challenges. **Advances in Water Resources** 51, 3–26.

Alcamo, J., Henrichs, T., Rösch, T., 2000. World Water in 2025 World Commission on Water for the 21 Century. pp 49.

Allen, D.M., Suchy, M., 2001. Geochemical evolution of groundwater on Saturna Island, British Columbia. **Canadian Journal of Earth Sciences** 38, 1059–1080.

Andersen, M.S., Nyvang, V., Jakobsen, R., Postma, D., 2005. Geochemical processes and solute transport at the seawater/freshwater interface of a sandy aquifer. **Geochimica et Cosmochimica Acta** 69, 3979–3994.

Anderson, M.P., Woessner, W.W., 1992. Applied groundwater modeling, Academic, San Diego, Calif. pp 381.

Appelo, C.A.J., Postma, D., 2004. Geochemistry, groundwater and pollution. CRC press.

Arfib, B., De Marsily, G., 2004. Modeling the salinity of an inland coastal brackish karstic spring with a conduit-matrix model. **Water Resources Research** 40, 1–10.

Baena-Ruiz, L., Pulido-Velazquez, D., Collados-Lara, A.J., Renau-Pruñonosa, A., Morell, I., 2018. Global Assessment of Seawater Intrusion Problems (Status and Vulnerability). **Water Resources Management** 32, 2681–2700.

Barlow, P.M., 2013. Ground Water in fresh water-salt water environments of the Atlantic, Geological Survey (USGS).

Barlow, P.M., Reichard, E.G., 2010. Saltwater intrusion in coastal regions of North America. **Hydrogeology Journal** 18, 247–260.

Basu, A. R., Jacobsen, S. B., Poreda, R. J., Dowling, C. B., Aggarwal, P. K. 2001. Large groundwater strontium flux to the oceans from the Bengal Basin and the marine strontium isotope record. **Science** 293 1470-1473.

Bear, J., Cheng, A.H.-D., Sorek, S., Ouazar, D., Herrera, I., 1999. Seawater intrusion in coastal aquifers: concepts, methods and practices. Springer Science & Business Media. pp 632.

Behera, A.K., Chakrapani, G.J., and Kumar, S. 2018. Identification of seawater intrusion signatures through geochemical evolution of groundwater: A case study based on coastal region of the Mahanadi delta, Bay of Bengal, India. (Manuscript submitted to journal and is under consideration for publication).

Behera, A.K., Kumar, S. and Chakrapani G.J. Groundwater dynamics in shallow coastal aquifers of Mahanadi delta, Bay of Bengal Coast, India. (Manuscript submitted to journal and is under review process).

Biswal, S., Jha, M.K., Sharma, S.P., 2018. Hydrogeologic and hydraulic characterization of aquifer and nonaquifer layers in a lateritic terrain (West Bengal, India). **Hydrogeology Journal** 26, 1947–1973.

Bobba, A.G., 2002. Numerical modelling of salt-water intrusion due to human activities and sea-level change in the Godavari Delta, India. **Hydrological Sciences Journal** 47, S67–S80.

Callahan, T.J., Vulava, V.M., Passarello, M.C., Garrett, C.G., 2012. Estimating groundwater recharge in lowland watersheds. **Hydrological Processes** 26, 2845–2855.

Calvache, M.L., Pulido-Bosch, A., 1994. Modeling the Effects of Salt-Water Intrusion Dynamics for a Coastal Karstified Block Connected to a Detrital Aquifer. **Groundwater** 32, 767–777.

Cary, L., Petelet-Giraud, E., Bertrand, G., Kloppmann, W., Aquilina, L., Martins, V., Hirata, R., Montenegro, S., Pauwels, H., Chatton, E., Franzen, M., Aurouet, A., Lasseur, E., Picot, G., Guerrot, C., Fléhoc, C., Labasque, T., Santos, J.G., Paiva, A., Braibant, G., Pierre, D., 2015. Origins and processes of groundwater salinization in the urban coastal aquifers of Recife (Pernambuco, Brazil): A multi-isotope approach. **Science of the Total Environment** 530–531, 411–429.

CGWB, 2014. Report on Status of Ground Water Quality in Costal Aquifers of India. pp 130.

CGWB, 2013. Groundwater Information Booklet. pp 25.

Chandrajith, R., Diyabalanage, S., Premathilake, K.M., Hanke, C., van Geldern, R., Barth, J.A.C., 2016. Controls of evaporative irrigation return flows in comparison to seawater intrusion in coastal karstic aquifers in northern Sri Lanka: Evidence from solutes and stable isotopes. **Science of the Total Environment** 548–549, 421–428.

Chang, S.W., Clement, T.P., Simpson, M.J., Lee, K.-K., 2011. Does sea-level rise have an impact on saltwater intrusion? **Advances in Water Resources** 34, 1283–1291.

Charette, M. A., Sholkovitz, E. R., Hansel, C. M. 2005. Trace element cycling in a subterranean estuary: Part 1. Geochemistry of the permeable sediments. **Geochimica et Cosmochimica Acta** 69, 2095-2109.

Charette, M. A., Sholkovitz, E. R. 2002. Oxidative precipitation of groundwater-derived ferrous iron in the subterranean estuary of a coastal bay. **Geophysical research letters** 29, 85-1.

Chhotray, V., Few, R., 2012. Post-disaster recovery and ongoing vulnerability: Ten years after the super-cyclone of 1999 in Orissa, India. **Global Environmental Change** 22, 695–702.

Clark, I.D., Fritz, P., 2013. Environmental isotopes in hydrogeology. CRC press. pp 312.

Custodio, E., 2010. Coastal aquifers of europe: an overview. **Hydrogeology Journal** 18, 269–280.

Custodio, E., 1987. Seawater intrusion in the Llobregat delta, near Barcelona (Catalonia, Spain). **Groundwater Problems in Coastal Areas. Studies and Reports in Hydrogeology** 436–463.

Custodio, E., Bruggeman, G.A., 1987. Groundwater problems in coastal areas. Cambridge University Press, Cambridge. pp 610.

Das, A., Datta, B., 2001. Simulation of seawater intrusion in coastal aquifers: Some typical responses. **Sadhana** 26, 317–352.

Das, A., Datta, B., 2000. Optimization based solution of density dependent seawater intrusion in coastal aquifers. **Journal of Hydrologic Engineering** 5, 82–89.

Das, A., Datta, B., 1995. Simulation of density dependent 2-D seawater intrusion in coastal aquifers using nonlinear optimization algorithm. **American Water Resources Association, 950 Herndon Parkway, Suite 300, Herndon, Va 22070-5528 (USA). Vp.**

Das, P.P., Sahoo, H.K., Mohapatra, P.P., 2016. An integrative geospatial and hydrogeochemical analysis for the assessment of groundwater quality in Mahakalapara Block, Odisha, India. **Environmental Earth Sciences** 75, 1–18.

Datta, B., Vennalakanti, H., Dhar, A., 2009. Modeling and control of saltwater intrusion in a coastal aquifer of Andhra Pradesh , India. **Journal of Hydro-Environment Research** 3, 148–159.

Debnath, P., Mukherjee, A. 2016. Quantification of tidally-influenced seasonal groundwater discharge to the Bay of Bengal by seepage meter study. **Journal of hydrology** 537, 106-116.

Debnath, P., Mukherjee, A., Das, K. 2018. Characterization of tidally influenced seasonal nutrient flux to the Bay of Bengal and its implications on the coastal ecosystem. **Hydrological processes** 32, 1282-1300.

de Montety, V., Radakovitch, O., Vallet-Coulomb, C., Blavoux, B., Hermitte, D., Valles, V., 2008. Origin of groundwater salinity and hydrogeochemical processes in a confined coastal aquifer: Case of the Rhône delta (Southern France). **Applied Geochemistry** 23, 2337–2349.

Delottier, H., Pryet, A., Dupuy, A., 2017. Why Should Practitioners be Concerned about Predictive Uncertainty of Groundwater Management Models? **Water Resources Management** 31, 61–73.

Delsman, J.R., 2015. Saline groundwater – Surface water interaction in coastal lowlands, IOS Press. pp 194.

Demirel, Z., 2004. The history and evaluation of saltwater intrusion into a coastal aquifer in Mersin , Turkey. **Journal of Environmental Management** 70, 275–282.

Demlie, M., Wohnlich, S., Gizaw, B., Stichler, W., 2007. Groundwater recharge in the Akaki catchment, central Ethiopia: evidence from environmental isotopes ($\delta^{18}O$, $\delta^{2}H$ and ^{3}H) and chloride mass balance. **Hydrological Processes** 21, 807–818.

Doherty, J., 2018. PEST Surface Water Utilities User's Manual. pp 364.

Dube, S.K., Chittibabu, P., Rao, A.D., Sinha, P.C., Murty, T.S., 2000. Sea levels and coastal inundation due to tropical cyclones in indian coastal regions of andhra and orissa. **Marine Geodesy** 23, 65–73.

Eissa, M.A., Thomas, J.M., Pohll, G., Shouakar-Stash, O., Hershey, R.L., Dawoud, M., 2016. Groundwater recharge and salinization in the arid coastal plain aquifer of the Wadi Watir delta, Sinai, Egypt. **Applied Geochemistry** 71, 48–

62.

Epstein, S., Mayeda, T., 1953. Variation of O^{18} content of waters from natural sources. **Geochimica et Cosmochimica Acta** 4, 213–224.

Essaid, H.I., 1990. A multilayered sharp interface model of coupled freshwater and saltwater flow in coastal systems: model development and application. **Water Resources Research** 26, 1431–1454.

Fass, T., Cook, P.G., Stieglitz, T., Herczeg, A.L., 2007. Development of saline ground water through transpiration of sea water. **Ground Water** 45, 703–710.

Ferguson, G., Gleeson, T., 2012. Vulnerability of coastal aquifers to groundwater use and climate change. **Nature Climate Change** 2, 342-345.

Finney, B.A., Samsuhadi, Willis, R., 1992. Quasi-three-dimensional optimization model of Jakarta basin. **Journal of Water Resources Planning and Management** 118, 18–31.

Flores-Márquez, E.L., Campos-Enríquez, J.O., Chávez-Segura, R.E., Castro-García, J.A., 1998. Saltwater intrusion of the Costa de Hermosillo aquifer, Sonora, Mexico: A numerical simulation. **Geofisica Internacional** 37, 133–151.

Galeati, G., Gambolati, G., Neuman, S.P., 1992. Coupled and partially coupled Eulerian-Lagrangian model of freshwater-seawater mixing. **Water Resources Research** 28, 149–165.

Ghabayen, S.M.S., McKee, M., Kemblowski, M., 2006. Ionic and isotopic ratios for identification of salinity sources and missing data in the Gaza aquifer. **Journal of Hydrology** 318, 360–373.

Giambastiani, B.M.S., Antonellini, M., Oude Essink, G.H.P., Stuurman, R.J., 2007. Saltwater intrusion in the unconfined coastal aquifer of Ravenna (Italy): A numerical model. **Journal of Hydrology** 340, 91–104.

Gleeson, T., Befus, K.M., Jasechko, S., Luijendijk, E., Cardenas, M.B., 2016. The global volume and distribution of modern groundwater., Nature Geoscience.

Green, N.R., MacQuarrie, K.T.B., 2014. Une évaluation de l'importance relative des effets du changement climatique et du prélèvement d'eau souterraine sur l'intrusion d'eau marine dans les aquifères côtiers du Canada atlantique. **Hydrogeology Journal** 22, 609–623.

Guo, W., Langevin, C.D. and Bennett, G.D., 2001. Improvements to SEAWAT and Applications of the Variable-Density Modeling Program in Southern Florida. In Poeter, E., and others, MODFLOW 2001 and Other Modeling Odysseys Conference, Colorado School of Mines, Golden, Colorado. 2, 621-627.

Gupta, S.K., Deshpande, R.D., 2005. Groundwater isotopic investigations in India: What has been learned? **Current Science** 89, 825–835.

Gupta, S.K., Deshpande, R.D., Bhattacharya, S.K., Jani, R.A., 2005. Groundwater δ18O and δD from central Indian Peninsula: Influence of the Arabian Sea and the Bay of Bengal branches of the summer monsoon. **Journal of Hydrology** 303, 38–55.

Gurunadha Rao, V.V.S., Tamma Rao, G., Surinaidu, L., Mahesh, J., Mallikharjuna Rao, S.T., Mangaraja Rao, B., 2013. Assessment of geochemical processes occurring in groundwaters in the coastal alluvial aquifer. **Environmental Monitoring and Assessment** 185, 8259–8272.

Hallaji, K., Yazicigil, H., 1996. Optimal Management of a Coastal Aquifer in Southern Turkey. **Journal of Water Resources Planning and Management** 122, 233–244.

Han, D., Kohfahl, C., Song, X., Xiao, G., Yang, J., 2011. Geochemical and isotopic evidence for palaeo-seawater intrusion into the south coast aquifer of Laizhou Bay, China. **Applied Geochemistry** 26, 863–883.

Han, D., Post, V.E.A., Song, X., 2015. Groundwater salinization processes and reversibility of seawater intrusion in coastal carbonate aquifers. **Journal of Hydrology** 531, 1067–1080.

Han, D.M., Song, X.F., Currell, M.J., Tsujimura, M., 2012. Using chlorofluorocarbons (CFCs) and tritium to improve conceptual model of groundwater flow in the South Coast Aquifers of Laizhou Bay, China.

Hydrological Processes 26, 3614–3629.

Han, D.M., Song, X.F., Currell, M.J., Yang, J.L., Xiao, G.Q., 2014. Chemical and isotopic constraints on evolution of groundwater salinization in the coastal plain aquifer of Laizhou Bay, China. **Journal of Hydrology** 508, 12–27.

Harbaugh, A.W., Banta, E.R., Hill, M.C., McDonald, M.G., 2000. MODFLOW-2000, The U. S. Geological Survey Modular Ground-Water Model-User Guide to Modularization Concepts and the Ground-Water Flow Process. **Open-File Report. U. S. Geological Survey** 134.

Harmon, C., 1961. Standard for Reporting Concentrations of Deuterium and Oxygen-18 in Natural Waters. **Science** 133, 1833–1834.

Hinrichsen, D., 2007. Ocean planet in decline. **People and the Planet. Available:[Online] Http://Www. Peopleandplanet. Net**.

Holländer, H.M., Mull, R., Panda, S.N., 2009. A concept for managed aquifer recharge using ASR-wells for sustainable use of groundwater resources in an alluvial coastal aquifer in Eastern India. **Physics and Chemistry of the Earth** 34, 270–278.

Huang, G., Sun, J., Zhang, Y., Chen, Z., Liu, F., 2013. Impact of anthropogenic and natural processes on the evolution of groundwater chemistry in a rapidly urbanized coastal area, South China. **Science of The Total Environment** 463–464, 209–221.

Huyakorn, P.S., Andersen, P.F., Mercer, J.W., White, H.O., 1987. Saltwater intrusion in aquifers: Development and testing of a three-dimensional finite element model. **Water Resources Research** 23, 293–312.

Intergovernmental Panel on Climate Change, 2007.

Jacobson, G., Lau, J.E., 1994. Groundwater pollution in Australian regional aquifers.

Kanagaraj, G., Elango, L., Sridhar, S.G.D., Gowrisankar, G., 2018. Hydrogeochemical processes and influence of seawater intrusion in coastal aquifers south of Chennai, Tamil Nadu, India. **Environmental Science and**

Pollution Research 25, 8989–9011.

Knowling, M.J., Werner, A.D., 2016. Estimability of recharge through groundwater model calibration: Insights from a field-scale steady-state example. **Journal of Hydrology** 540, 973–987.

Kumar, K.S.A., Priju, C.P., Prasad, N.B.N., 2015. Study on Saline Water Intrusion into the Shallow Coastal Aquifers of Periyar River Basin, Kerala Using Hydrochemical and Electrical Resistivity Methods. **Aquatic Procedia** 4, 32–40.

Kumar, M., Herbert, R., Ramanathan, A., Someshwar Rao, M., Kim, K., Deka, J.P., Kumar, B., 2013. Hydrogeochemical zonation for groundwater management in the area with diversified geological and land-use setup. **Chemie Der Erde - Geochemistry** 73, 267–274.

Lacombe, P.J., Carleton, G.B., 2002. Hydrogeologic framework, availability of water supplies, and saltwater intrusion, Cape May County, New Jersey, USGS, Water-Resources Investigations Report 01-4246. pp 165.

Langevin, C.D., 2003. Simulation of Submarine Ground Water Discharge to a Marine Estuary: Biscayne Bay, Florida. **Ground Water** 41, 758–771.

Larsen, F., Tran, L.V., Van Hoang, H., Tran, L.T., Christiansen, A.V., Pham, N.Q., 2017. Groundwater salinity influenced by Holocene seawater trapped in incised valleys in the Red River delta plain. **Nature Geoscience** 10, 376–381.

Lathashri, U.A., Mahesha, A., 2015. Simulation of Saltwater Intrusion in a Coastal Aquifer in Karnataka, India. **Aquatic Procedia** 4, 700–705.

Ledesma-Ruiz, R., Pastén-Zapata, E., Parra, R., Harter, T., Mahlknecht, J., 2015. Investigation of the geochemical evolution of groundwater under agricultural land: A case study in northeastern Mexico. **Journal of Hydrology** 521, 410–423.

Lee, J.Y., Song, S.H., 2007. Evaluation of groundwater quality in coastal areas: Implications for sustainable agriculture. **Environmental Geology** 52, 1231–1242.

Lin, J., Snodsmith, J.B., Zheng, C., Wu, J., 2009. A modeling study of seawater intrusion in Alabama Gulf Coast, USA. **Environmental Geology** 57, 119–130.

Liu, F., Song, X., Yang, L., Han, D., Zhang, Y., Ma, Y., Bu, H., 2015. The role of anthropogenic and natural factors in shaping the geochemical evolution of groundwater in the Subei Lake basin, Ordos energy base, Northwestern China. **Science of the Total Environment** 538, 327–340.

Loáiciga, H.A., Pingel, T.J., Garcia, E.S., 2012. Sea water intrusion by sea-level rise: Scenarios for the 21st century. **Groundwater** 50, 37–47.

Mahalik, N.K., 2000. Mahanadi Delta: geology, resources & biodiversity. pp 169.

Mahalik, N.K., Das, C., Maejima, W., 1996. Geomorphology and evolution of the Mahanadi delta, India. **Journal of Geosciences Osaka City University** 39, 111–122.

Martínez, D., Bocanegra, E., 2002. Hydrogeochemistry and cation-exchange processes in the coastal aquifer of Mar Del Plata, Argentina. **Hydrogeology Journal** 10, 393–408.

Masterson, J. P., Garabedian, S. P. 2007. Effects of sea-level rise on ground water flow in a coastal aquifer system. **Groundwater** 45, 209-217.

Maupin, M.A., Barber, N.L., 2005. Estimated withdrawals from principal aquifers in the United States, 2000, US Geological Survey Circular 1279.

McDonald, M.G., Harbaugh, A.W., 1988. A modular three-dimensional finite-difference ground-water flow model. US Geological Survey Reston, VA. pp 875.

Mercer, J.W., Larson, S.P., Faust, C.R., 1980. Simulation of Salt-Water Interface Motion. **Groundwater** 18, 374–385.

Michael, H. A., Mulligan, A. E., Harvey, C. F. 2005. Seasonal oscillations in water exchange between aquifers and the coastal ocean. **Nature**, 1145.

Mohanty, S., Jha, M.K., Kumar, A., Jena, S.K., 2012. Hydrologic and hydrogeologic characterization of a deltaic aquifer system in Orissa, eastern

India. **Water Resources Management** 26, 1899–1928.

Mohsen, M.S., Singh, V.P., Amer, A.M., 1990. A note on saltwater intrusion in coastal aquifers. **Water Resources Management** 4, 123–134.

Mondal, N.C., Singh, V.P., Singh, V.S., Saxena, V.K., 2010. Determining the interaction between groundwater and saline water through groundwater major ions chemistry. **Journal of Hydrology** 388, 100–111.

Moore, W. S. 2003. Sources and fluxes of submarine groundwater discharge delineated by radium isotopes. **Biogeochemistry**, 66, 75-93.

Morgan, L.K., Werner, A.D., 2014. Seawater intrusion vulnerability indicators for freshwater lenses in strip islands. **Journal of Hydrology** 508, 322–327.

Morgan, L.K., Werner, A.D., Simmons, C.T., 2012. On the interpretation of coastal aquifer water level trends and water balances: A precautionary note. **Journal of Hydrology** 470–471, 280–288.

Mukherjee, A. (Ed.). 2018. Groundwater of South Asia. Springer.

Mukherjee, A., Fryar, A. E. 2008. Deeper groundwater chemistry and geochemical modeling of the arsenic affected western Bengal basin, West Bengal, India. **Applied Geochemistry,** 23, 863-894.

Mukherjee, A., Fryar, A. E., Howell, P. D. 2007. Regional hydrostratigraphy and groundwater flow modeling in the arsenic-affected areas of the western Bengal basin, West Bengal, India. **Hydrogeology Journal**, 15, 1397.

Nadler, A., Magaritz, M., Mazor, E., 1980. Chemical reactions of sea water with rocks and freshwater: Experimental and field observations on brackish waters in Israel. **Geochimica et Cosmochimica Acta** 44, 879–886.

Naik, P.C., 2018. Seawater Intrusion in the Coastal Alluvial Aquifers of the Mahanadi Delta, SpringerBriefs in Water Science and Technology. Springer International Publishing, Cham. pp 121.

Nair, I.S., Rajaveni, S.P., Schneider, M., Elango, L., 2015. Geochemical and isotopic signatures for the identification of seawater intrusion in an alluvial

aquifer. **Journal of Earth System Science** 124, 1281–1291.

Nayak, S.R., Sarangi, R.K., Rajawat, A.S., 2001. Application of IRS-P4 OCM data to study the impact of cyclone on coastal. **Current Science** 80.

Oteri, A.U., 1988. Electric log interpretation for the evaluation of salt water intrusion in the eastern Niger Delta. **Hydrological Sciences Journal** 33, 19–30.

Oude Essink, G.H.P., 2001. Salt water intrusion in a three-dimensional groundwater system in the Netherlands: A numerical study. **Transport in Porous Media** 43, 137–158.

Panda, D.K., Mishra, A., Jena, S.K., James, B.K., Kumar, A., 2007. The influence of drought and anthropogenic effects on groundwater levels in Orissa, India. **Journal of Hydrology** 343, 140–153.

Panday, S., Huyakorn, P.S., Robertson, J.B., McGurk, B., 1993. A density-dependent flow and transport analysis of the effects of groundwater development in a freshwater lens of limited areal extent: The Geneva area (Florida, U.S.A.) case study. **Journal of Contaminant Hydrology** 12, 329–354.

Parkhurst, D.L., Appelo, C.A.J., 2013. Description of input and examples for PHREEQC version 3: a computer program for speciation, batch-reaction, one-dimensional transport, and inverse geochemical calculations. US Geological Survey.

Piper, A.M., 1944. A graphic procedure in the geochemical interpretation of water-analyses. **Transactions, American Geophysical Union** 25, 914.

Planning and Convergence Department, Odisha., 2016. Comprehensive District Plan (2015-16) for Jagatsinghpur District.

Post, V.E.A., Kooi, H., 2003. Rates of salinization by free convection in high-permeability sediments: Insights from numerical modeling and application to the Dutch coastal area. **Hydrogeology Journal** 11, 549–559.

Praveena, S.M., Aris, A.Z., 2010. Groundwater resources assessment using

numerical model: A case study in low-lying coastal area. **International Journal of Environmental Science & Technology** 7, 135–146.

Pulido-Leboeuf, P., 2004. Seawater intrusion and associated processes in a small coastal complex aquifer (Castell de Ferro, Spain). **Applied Geochemistry** 19, 1517–1527.

Pulido-Leboeuf, P., Pulido-Bosch, A., Calvache, M.L., Vallejos, Á., Andreu, J.M., 2003. Strontium, SO_4^{2-}/Cl^- and Mg^{2+}/Ca^{2+} ratios as tracers for the evolution of seawater into coastal aquifers: the example of Castell de Ferro aquifer (SE Spain). **Comptes Rendus Geoscience** 335, 1039–1048.

Putti, M., Paniconi, C., 1995. Picard and Newton linearization for the coupled model of saltwater intrusion in aquifers. **Advances in Water Resources** 18(3), 159–170.

Radhakrishna, I., 2001. Saline fresh water interface structure in Mahanadi delta region, Orissa, India. **Environmental Geology** 40, 369–380.

Rai, S.P., Purushothaman, P., Kumar, B., Jacob, N., Rawat, Y.S., 2014. Stable isotopic composition of precipitation in the River Bhagirathi Basin and identification of source vapour. **Environmental Earth Sciences** 71, 4835–4847.

Raju, N.J., Patel, P., Reddy, B.C.S.R., Suresh, U., Reddy, T.V.K., 2016. Identifying source and evaluation of hydrogeochemical processes in the hard rock aquifer system: geostatistical analysis and geochemical modeling techniques. **Environmental Earth Sciences** 75, 1157.

Ramakrishnan, D., Bandyopadhyay, A., Kusuma, K.N., 2009. SCS-CN and GIS-based approach for identifying potential water harvesting sites in the Kali Watershed, Mahi River Basin, India. **Journal of Earth System Science** 118, 355–368.

Rao, S.A., Behera, S.K., Masumoto, Y., Yamagata, T., 2002. Interannual subsurface variability in the tropical Indian Ocean with a special emphasis on the Indian Ocean Dipole. **Deep-Sea Research Part II: Topical Studies in Oceanography** 49, 1549–1572.

Reichard, E.G., Johnson, T.A., 2005. Assessment of regional management strategies for controlling seawater intrusion. **Journal of Water Resources Planning and Management** 131, 280–291.

Rejani, R., Jha, M.K., Panda, S.N., 2009. Simulation-Optimization Modelling for Sustainable Groundwater Management in a Coastal Basin of Orissa, India. **Water Resources Management** 23, 235–263.

Rejani, R., Jha, M.K., Panda, S.N., Mull, R., 2008. Simulation Modeling for Efficient Groundwater Management in Balasore Coastal Basin, India. **Water Resources Management** 22, 23–50.

Rejani, R., Jha, M.K., Panda, S.N., Mull, R., 2003. Hydrologic and hydrogeologic analyses in a coastal groundwater basin, Orissa, India. **Applied Engineering in Agriculture** 19, 177.

Riedel, T., Lettmann, K., Beck, M., Brumsack, H.J., 2010. Tidal variations in groundwater storage and associated discharge from an intertidal coastal aquifer. **Journal of Geophysical Research: Oceans** 115, 1–10.

Rosenthal, E., 1987. Chemical composition of rainfall and groundwater in recharge areas of the Bet Shean-Harod multiple aquifer system, Israel. **Journal of Hydrology** 89, 329–352.

Rozell, D.J., Wong, T., 2010. Effects of climate change on groundwater resources at Shelter Island, New York State, USA. **Hydrogeology Journal** 18, 1657–1665.

Sadeg, S., Karahanoðlu, N., 2001. Numerical assessment of seawater intrusion in the Tripoli region, Libya. **Environmental Geology** 40, 1151–1168.

Sahoo, S., Jha, M.K., 2017. Numerical groundwater-flow modeling to evaluate potential effects of pumping and recharge: implications for sustainable groundwater management in the Mahanadi delta region, India. **Hydrogeology Journal** 2489–2511.

Saldi, G.D., Noireaux, J., Louvat, P., Faure, L., Balan, E., Schott, J., Gaillardet, J., 2018. Boron isotopic fractionation during adsorption by calcite – Implication

for the seawater pH proxy. **Geochimica et Cosmochimica Acta** 240, 255–273.

Sanford, W.E., Pope, J.P., 2010. Current challenges using models to forecast seawater intrusion: lessons from the Eastern Shore of Virginia, USA. **Hydrogeology Journal** 18, 73–93.

Santha Sophiya, M., Syed, T.H., 2013. Assessment of vulnerability to seawater intrusion and potential remediation measures for coastal aquifers: a case study from eastern India. **Environmental Earth Sciences** 70, 1197–1209.

Saravana Kumar, U., Sharma, S., Navada, S. V., Deodhar, A.S., 2009. Environmental isotopes investigation on recharge processes and hydrodynamics of the coastal sedimentary aquifers of Tiruvadanai, Tamil Nadu State, India. **Journal of Hydrology** 364, 23–39.

Schneider, J.C., Kruse, S.E., 2006. Assessing selected natural and anthropogenic impacts on freshwater lens morphology on small barrier Islands: Dog Island and St. George Island, Florida, USA. **Hydrogeology Journal** 14, 131–145.

Sengupta, S., Sarkar, A., 2006. Stable isotope evidence of dual (Arabian Sea and Bay of Bengal) vapour sources in monsoonal precipitation over north India. **Earth and Planetary Science Letters** 250, 511–521.

Sherif, M., 1999. Nile Delta Aquifer in Egypt. In: Bear, J., Cheng, A.H.-D., Sorek, S., Ouazar, D., Herrera, I. (Eds.). Springer Netherlands, Dordrecht, 559–590.

Singh, A., 2014. Optimization modelling for seawater intrusion management. **Journal of Hydrology** 508, 43–52.

Singh, A., 2013. Groundwater modelling for the assessment of water management alternatives. **Journal of Hydrology** 481, 220–229.

Skrzypek, G., Dogramaci, S., Grierson, P.F., 2013. Geochemical and hydrological processes controlling groundwater salinity of a large inland wetland of northwest Australia. **Chemical Geology** 357, 164–177.

Smith, A.J., Turner, J. V., 2001. Density-dependent surface water-groundwater interaction and nutrient discharge in the Swan - Canning estuary.

Hydrological Processes 15, 2595–2616.

Soumya, B.S., Sekhar, M., Riotte, J., Banerjee, A., Braun, J.J., 2013. Characterization of groundwater chemistry under the influence of lithologic and anthropogenic factors along a climatic gradient in Upper Cauvery basin, South India. **Environmental Earth Sciences** 69, 2311–2335.

Spechler, B.R.M., 2001. The Relation Between Structure and Saltwater Intrusion in the Floridan Aquifer System , Northeastern Florida. 92-4274. pp 84.

Sprinkle, C.L., 1989. Geochemistry of the Floridan aquifer system in Florida and in parts of Georgia, South Carolina, and Alabama. United States Geological Survey, Professional Paper; (USA); Journal Volume: 1403-I

Steinich, B., Escolero, O., Marín, L.E., 1998. Salt-water intrusion and nitrate contamination in the Valley of Hermosillo and El Sahuaral coastal aquifers, Sonora, Mexico. **Hydrogeology Journal** 6, 518–526.

Steyl, G., Dennis, I., 2010. Review of coastal-area aquifers in Africa. **Hydrogeology Journal** 18, 217–225.

Stigter, T.Y., Van Ooijen, S.P.J., Post, V.E.A., Appelo, C.A.J., Carvalho Dill, A.M.M., 1998. A hydrogeological and hydrochemical explanation of the groundwater composition under irrigated land in a Mediterranean environment, Algarve, Portugal. **Journal of Hydrology** 208, 262–279.

Subba Rao, N., Saroja Nirmala, I., Suryanarayana, K., 2005. Groundwater quality in a coastal area: A case study from Andhra Pradesh, India. **Environmental Geology** 48, 543–550.

Taylor, G.C., 1959. Ground-water provinces of India. **Economic Geology** 54, 683–697.

Taylor, R.G., Scanlon, B., Döll, P., Rodell, M., Van Beek, R., Wada, Y., Longuevergne, L., Leblanc, M., Famiglietti, J.S., Edmunds, M., 2013. Ground water and climate change. **Nature Climate Change** 3, 322.

Todd, D.K., 1959. Ground water hydrology. John Wiley and Sons, Inc, New York.

Tsujimura, M., Abe, Y., Tanaka, T., Shimada, J., Higuchi, S., Yamanaka, T., Davaa, G., Oyunbaatar, D., 2007. Stable isotopic and geochemical characteristics of groundwater in Kherlen River basin, a semi-arid region in eastern Mongolia. **Journal of Hydrology** 333, 47–57.

Tyagi, J.V., Kumar, S., 2000. Estimation of rainfall recharge in a coastal area through inverse groundwater modeling. **Proceedings of the International Conference on Integrated Water Resources Management for Sustainable Development**. 312–322.

Van Weert, F., Van der Gun, J., Reckman, J.W.T.M., 2009. Global overview of saline groundwater occurrence and genesis. **IGRAC Report GP 2009-1** 105.

Vengosh, A., Rosenthal, E., 1994. Saline groundwater in Israel: its bearing on the water crisis in the country. **Journal of Hydrology** 156, 389–430.

Vijay, R., Mohapatra, P.K., 2016. Hydrodynamic assessment of coastal aquifer against saltwater intrusion for city water supply of puri, India. **Environmental Earth Sciences** 75, 1–8.

Volker, R.E., Rushton, K.R., 1982. An assessment of the importance of some parameters for seawater intrusion in aquifers and a comparison of dispersive and sharp-interface modelling approaches. **Journal of Hydrology** 56, 239–250.

Wada, Y., Van Beek, L.P.H., Van Kempen, C.M., Reckman, J.W.T.M., Vasak, S., Bierkens, M.F.P., 2010. Global depletion of groundwater resources. **Geophysical Research Letters** 37, 1–5.

Walther, M., Delfs, J., Grundmann, J., Kolditz, O., Liedl, R., 2012. Journal of Computational and Applied Saltwater intrusion modeling : Verification and application to an agricultural coastal arid region in Oman. **Journal of Computational and Applied Mathematics** 236, 4798–4809.

Wang, Y., Jiao, J.J., 2012. Origin of groundwater salinity and hydrogeochemical processes in the confined Quaternary aquifer of the Pearl River Delta, China. **Journal of Hydrology** 438–439, 112–124.

Webb, M.D., Howard, K.W.F., 2011. Modeling the transient response of saline intrusion to rising sea-levels. **Groundwater** 49, 560–569.

Werner, A.D., 2010. A review of seawater intrusion and its management in Australia. **Journal of Hydrogeology** 18, 281–285.

Willis, R., Finney, B.A., 1988. Planning model for optimal control of saltwater intrusion. **Journal of Water Resources Planning and Management** 114, 163–178.

Yidana, S.M., Chegbeleh, L.P., 2013. The hydraulic conductivity field and groundwater flow in the unconfined aquifer system of the Keta Strip, Ghana. **Journal of African Earth Sciences** 86, 45–52.

Zhang, J., Tsujimura, M., Song, X., Sakakibara, K., 2016. Using stable isotopes and major ions to investigate the interaction between shallow and deep groundwater in Baiyangdian Lake Watershed, North China Plain. **Hydrological Research Letters** 10, 67–73.

Zen, C., P. P. Wang. 1999. MT3DMS: A modular three-dimensional multi-species model for simulation of advection, dispersion and chemical reactions of contaminants in groundwater systems. Documentation and User's Guide. Contract Report SERDP-99-1, US Army Engineer Research and Development Center, Vicksburg.

Zhou, P., Li, G., Lu, Y., Li, M., 2014. Numerical modeling of the effects of beach slope on water-table fluctuation in the unconfined aquifer of Donghai Island, China. **Hydrogeology Journal** 22, 383–396.

Annexure I: Hydraulic head data (2004-2009)

YEAR		OBSERVATION WELLS										
		OW9	***OW11***	***OW2***	***OW7***	***OW5***	***OW8***	***OW4***	***OW1***	***OW6***	***OW10***	***OW3***
CALIBRATION 2004-2005	**1**	2.75	4.8	13.83	4.68	7.59	3.81	9.31	5.72	9.99	1.32	11.7
	89	2.7	3.6	12.81	3.51	7.42	3.25	8.43	5.15	9.53	0.7	11.42
	243	3.35	5.66	14.76	5.52	8.6	5.42	10.43	7.32	12.6	1.95	14.42
	334	3.05	5.16	14.53	5.43	7.81	4.64	10.35	6.36	11.46	1.62	12.52
	366	2.6	4.56	14.01	4.56	8	3.47	9.33	5.32	10.36	1.55	11.62
	454	2.65	3.46	13.26	3.54	7.67	3.02	8.43	5.92	9.39	0.9	11.12
	608	3.15	5.76	14.59	5.54	7.95	5.37	10.45	7.37	12.34	1.7	12.62
	699	4.11	5.29	14.96	5.24	7.78	4.54	10.28	6.15	10.61	1.53	12.48
	731	3.15	4.91	13.79	4.51	7.82	3.17	8.93	4.86	10.03	1.78	11.11
VALIDATION 2006-2009	**1**	3.15	4.91	13.79	4.51	7.82	3.17	8.93	4.86	10.03	1.78	11.11
	88	2.33	4.24	12.06	3.5	5.95	3.29	8.08	3.67	9.53	0.77	10.77
	242	3.82	5.73	14.91	5.53	6.9	5.82	10.38	7.3	12.51	2.5	12.88
	333	4.08	5.15	14.53	5.44	6.5	4.69	10.35	6.38	11.36	1.65	11
	365	3.6	4.85	13.88	3.46	5.93	3.77	9.17	5.64	9.97	1.45	10.76
	453	3.89	3.91	13.69	3.85	6.95	3.8	9.38	5.1	10.08	0.8	10.3
	607	4.69	5.58	14.83	5.73	7.59	5.32	10.28	7.32	12.5	2.33	12.49
	698	4.06	4.97	14.47	5.64	7.64	4.75	10.3	6.24	10.08	1.5	12.4
	730	2.82	3.39	12.86	4.06	6.93	2.65	8.74	3.89	9.59	1.12	11.21
	819	3.5	2.86	13.06	4.39	5.85	3.74	8.66	5.42	10.62	0.85	11.14
	973	4.62	5.58	14.47	5.73	7.94	4.91	10.2	7.28	12.42	2.38	12.59
	1064	4.55	4.49	14.21	5.02	6.68	3.74	10.26	6.61	11.47	1.34	12.51
	1096	3.05	3.66	13.92	4.64	7.58	3.94	11.33	5.92	10.29	0.89	10.43
	1184	3.36	2.62	12.45	3.49	5.73	3.69	8.09	4.59	10.1	0.85	10.21
	1338	4.58	4.99	14.74	5.34	7.78	5.08	10.27	7.01	12.15	2.74	12.62
	1429	3.86	4.17	14.45	5.15	7.94	4.8	10.19	6.49	11.38	1.5	12.51
	1461	3.38	3.18	13.95	4.56	7.62	3.36	9.12	5.81	11.22	0.66	10.24

Annexure IIA Lithologs of some boreholes data collected from CGWB, Bhubaneswar

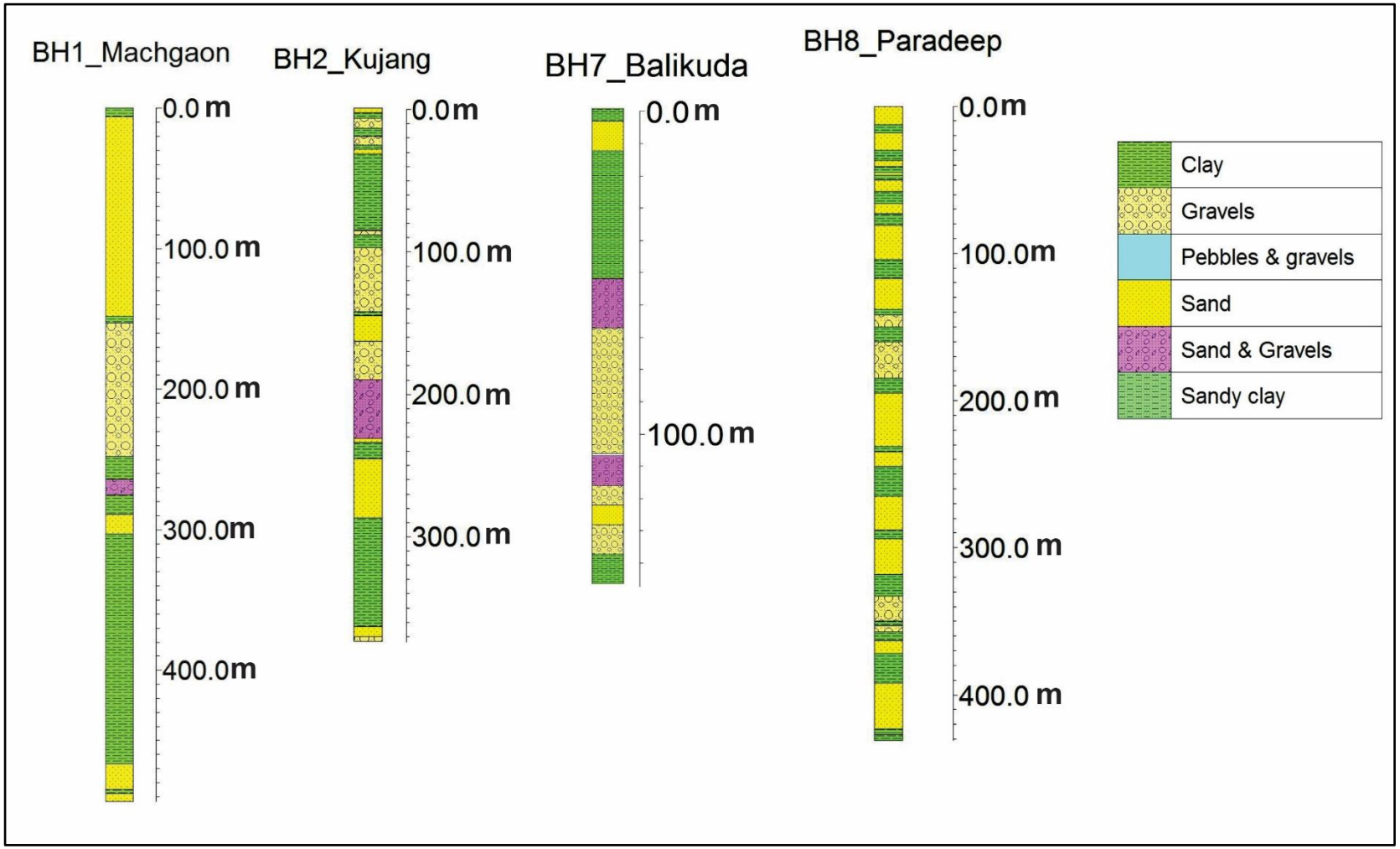

Annexure IIIB Lithologs of some boreholes data collected from CGWB, Bhubaneswar

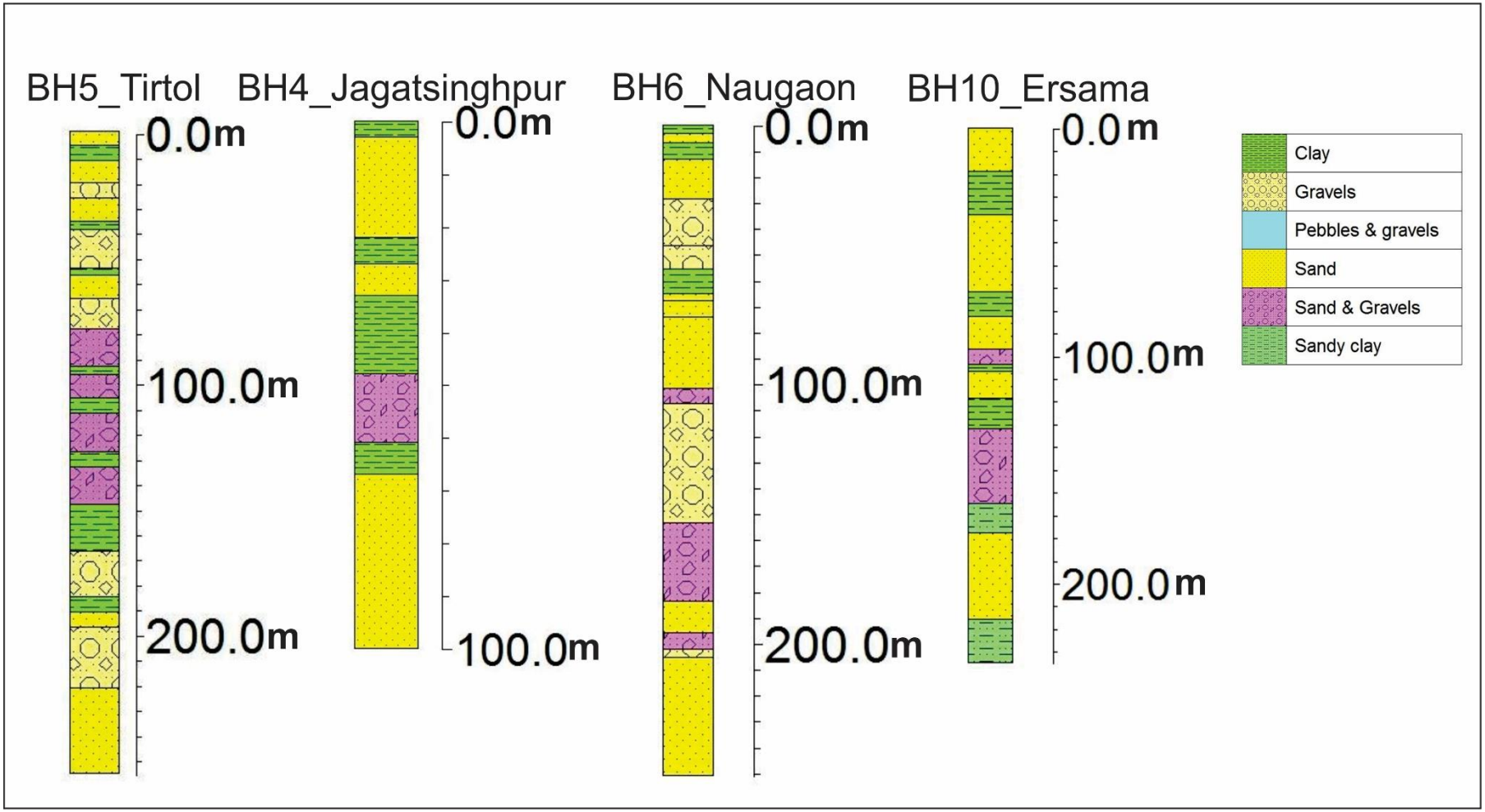

Annexure IV Calibration of Recharge zones (2004-2005)

Start time	*Stop time*	*ZONE 1*	*ZONE 2*	*ZONE 3*	*ZONE 4*	*ZONE 5*	*ZONE 6*	*ZONE 7*	*ZONE 8*	*ZONE 9*	*ZONE 10*	*ZONE 11*
1	30	-0.0008	-0.0002	-0.00009	-0.0008	-0.00018	-9.6E-05	-0.00077	-0.001	-0.00015	-0.00232	-0.00102
30	60	-0.00058	-0.0002	0.0000125	-0.0008	-0.00018	0	-0.00071	-0.00094	-0.0003	-0.00226	-0.0008
60	90	-0.0008	-0.0002	-0.000144	-0.0012	-0.00018	-0.00024	-0.00072	-0.00114	-0.0003	-0.00245	-0.00102
90	120	0.000715	0.000296	0.000904	0.000246	0.000388	0.00146	0.000452	0.000338	-6.2E-05	-0.00159	0.000715
120	150	0.000192	-0.00016	0.0002595	-0.00006	-0.00011	0	-0.00048	-0.00095	-0.00029	-0.00245	0.00019
150	180	0.00077	0.00171	0.000924	0.000462	0.0007	0.0006	0.000688	0.000641	0.00046	0.000521	0.00077
180	210	0.00079	0.002	0.0012	0.00086	0.000452	0.0024	0.000825	0.000125	0.00116	0.0006	0.00057
210	240	0.0012	0.002	0.00102	0.0011	0.00105	0.002368	0.0009	0.00095	0.0013	0.0006	0.001158
240	270	0.000485	0.001696	0.000749	0.00073	0.0003	0.001236	0.00044	0.000692	-6.8E-05	4.2E-05	0.000295
270	300	0.000824	0.001917	0.00084	0.000368	0.001028	0.002	0.0009	0.000908	0.0013	0.0006	0.0012
300	330	-0.002	-0.00035	-0.00135	-0.0015	-0.0006	-0.0004	-0.0012	-0.00143	-0.0012	-0.0026	-0.00102
330	365	-0.002	-0.0007	-0.00135	-0.0015	-0.0006	-0.00048	-0.0012	-0.0019	-0.0009	-0.0024	-0.00102
365	395	-0.00071	0.000109	0.0002125	-0.00024	0.0001	-0.00023	-0.00065	-0.00097	-0.00023	-0.00229	-0.00093
395	425	-0.0008	-0.00035	-0.00009	-0.0008	-0.00018	-0.00042	-0.0008	-0.00114	-0.0003	-0.00245	-0.00102
425	455	-0.00045	0.00102	0.0002625	-0.00067	-0.00072	-9.6E-05	-0.00047	-0.00095	-6E-06	-0.00227	-0.00066
455	485	0.000016	0.000718	-0.000488	0.000012	-0.00025	-0.00017	-0.00048	-0.00095	-0.00023	-0.00245	0.00001
485	515	-2.8E-05	0.000515	-0.000504	-0.0002	2E-06	-0.00008	0.00036	2.75E-05	0.000176	-0.00166	-3.5E-05
515	545	0.000805	0.001466	0.000785	0.000445	0.000784	0.00115	0.00022	-0.00037	0.000323	-0.00015	0.000805
545	575	0.0012	0.002	0.0012	0.001029	0.00075	0.002113	0.0009	0.00095	0.00127	0.0006	0.0012
575	605	0.00055	0.001942	-0.000262	-0.0004	0.000308	0.001949	0.0009	0.00095	0.0013	0.0006	0.00005
605	635	0.00076	0.002	0.00084	0.0011	0.00075	0.001546	0.0009	0.00095	0.0013	0.0006	0.0012
635	665	0.000824	0.002	0.00084	0.00097	0.00075	0.0017	0.0009	0.00095	0.0013	0.0006	0.0012
665	695	-0.00155	-2.6E-05	-0.001314	-0.00147	-0.0006	-2.5E-05	-0.00107	-0.00129	-0.00113	-0.00247	-0.0003
695	731	-0.002	-0.0007	-0.00135	-0.0015	-0.0006	-0.00084	-0.0012	-0.0019	-0.0009	-0.0024	-0.00102

Annexure V Validation Recharge Zones (2006-07)

Start time	*Stop time*	*ZONE 1*	*ZONE 2*	*ZONE 3*	*ZONE 4*	*ZONE 5*	*ZONE 6*	*ZONE 7*	*ZONE 8*	*ZONE 9*	*ZONE 10*	*ZONE 11*
1	**30**	-0.0008	-0.0002	-0.00009	-0.0008	-0.00018	-0.00024	-0.0009	-0.00114	-0.00015	-0.00245	-0.00084
30	**60**	-0.0008	-0.0002	-0.00009	-0.0008	-0.00018	-0.00024	-0.0009	-0.00114	-0.00015	-0.00245	-0.00084
60	**90**	-0.0008	-0.0002	-0.00018	-0.0012	-0.00018	-0.00024	-0.00072	-0.00114	-0.00015	-0.00245	-0.00084
90	**120**	-0.00016	-0.0004	-0.0009	-0.00032	-0.0006	-0.00028	-0.00054	-0.00095	-0.00015	-0.00245	-0.00014
120	**150**	0.000725	0.00159	0.00077	0.000824	0.00076	0.00032	0.000556	0.000542	0.000342	-0.00153	0.000725
150	**180**	0.00093	0.001905	0.001133	0.000764	0.00074	0.001844	0.000468	0.000202	0.00055	0.000354	0.00093
180	**210**	0.0012	0.002	0.0012	0.0011	0.00105	0.0024	0.0009	0.00095	0.0013	0.0006	0.0012
210	**240**	0.0012	0.002	0.00102	0.0011	0.00105	0.0024	0.0009	0.00095	0.0013	0.0006	0.0012
240	**270**	0.001104	0.002	0.000777	0.000428	0.00058	0.0024	0.00072	0.000776	0.00025	0.000336	0.000782
270	**300**	-0.00163	0.000568	0.000176	-0.001034	-0.00102	0.00036	-0.00091	-0.00171	0.000301	-0.00125	-0.00067
300	**330**	-0.00181	-0.00035	-0.00113	-0.0015	-0.00025	-0.0004	-0.00044	-0.00058	-0.00052	-0.00179	-0.00067
330	**365**	-0.002	-0.0007	-0.00135	-0.0015	-0.0006	-0.00048	-0.0012	-0.0019	-0.00045	-0.0024	-0.00084
365	**395**	-0.0008	-0.00035	-0.00009	-0.00064	-0.00018	-0.00042	-0.0008	-0.00114	-0.00015	-0.00245	-0.00084
395	**425**	-0.00023	0.00144	0.000668	7E-05	0.00028	0.00113	-0.00052	-0.00083	0.00018	-0.00215	-0.00029
425	**455**	-0.0008	-0.00035	-0.00018	-0.0012	-0.00108	-0.00042	-0.00064	-0.00114	-0.00015	-0.00245	-0.00084
455	**485**	-0.00016	-0.0007	-0.0009	-0.00032	-0.0006	-0.00049	-0.00048	-0.00095	-0.00015	-0.00245	-0.00014
485	**515**	0.001016	0.001878	0.000758	0.000812	0.000304	0.000352	0.000556	0.000542	0.000672	-0.00153	0.001016
515	**545**	0.001105	0.001802	0.000928	0.000848	0.00064	0.002288	0.00071	0.000665	0.000178	0.000533	0.001105
545	**575**	0.000059	0.001758	-9E-06	-0.000352	0.000298	0.001525	0.000304	-0.00138	-0.00022	-0.00045	-0.00018
575	**605**	0.0012	0.002	0.0012	0.0011	0.000924	0.0024	0.0009	0.00095	0.0013	0.0006	0.0012
605	**635**	0.00076	0.002	0.00084	0.0011	0.00075	0.001546	0.0009	0.00095	0.0013	0.0006	0.0012
635	**665**	0.00003	0.000749	0.000236	-0.000338	0.000154	0.00022	-0.00066	-0.00143	-0.00012	-0.00099	-0.00079
665	**695**	-0.002	-0.00035	-0.00135	-0.0015	-0.0006	-0.0007	-0.0012	-0.00143	-0.0006	-0.0026	-0.00084
695	**730**	-0.002	-0.0007	-0.00135	-0.0015	-0.0006	-0.00084	-0.0012	-0.0019	-0.00045	-0.0024	-0.00084